REVIEW OF FIBER REINFORCED POLYMERS (FRP) USAGE IN TIMBER FRAME ELEMENTS

A THESIS SUBMITTED TO
GRADUATE SCHOOL OF NATURAL AND APPLIED SCIENCES
OF
KOCAELI UNIVERSITY

BY

SUHAIB SALAHUDDIN ALZUBAIR SULIMAN

IN PARTIAL FULFILLMENT OF THE REQUIREMENTS
FOR
THE DEGREE OF MASTER OF SCIENCE
IN
CIVIL ENGINEERING

KOCAELI 2025

REVIEW OF FIBER REINFORCED POLYMERS (FRP) USAGE IN TIMBER FRAME ELEMENTS

A THESIS SUBMITTED TO
GRADUATE SCHOOL OF NATURAL AND APPLIED SCIENCES
OF
KOCAELI UNIVERSITY

BY

SUHAIB SALAHUDDIN ALZUBAIR SULIMAN

IN PARTIAL FULFILLMENT OF THE REQUIREMENTS
FOR
THE DEGREE OF MASTER OF SCIENCE
IN
CIVIL ENGINEERING

Asst. Prof. Dr. Erkan AKPINAR **..……**
Supervisor, Kocaeli University

Prof. Dr. Seval PINARBAŞI ÇUHADAROĞLU **...……...**
Jury Member, Kocaeli University

Assoc. Prof. Dr. Barış Erdil **…...……**
Jury Member, Van Yüzüncü Yıl University

Thesis Defense Date: 22.01.2025

ETHICAL DECLARATION AND RESEARCH FUND SUPPORT

According to the thesis writing rules of the Graduate School of Natural and Applied Sciences, Kocaeli University, in this thesis that I have prepared:

- I declare that this thesis is my original work.
- I affirm that I have adhered to scientific ethical principles and rules throughout all stages of preparation, data collection, analysis, and information presentation.
- I acknowledge and provide references for all data and information obtained in this study, and I have included these sources in the references section.
- I affirm that this work meets the criteria set by the Graduate School of Natural and Applied Sciences at Kocaeli University through the use of plagiarism detection software subscribed to by the university.
- I confirm that there has been no manipulation of the data used.
- I declare that I have not submitted any part of this thesis as part of another thesis at this university or any other university.

No stage of this thesis has been financially or infrastructurally supported by any institution/organization. I hereby acknowledge that if any contradiction to this statement is identified in relation to my work at any time, I accept all moral and legal consequences that may arise as a result.

……

Suhaib Salahuddin Alzubair Suliman

PUBLICATION AND INTELLECTUAL PROPERTY RIGHTS

I declare that I grant permission to Kocaeli University to archive and make available for use, in both printed and electronic formats, my entire master's thesis, or any part thereof, under the following conditions, as approved by the Graduate School of Natural and Applied Sciences. With this permission, all intellectual property rights, except for the usage rights granted to the university, will remain mine. The future use of my thesis, either in its entirety or in part, in works such as articles, books, presentations, licenses, patents, or similar endeavors, will be subject to my discretion and the acknowledgement of my supervisor's contribution.

I affirm and guarantee that the thesis is my original work, does not violate the rights of others, and that I am the sole owner of the thesis. I further declare that any copyrighted material used in my thesis has been obtained with written permission from the respective copyright holders, and I undertake to provide copies of these permissions to the university upon request.

In accordance with the guidelines published by the Council of Higher Education regarding the collection, organization, and accessibility of electronic thesis, my thesis will be made accessible in the YOK National Thesis Center/Kocaeli University Libraries Open Access System, except under the condition specified below.

No confidentiality decision has been made regarding my thesis.

Suhaib Salahuddin Alzubair Suliman

PREFACE AND ACKNOWLEDGEMENTS

This thesis, titled "Review of Fiber Reinforced Polymers (FRP) Usage in Timber Frame Elements" marks the culmination of my graduate studies at Kocaeli University. This work represents a comprehensive exploration of how FRP materials can enhance timber structural components, an area that has presented numerous challenges and rewards throughout my research journey. I am deeply grateful for the support and encouragement I have received along the way.

First and foremost, I wish to express my heartfelt gratitude to my supervisor, Dr. Erkan Akpinar. His unwavering support, insightful guidance, and extensive expertise have been instrumental in shaping the course of my research. I truly appreciate his mentorship, which has been a guiding force in the development and completion of this thesis.

Additionally, I am thankful to my fellow graduate students for their collaboration and assistance during various stages of this project. Their camaraderie and support greatly enriched my experience and contributed to the successful completion of the review.

Above all, I am profoundly grateful to my family for their relentless support, love, and understanding throughout this academic journey. I am especially thankful to my mother for her encouragement and unwavering belief in my abilities. Their sacrifices and support have been fundamental to my success, and I dedicate this thesis to them in recognition of my heartfelt appreciation.

Finally, I extend my thanks to all individuals, colleagues, and friends who have provided guidance, feedback, and assistance in various forms throughout the course of this research.

It is my hope that this thesis contributes to the growing knowledge on the advantages of FRPs in timber structural components, serving as a foundation for future research endeavors in this vital field.

January - 2025 Suhaib Salahuddin Alzubair Suliman

CONTENTS

ETHICAL DECLARATION AND RESEARCH FUND SUPPORT i
PUBLICATION AND INTELLECTUAL PROPERTY RIGHTS ii
PREFACE AND ACKNOWLEDGEMENTS iii
CONTENTS iv
LIST OF FIGURES vi
LIST OF TABLES xi
INDEX OF SYMBOLS AND ABBREVIATIONS xii
ÖZET xiii
ABSTRACT xiv
1. INTRODUCTION 1
1.1. Objectives of the Study 5
2. TIMBER AS STRUCTURAL MATERIAL 6
2.1. Types of Timber 8
2.1.1. Softwood 8
2.1.2. Hardwood 9
2.2. Natural Characteristics of Wood 10
2.2.1. Knots 10
2.2.2. Splits or Checks in Wood 10
2.2.3. Shake Defect 10
2.2.4. Decay 11
2.3. Physical and Mechanical Properties of Wood 11
2.3.1. Physical Properties 11
2.3.2. Directional Properties 12
2.3.3. Moisture Content 12
2.3.4. Shrinkage and Swelling 13
2.3.5. Distortion of Timber 14
2.4. Mechanical Properties 15
2.4.1. Modulus of Elasticity (MOE) 15
2.4.2. Shear Modulus 15
2.4.3. Modulus of Rupture (MOR) 16
2.4.4. Hardness 17
2.4.5. Density 17
2.5. Wood Products: 18
2.5.1. Solid Timber 19
2.5.2. Glulam 20
2.5.3. Cross-Laminated Timber 23
2.5.4. Laminated Veneer Lumber (LVL) 26
2.5.5. Plywood 28
2.5.6. Oriented Strand Board (OSB) 29
2.5.7. Laminated Strand Lumber (LSL) 30
2.5.8. Parallel Strand Lumber (PSL) 32
3. TIMBER STRUCTURAL ELEMENTS 35
3.1. Beam 35
3.2. Column 38
4. FIBER REINFORCED POLYMER (FRP) 41

5. APPLICATIONS OF FRP REINFORCEMENT IN TIMBER STRUCTURES IN THE PREVIOUS STUDIES 46
5.1. Beams 46
5.1.1. Side Face Reinforcement 47
5.1.2. Bottom Face Reinforcement 48
5.1.3. U-Wrap Configuration 66
5.1.4. Near-Surface Mounted 72
5.1.5. Pultruded FRP Bars 76
5.2. Columns 94
5.2.1. Studies Conduct Full Wrapping Method 94
5.2.2. Studies Conduct Partial Wrapping Method 110
5.2.3. Studies Conduct both Methods (Full + Partial) 119
5.2.4. Studies Conduct Longitudinal FRP Reinforcement 128
5.2.5. Studies Conduct Hybrid Reinforcement Techniques 130
6. CONCLUSION AND RECOMMENDATIONS 138
REFERENCES 140
PUBLICATIONS AND WORKS 148
BIOGRAPHY 148

LIST OF FIGURES

Figure 1.1. Urnes Stave Church (Norway) 1
Figure 1.2. Iglesia Santa María de Loreto de Achao 2
Figure 1.3. Greensted Church 3
Figure 1.4. Image by patrick degerman 4
Figure 2.1. Hierarchical levels of wood 7
Figure 2.2. Cross-section of tree trunk 8
Figure 2.3. Schematic structure of softwood 9
Figure 2.4. Schematic structure of hardwood 9
Figure 2.5. A knot observed from every angle of a wood piece 10
Figure 2.6. Common defects in wood 11
Figure 2.7. Overall correlation between moisture content and strength and/or stiffness 13
Figure 2.8. Relative humidity and the moisture content at equilibrium 13
Figure2.9. Diagrammatic representation of the arrangement of microfibrils and shrinkage in both compressed and normal wood 14
Figure 2.10. Definition of distortion/warp modes 14
Figure 2.11. The relation between the ultimate strength of failure 16
Figure 2.12. Shear in different directions 16
Figure 2.13. Schematic illustration of the influence of density 18
Figure 2.14. Squared wood with knots, drying cracks, and pith 19
Figure 2.15. Glued laminated timber 20
Figure 2.16. Typical stages of glulam production 22
Figure 2.17. Cross-laminated timber layup 24
Figure 2.18. Laminated Veneer Lumber 26
Figure 2.19. LVL production includes multiple steps, and if green veneer is used, it undergoes drying before resin application 27
Figure 2.20. Examples of plywood and wood core plywood 29
Figure 2.21. Oriented Strand Board 30
Figure 2.22. Laminated Strand Lumber 30
Figure 2.23. Flowchart illustrating the manufacturing procedure for laminated strand lumber 31
Figure 2.24. Parallel Strand Lumber 32
Figure 3.1. a) Principal drawing of bending failure, b) failure of tension during bending 36
Figure 3.2. (a) Key design representation for compression failure at the support point, (b) compression failure 36
Figure 3.3. Shear failure 37
Figure 3.4. Crack and split of timber beam. 37
Figure 3.5. Images showing the failure modes 39
Figure 4.1. Stress Strain Diagram for Composite Phases 42
Figure 4.2. Typical FRPs 42
Figure 4.3. Stress-strain graphs for various unidirectional FRPs and steel under uniaxial tension 43
Figure 5.1. Shape and structure of wood beams that have been tested 47

Figure 5.2. The MTS testing apparatus alongside one of the specimens prepared for the bending test 49
Figure 5.3. The test specimen is positioned upside down after the experiment, revealing the CFRP strip bonded to the beam's tensile face across its full width 49
Figure 5.4. The failure mechanisms of the samples are shown in a grid, featuring images of different failures such as tension, compression, shearing, cross-graining, and CFRP 49
Figure 5.5. All Specimens 51
Figure 5.6. Crack formations for timber beams (B1, B3, B6, and B9) 52
Figure 5.7. Analyzing how varying the widths/ lengths of CFRP strips influence the maximum load capacity of timber beams with different widths of CFRP strips 52
Figure 5.8. Illustration of the test configuration; a schematic representation, (a) bond width of 45 mm, (b) bond width of 30 mm 53
Figure 5.9. Failure mode of timber beams 54
Figure 5.10. Comparison of Load-Bearing Capacity and Width and length Utilization in Timber Beams Reinforced with CFRP 54
Figure 5.11. Reinforcement method: a) apply an initial layer of epoxy resin, b) fibers can be easily trimmed with scissors, c) several layers of fibers can be applied in succession and interchanged 56
Figure 5.12. Test setup, with LVDT placements at one-quarter and three-quarters of the span, as well as at the midpoint 56
Figure 5.13. Tension failure types include: a) failure caused by a knot on the tension side, b) standard tension failure in a straight-grained beam, and c) and d) tension failure in cross-grained scenarios 56
Figure 5.14. Various retrofitting techniques utilizing FRP) include: (a) applying FRP sheets; (b) positioning FRP pultruded elements on the compression side; and (c) using CFR) laminae 57
Figure 5.15. Experimental test configuration: (a) small beams; (b) large beams. (rafters) 57
Figure 5.16. The four-point bending tests, with simply supported ends, measure the relationship between load and mid-span deflection for both unreinforced non-defective (ND Series) and defective samples. (KD Series) 58
Figure 5.17. Beams set up for destructive evaluation: unreinforced beams and those reinforced with CFRP Glued Laminated Timber 59
Figure 5.18. Examples of failures for each group of analysed samples are shown: Beam No. 0/4 (a), Beam No. 1/2 (b), Beam No. 3/3 (c), and Beam No. 5/4 (d) 59
Figure 5.19. (a) Production of prestressed beams, (b) Test set-up 60
Figure 5.20. View of the damaged prestressed beam 61

Figure 5.21. Failure mechanisms for specimens without FRP (above) and those reinforced with FRP (below): (a) side surface, (b) bottom surface, and (c) end surface 62
Figure 5.22. Beam with Bottom Face Reinforcement .....
Figure 5.23. FRP reinforced beams in the De La Rosa García, et al. 2013 research 67
Figure 5.24. Test schème..... 67
Figure 5.25. Failure mode of tested beams 68
Figure 5.26. (a) Test Setup; (b) Diagram illustrating the structure of a device used for bending tests 69
Figure 5.27. Common failure types in unreinforced timber beams 69
Figure 5.28. Common failure types in unreinforced timber beams 70
Figure 5.29. Test set-up..... 71
Figure 5.30. (a) modes of failure for (+M) bending group; (b) for (-M) bending group 71
Figure 5.31. NSM reinforcement configurations: Bottom single reinforcement with 2, 3 bars in rectangular grooves, with in the lateral side and double bottom and top 73
Figure 5.32. Experimental set-up..... 73
Figure 5.33. Typical failure modes 74
Figure 5.34. (A) Specimen number and characteristics, (B) Reinforcing process of test specimens..... 75
Figure 5.35. (a) Failure modes of unreinforced specimens; (b) NSM reinforcement circular specimens, (c) NSM reinforcement square specimens, (d) Bottom external bonding reinforcement 76
Figure 5.36. (a) Test setup, (b) Specimens configuration 77
Figure 5.37. Tension failure (a) GFRP flexural reinforcement, (b) beams reinforced with dowels 78
Figure 5.38. The effect of strengthening on load–deflection behaviour 78
Figure 5.39. Reinforcement configurations (a) for short term; (b) for creep test specimens 79
Figure 5.40. (a) Test rig with beam D3 subjected to bending test, (b) Mechanism of failure of beam 81
Figure 5.41. (a) Beam arrangements, (b) Stiffness test arrangement..... 82
Figure 5.42. (a) Tension failure at defect in the Beam, (b) Compression wrinkling, (c) GF attached to sacrificial lamination demonstrating quality of bond, (d) Failure initiated from knot..... 82
Figure 5.43. Test setup of tested specimens 83
Figure 5.44. Failure modes for control specimens..... 84
Figure 5.45. (a) SCR (CFRP + epoxy resin), (b) SCM (CFRP + melamine glue), (c) SVR (GFRP + epoxy resin), (d) SVM (GFRP + melamine 84
Figure 5.46. (a) specimens HV (GFRP + epoxy resin), (b) specimens (basalt rods + epoxy resin)..... 84
Figure 5.47. Beam configurations..... 85

Figure 5.48. Typical beam failure modes include (a) unreinforced beams failing under tension; (b) weakly reinforced beams failing under tension; (c) moderately reinforced beams failing under compression; (d) compression failure of moderately reinforced beams by vertically CFRP plate reinforced beams 86
Figure 5.49. Configurations of strengthened beams: (a) Phase A, (b) Phase B, (c) Phase C, (d) Phase D, (e) Phase E, and (f) Phase F (mm) 87
Figure 5.50. Each phase's typical load-deflection behaviour 88
Figure 5.51. Typical failure modes for all phases 88
Figure 5.52. Properties of carbon FRP fan-type anchors 90
Figure 5.53. Specimen failure modes 91
Figure 5.54. Epoxy and FRP application 95
Figure 5.55. Specimens strengthened with (a) three, (b) one layers of GFRP showed representative failure mechanisms 96
Figure 5.56. (a) GLT and CLT column specimen dimensions, (b) Manufacturing process 97
Figure 5.57. Common failure patterns observed in unconfined specimens 97
Figure 5.58. Common failure characteristics of the confined specimens 97
Figure 5.59. Typical examples of failure modes 98
Figure 5.60. Test setup 99
Figure 5.61. load-displacement curve 100
Figure 5.62. Typical failure pattern 100
Figure 5.63. Failure mode for unconfined specimen 101
Figure 5.64. AFRP confined specimen’s failure mode (a) End crushing; (b) Bending 102
Figure 5.65. C-section of the HFT (arrow heads indicate the FRP fiber and the timber grain directions) 103
Figure 5.66. Local failure modes 103
Figure 5.67: Comparative Column Capacity Results for Fully Reinforced Timber Members with Various FRP Materials 109
Figure 5.68. (a) Tested specimens (unit mm), (b) Test setup 111
Figure 5.69. Failure Modes 112
Figure 5.70. (a) Hooped type, (b) Spiral type 113
Figure 5.71. Load-displacement curve 113
Figure 5.72. The failure modes 113
Figure 5.73. Column Samples: (a) LCLT-0, (b) LCLT-B, (c) LCLT-S, (d) LCLT-SH and (e) 115
Figure 5.74. Failure patterns of columns (a) LCLT-0, (b) LCLT-B, (c) LCLT-S, (d) LCLT-SH 115
Figure 5.75: Comparative Column Capacity Results for Partially Reinforced Timber Members with Various FRP Materials 118
Figure 5.76. Typical carbon reinforcement and column specimens 120
Figure 5.77. Shear failure a specimen with spirals; b specimens with full wrapping 121
Figure 5.78. The columns' cross sections are (a) pinned and (b) fixed 122

Figure 5.79. Response averages for pinned–pinned GFRP columns: (a) 950 mm, (b) 1400 mm, (c) 1850 mm 122
Figure 5.80. Response averages for fixed–fixed GFRP columns: (a) 1450 mm, (b) 1900 mm, ... 123
Figure 5.81. (a) Illustration of wrapping of FRP methods, (b) Test setup 124
Figure 5.82. Failure modes of specimens tested 124
Figure 5.83. Strengthening scheme of timber columns (mm) 125
Figure 5.84. Test setup 126
Figure 5.85. Modes of specimen failure 126
Figure 5.86. FRP types 127
Figure 5.87. Test specimens 127
Figure 5.88. Ultimate load–displacement curve of group two 128
Figure 5.89. Shape of the compression strength specimen 130
Figure 5.9 . The reinforced-specimen failure modes 130
Figure 5.91. Specimen types 131
Figure 5.92. Illustration of the loading mechanism and measurement apparatus 131
Figure 5.93. (a) Group 1, (b) Group 2, (c) Group 3 132
Figure 5.94. Plan and sectional views of full-scale 133
Figure 5.95. Full-scale column test arrangement and schematic design (mm) 134
Figure 5.96. A typical composite column made of concrete, steel tubes, timber, and GFRP 136
Figure 5.97. Cross-sections of all specimens 136
Figure 5.98. Modes of failure of GTSCs 137

LIST OF TABLES

Table 3.1. Classification of timber beams types 35
Table 3.2. According to Geometry 35
Table 4.1. Fibre and Polymer properties 43
Table 5.1. Summary of the results 48
Table 5.2. Increases in average values compared to the reference group S0 50
Table 5.3. Summary of Studies on Timber Beams Reinforced with FRP on the Bottom Face 63
Table 5.4. Failure mechanism of tested beams 68
Table 5.5. Modes of failure. Bending tests (+M) 72
Table 5.6. Summary of Studies on Timber Beams Reinforced with FRP on U-Configuration 72
Table 5.7. Beam Configurations 80
Table 5.8. Comparison of experimentally obtained results 86
Table 5.9. Specimens details and failure modes 90
Table 5.10: Summary of Key Findings on FRP-Reinforced Timber Beams 92
Table 5.11. Specimens' parameters 99
Table 5.12. Result of specimens 101
Table 5.13: Summary of Experimental Studies on Full-Reinforcement of Timber Columns 109
Table 5.14. Details of the Specimens 111
Table 5.15. Number of specimens and key parameters 112
Table 5.16. Summary of Experimental Studies on Partial-Reinforcement of Timber Columns 116
Table 5.17. Results of group one 128
Table 5.18. Details of tested specimens 134
Table 5.19. Summary of results 134

INDEX OF SYMBOLS AND ABBREVIATIONS

Abbreviations

AFRP	: Aramid Fiber Reinforced Polymer
BFRP	: Basalt Fiber Reinforced Polymer
CFRP	: Carbon Fiber Reinforced Polymer
CFST	: Concrete-Filled Steel Tube
CLT	: Cross-Laminated Timber
EBR	: Externally Bonded Reinforcement
EC 5	: Eurocode 5
FRP	: Fibre Reinforced Polymers
GFRP	: Glass Fiber Reinforced Polymer
GLT	: Glued Laminated Timber
GTSC	: Glass fiber-reinforced polymer (GFRP)-Timber-Steel Tube- Concrete
HFRP	: Hybrid Fiber-Reinforced Polymer
HM	: High Modulus
HPBBC	: High-Performance Bamboo-Based Composites
HS	: High Strength
LBL	: Laminated Bamboo Lumber
LSL	: Laminated Strand Lumber
LVL	: Laminated Veneer Lumber
MC	: Moisture Content
MOE	: The Modulus of Elasticity
MOR	: Modulus Of Rupture
MT	: Mass Timber
NSM	: Near-Surface Mounted
OSB	: Oriented Strand Board
PSL	: Parallel Strand Lumber
STS	: Self-Tapping Screws
TFST	: Timber-Filled Steel Tube

AHŞAP ÇERÇEVE ELEMANLARINDA LIFLI POLIMER (FRP) KULLANIMININ İNCELENMESI

ÖZET

Bu çalışmada, Lifli Polimerlerin (FRP), özellikle kirişler ve kolonlar olmak üzere ahşap yapı elemanlarında güçlendirme amaçlı literatürde yer alan kullanımı, kapsamlı bir şekilde incelenmiştir. Eleman alt yüzünden, yan yüzeylerinden yapıştırma, yüzeye yakın gömme, tam ve kısmi sargılama teknikleri, hibrit yöntemler gibi çeşitli güçlendirme teknikleri, deneysel çalışmaların kapsamlı bir değerlendirmesi ile incelenmiştir. FRP türü, katman sayısı, lif yönelimi, yapıştırma yöntemleri ve hasar mekanizmaları gibi kritik faktörler, yapısal performans üzerindeki etkilerini değerlendirmek amacıyla değerlendirilmiştir. Çalışmanın bulguları, FRP güçlendirmesinin ahşap kirişlerin eğilme dayanımı, rijitliği ve yük taşıma kapasitesini önemli ölçüde artırdığını ve yüzeye yakın gömme ile U-sargı konfigürasyonlarının eğilme dayanımı açısından en iyi sonuçları verdiğini göstermektedir. Ahşap kolonlarda ise tam FRP sargılamanın basınç dayanımı ve süneklik açısından en etkili yöntem olduğu, özellikle karbon lifli polimerlerin (CFRP) en yüksek performans kazancını sağladığı belirlenmiştir. Ancak, FRP ile çelik veya harç dolgulu kılıfların birleştirildiği hibrit takviye yöntemlerinin, yapısal bütünlüğü korurken maliyet açısından daha verimli çözümler sunduğu görülmüştür. Ayrıca, FRP katmanlarının aşırı arttırılmasının her zaman orantılı dayanım artışı sağlamadığı ve yapışma ile gerilme dağılımı açısından sınırlamalar oluşturabileceği vurgulanmıştır. Bu bulgular, FRP güçlendirme stratejilerinin verimlilik, dayanıklılık ve maliyet etkinliği açısından optimize edilmesi gerektiğini ortaya koymaktadır. Bu derleme çalışması, FRP ile güçlendirmenin mekanik özellikleri iyileştirmedeki rolünü, servis ömrünü uzatmadaki etkisini ve sürdürülebilir yapı uygulamalarını teşvik etmedeki önemini ortaya koyarak, ahşap yapı teknolojilerinin ilerlemesine katkıda bulunmaktadır.

Anahtar Kelimeler: Ahşap Hasar Mekanizmaları, Ahşap Kirişler, Ahşap Kolonlar, FRP, Yapısal Güçlendirme.

REVIEW OF FIBER REINFORCED POLYMERS (FRP) USAGE IN TIMBER FRAME ELEMENTS

ABSTRACT

In this study, the use of Fiber Reinforced Polymers (FRP) for the strengthening of timber structural elements, particularly beams and columns, in the literature has been extensively reviewed. Various reinforcement techniques, including bottom-face reinforcement, side-face bonding, near-surface mounted (NSM) techniques, fully and partially wrapping, and hybrid approaches, were examined through an extensive evaluation of experimental studies. Key factors such as the type of FRP, number of layers, fiber orientation, bonding methods, and failure mechanisms were investigated to assess their impact on structural performance. Findings indicate that FRP reinforcement significantly enhances the flexural strength, stiffness, and load-bearing capacity of timber beams, with NSM and U-wrap configurations providing optimal results for bending resistance. In timber columns, full FRP wrapping is the most effective method for improving compressive strength and ductility, with CFRP yielding the highest performance gains. However, hybrid reinforcement methods, such as combining FRP with steel or grout-filled sleeves, offer cost-effective solutions while maintaining structural integrity. The study also highlights that excessive FRP layering does not always lead to proportional strength improvements due to bonding limitations and stress distribution challenges. These findings emphasize the need for optimized reinforcement strategies to maximize efficiency, durability, and cost-effectiveness. This review contributes to the advancement of timber construction technologies by providing insights into the role of FRP reinforcement in enhancing mechanical properties, extending service life, and promoting sustainable building practices.

Keywords: Timber Failure Mode, Timber Beams, Timber Columns, Fiber Reinforced Polymers, Structural Strengthening.

1. INTRODUCTION

Timber has been a vital construction material for millennia, valued for its durability, adaptability, and sustainable nature. Its advantages include a favorable strength-to-weight ratio, aesthetic flexibility, and exceptional thermal insulation properties, which enhance the energy efficiency of buildings by reducing dependence on mechanical heating and cooling systems. This remarkable resource also plays a significant role in carbon sequestration, making it an environmentally responsible choice for modern architecture. As trees grow, they absorb carbon dioxide from the atmosphere, effectively reducing the carbon footprint of both the construction process and the built environment. Additionally, timber's ability to be sourced sustainably from managed forests further underscores its role as a green building material. Its usage increased significantly during the Middle Ages as carpenters and woodworkers emerged as skilled tradespeople. There are numerous examples of ancient buildings that were constructed hundreds or even thousands of years ago.

Here are a few instances of historic buildings that date back hundreds or even thousands of years:

Norway's stave churches, constructed between the 12th and 14th centuries, represent remarkable examples of medieval wooden architecture. Among them, Borgund Stave Church stands out as a testament to Viking craftsmanship, featuring a framework of vertical wooden staves along with elaborate carvings. These structures demonstrate the advanced timber engineering practices that were emerging in early Europe.

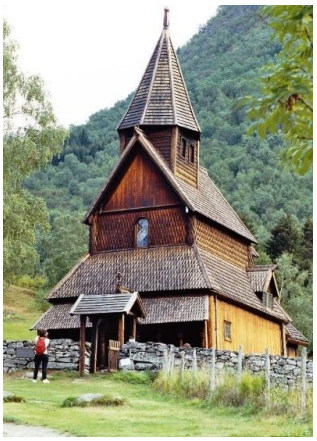


Figure 1.1. Urnes Stave Church (Norway) (URL-1)

The Saint Mary of Loreto Church in Achao, a significant Catholic temple located near the central square and the sea, was originally built by Jesuits around 1730 and later reconstructed in 1784 following a fire. Recognized as one of Chile's oldest churches, it features a wooden structure with three naves, measuring 46 meters in length and 14 meters in width, while its tower reaches 22 meters high. The exterior is adorned with larch shingles, and the interior showcases baroque architecture, including an intricately designed altarpiece and pulpit, alongside Solomonic columns and a carefully crafted wooden floor. Declared a National Monument in July 1951 and designated a UNESCO World Heritage site in 2000, the church celebrates its main feast day on December 10 in honor of its patron, Saint Mary of Loreto.



Figure 1.2. Iglesia Santa María de Loreto de Achao (URL-2)

Greensted Church, situated in the heart of the Essex countryside, holds the title of the oldest timber church globally and is recognized as a significant historical worship site. Dating back to a nave constructed between 998 and 1063 AD, it also stands as the oldest wooden structure in Europe. While only remnants of the original Saxon architecture remain, specifically the split oak tree logs that form the nave, the church continued to serve its community even after the Norman conquest of 1066. This ongoing use is supported by the discovery of some Norman-period flint embedded in the Chancel wall.



Figure 1.3. Greensted Church (URL-3)

Recent advancements in wood technology have broadened the scope of timber usage in construction. Innovations like cross-laminated timber (CLT) and glue-laminated timber (glulam) provide superior structural capabilities, enabling the creation of taller buildings and more complex designs that were once considered unfeasible with traditional wood. (Gilfillan, et al. 2003)

As architects and builders increasingly adopt these materials, they acknowledge that timber not only complies with stringent safety regulations but also contributes a warm, natural aesthetic to urban environments. Additionally, incorporating timber into architecture fosters a connection to nature, enhancing the wellbeing of occupants.

As the global population grows, the need for efficient and sustainable building solutions has led to innovations in timber engineering, notably through engineered wood products like glulam, CLT, and LVL. These advancements not only cater to structural resilience but also align with contemporary sustainability goals, leveraging timber's inherent properties as a carbon sink. (Lam, 2001) Moreover, the sustainability narrative surrounding timber is reinforced by improved forest management practices, resulting in enhanced availability and responsible harvesting. This shift supports the perception of timber as an eco-friendly construction option, further propelled by technological innovations such as Building Information Modeling (BIM), which streamline design processes and elevate timber's applicability across diverse structural scenarios. (Arriaga et al., 2023)

The Sara Cultural Centre, designed by White Arkitekter, has opened in Skellefteå, Sweden, standing at 75 meters tall and becoming one of the tallest timber buildings in the world. This innovative structure serves as a cultural venue and hotel that enhances the local community while promoting sustainable design. It pays homage to the city's rich timber architecture heritage, employing advanced construction techniques with (CLT) and (GLT) to achieve a carbon-negative footprint within 50 years. The project highlights White Arkitekter's commitment to carbon neutrality by 2030 and aims to inspire the global adoption of timber as a viable material for sustainable high-rise construction, eliminating concrete from its load-bearing framework to further reduce environmental impact.

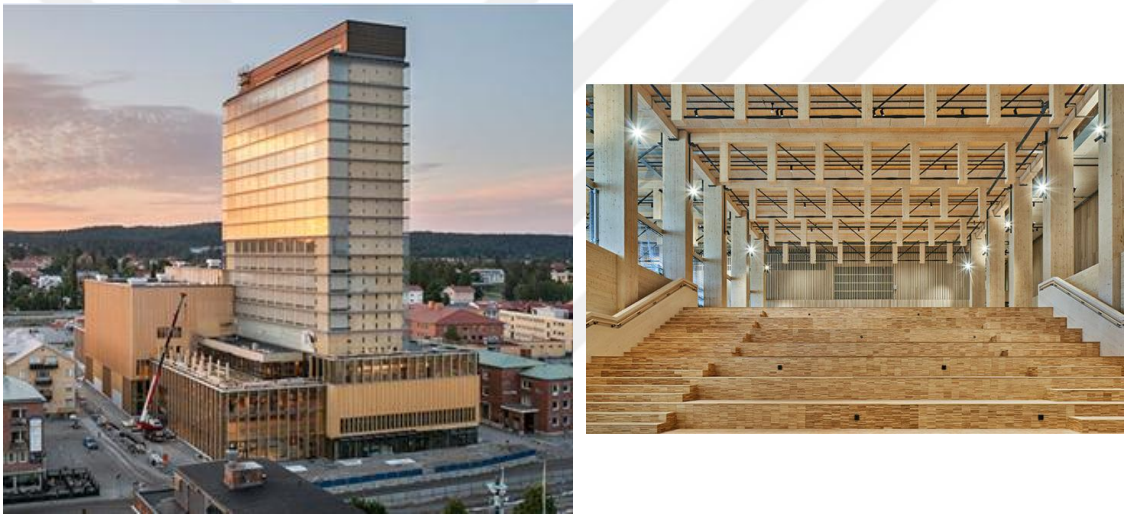


Figure 1.4. Image by patrick degerman (URL-4)

As timber construction gains traction, its aesthetic appeal and renewability become increasingly relevant. Notably, initiatives focused on improving timber's mechanical properties, especially through the integration of (FRPs), demonstrate potential for elevating structural performance. This synergy of traditional materials with modern reinforcement techniques is beneficial.(Vahedian, et al. 2019) Over the last 40 years, quite number of research has been done on the use of FRP composites to reinforce concrete, steel and timber structures. Since the mid-1980s, FRP technology has been used to strengthen the components of these structures. (Yang et al., 2019) (Bedon and Louter, 2017) Furthermore, the growing application of FRPs for reinforcing timber structures illustrates a promising intersection of innovative materials and traditional timber. Despite the benefits, there remain challenges in their widespread adoption, particularly

concerning the long-term implications of synthetic adhesives and the lack of standardized guidelines. (Schober et al., 2015)

Nonetheless, challenges associated with timber, including its vulnerability to pests, moisture, and fire, must be addressed. Nevertheless, advancements in treatment and technology have enhanced its durability and overall performance, alleviating many of these issues. Timber remains an essential and adaptive material in the construction sector, aesthetic appeal, and sustainability to satisfy the evolving demands of modern building practices. (Švajlenka and Kozlovská, 2020)

1.1. Objectives of the Study

This thesis aims to conduct a comprehensive state-of-the-art review on the use of FRPs in timber frame elements. The research seeks to assess the potential benefits of FRPs in improving the mechanical properties of timber components. The focus is on investigating the applications and advantages of FRPs strengthening of various timber structural elements, such as beams and columns. This study will contribute to a deeper understanding of the role of FRPs in the advancement of timber construction technologies.

2. TIMBER AS STRUCTURAL MATERIAL

Timber stands out as one of the oldest and most versatile materials in construction, celebrated for its remarkable strength-to-weight ratio, durability, and aesthetic qualities. Sourced from well-managed forests, timber serves as a sustainable resource that presents numerous environmental benefits compared to alternative building materials. It can be utilized in a variety of structural forms, including beams, columns, trusses, and girders, in addition to applications such as piles, decking, railway sleepers, and concrete formwork. Recent advancements in timber technology, particularly in engineered wood products and lamination techniques, have mitigated the challenges posed by natural defects and variations in log sizes. This progress has facilitated the creation of high-quality, durable timber structures in an array of forms and dimensions. Furthermore, timber's capacity for reshaping, repairing, and modification underscores its reliability for enduring construction projects. However, it is important to note that timber's performance can be significantly influenced by environmental conditions, especially moisture content, which directly impacts its strength, stiffness, and dimensional stability. (Porteous and Kermani, 2007)

In the United States, timber maintains a dominant presence as the primary building material, accounting for over 80% of all residential and commercial structures. Its versatility is reflected in a wide range of applications, spanning from one- to three-story residences to multifamily housing and hotels reaching up to four stories. The lightweight nature of timber, coupled with its ease of assembly and low maintenance requirements, makes it particularly suitable for specialized structures, such as supports for amusement park rides, which must endure repetitive cycles of dynamic loads. Although timber is not often the primary material in high-occupancy commercial or industrial buildings, it frequently serves as a vital secondary structural component, further showcasing its adaptability and reliability in various construction scenarios. (Aghayere and Vigil,, 2007)

A deeper understanding of the anatomy and microscopic structure of timber is crucial for maximizing its application in construction. As a natural, anisotropic material, wood possesses a unique cellular structure made up of cellulose, hemicellulose, lignin, and other components. Wood can be analysed at multiple levels, as shown in Figure 2.1. The mechanical properties of timber exhibit considerable variability depending on factors

such as grain orientation, cell wall arrangement, and the presence of growth anomalies. For example, wood exhibits markedly greater rigidity along the grain compared to across it, and its tensile strength can differ widely based on the material's quality. By investigating both macroscopic and microscopic characteristics, engineers can harness the potential of wood while effectively addressing challenges such as shrinkage, swelling, and variations in fiber alignment. The majority of timber utilized in construction consists of softwoods like spruce and fir, particularly in Europe, while hardwoods offer unique structural benefits in different contexts. (Blaß and Sandhaas, 2017)

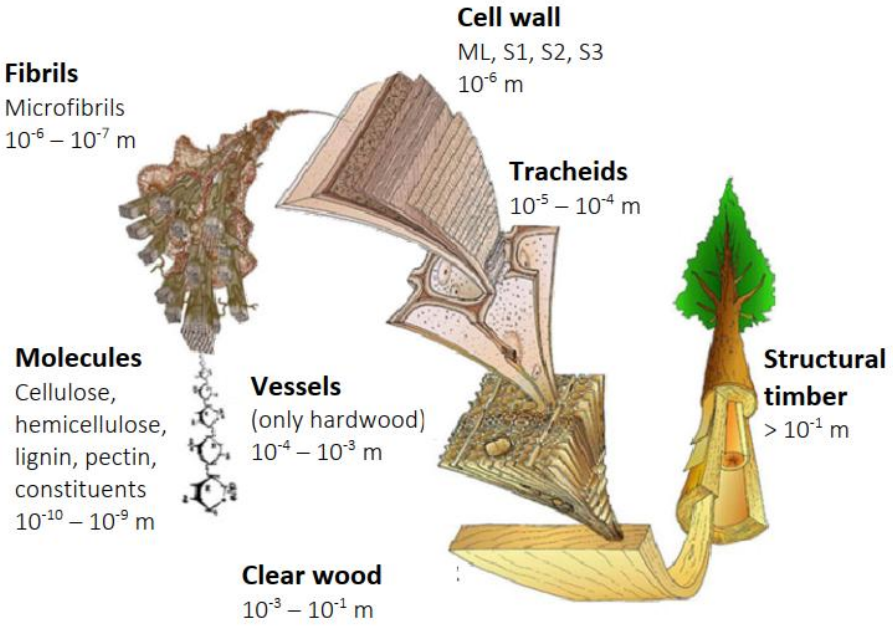


Figure 2.1. Hierarchical levels of wood (Blaß and Sandhaas, 2017)

Structural timber is derived from the trunk of a tree, which provides mechanical strength and support for the tree's crown. The trunk consists of various parts, as illustrated Figure 2.2 including bark, cambium (the growth layer), sapwood (active in transporting nutrients), and heartwood (which primarily offers support). Wood is made up of long tubular cells that are structured in a way to maximize strength, with growth rings indicating the age of the tree, formed from annual growth cycles. Trees in temperate climates develop distinct growth rings, comprising springwood (earlywood) from rapid growth in spring and summerwood (latewood) from slower summer growth. Sapwood is lighter and more susceptible to decay, while heartwood is denser and serves as a structural

support, making both vital for understanding timber properties. (Porteous and Kermani, 2007)

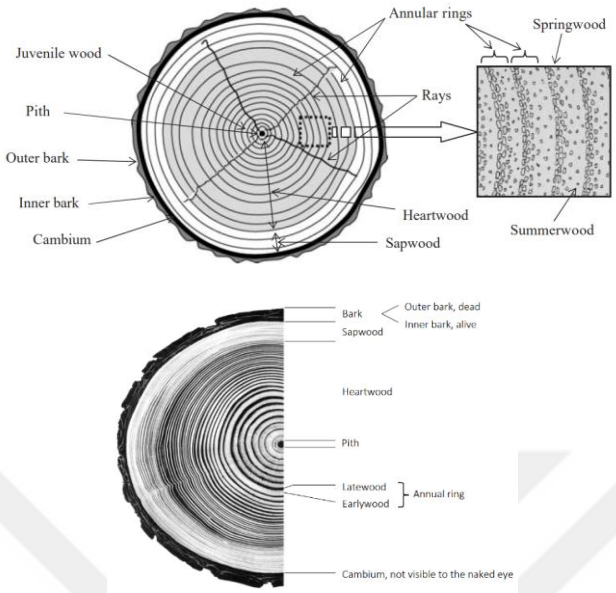


Figure 2.2. Cross-section of tree trunk (Porteous and Kermani, 2007)

2.1. Types of Timber

Commercial timbers and trees are categorized into two primary types: softwoods and hardwoods. This classification is based on the botanical origin of the timber and does not necessarily correspond to the wood's physical properties.

2.1.1. Softwood

Softwood, mainly represented by evergreen conifers, have distinctive structural properties that enhance their functional performance, primarily consisting of tracheids and parenchyma cells, with tracheids being the predominant type. These long, slender cells are organized into systems that extend longitudinally and radially, though most align longitudinally. Ray parenchyma, or rays, play essential roles in food storage and fluid movement, despite making up a smaller portion of the overall wood structure as shown in Figure 2.3 Common softwood species like spruce, larch, Scots pine, and Douglas fir generally share this cellular composition, though exceptions exist, such as yew, which lacks longitudinal parenchyma and resin canals, while fir species exhibit minimal longitudinal parenchyma and no resin canals in normal wood. Softwoods are characterized by rapid growth rates, enabling harvesting as early as 30 years post-

planting, resulting in low-density timber with lower strength and typically poor durability unless treated with preservatives. Due to their quick harvest cycles, softwoods are readily available in the market and are generally more affordable than hardwoods. (Blaß and Sandhaas, 2017; Porteous and Kermani, 2007)

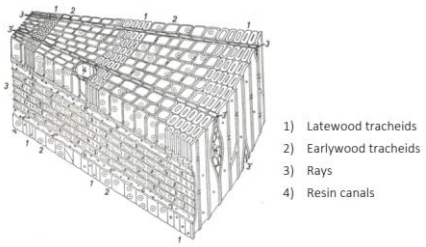


Figure 2.3. Schematic structure of softwood (Blaß and Sandhaas, 2017)

2.1.2. Hardwood

Hardwood has developed more complex structures compared to softwood, featuring a greater variety of cell types and specialized functions. It is characterized by various tracheids, which are dead cells, leading to a focus on fibers rather than tracheids in hardwood terminology. Libriform fibers primarily provide strength, while fiber tracheids have dual roles in both water transport and structural support. While both hardwood and softwood contain parenchyma cells for nutrient storage, hardwood rays can consist of multiple rows of parenchyma cells and are typically more visible as shown in Figure 2.4. (Blaß and Sandhaas, 2017)

Hardwoods generally grow more slowly than softwoods, leading to denser, stronger timber that can take over a century to mature. They also require fewer preservatives for durability and, due to longer growth periods and higher transportation costs especially for tropical varieties are typically more expensive than softwoods. (Porteous and Kermani, 2007)

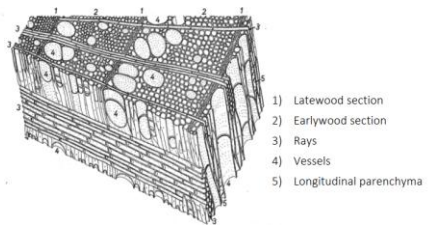


Figure 2.4. Schematic structure of hardwood (Blaß and Sandhaas, 2017)

2.2. Natural Characteristics of Wood

Several properties of wood may be regarded as defects in the context of engineering applications. Below, some of these characteristics is outlined.

2.2.1. Knots

Trees rely on leaves or needles for essential processes such as transpiration, respiration, and photosynthesis, necessitating an extensive leaf area that is distributed across branches. Annually, trees experience vertical growth at their tops while simultaneously developing new lateral branches. Over time, these branches become integrated into the trunk through the deposition of additional material on the outer surfaces of both the trunk and branches. The composition of branch wood mirrors that of the main stem, with interconnected tissue systems. A longitudinal examination of a knot reveals distorted fiber orientation, as fibers bend around the knot, which adversely impacts the mechanical properties of sawn timber. When timber is cut, fibers surrounding the knot become discontinuous, affecting its strength, especially in the primary fiber direction see Figure 2.5. The characteristics of knots such as size, shape, number, and location significantly determine the structural integrity of sawn timber, with timber containing fewer and smaller knots generally graded into higher quality classifications. (Swedish Wood, 2015)



Figure 2.5. A knot observed from every angle of a wood piece (Swedish Wood, 2015)

2.2.2. Splits or Checks in Wood

Separation of wood fibers at an angle to the growth rings, typically due to the drying process.(Aghayere and Vigil, 2007)

2.2.3. Shake Defect

Separation of wood fibers parallel to the growth rings. (Aghayere and Vigil, 2007)

2.2.4. Decay

Deterioration of wood caused by wood-destroying fungi. (Aghayere and Vigil, 2007)

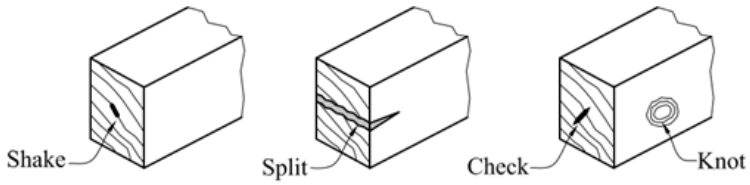


Figure 2.6. Common defects in wood (Aghayere and Vigil, 2007)

2.3. Physical and Mechanical Properties of Wood

Understanding the strength of wood necessitates a thorough examination of its physical and mechanical properties. Physical properties refer to the measurable characteristics of wood and its reactions to external influences, while mechanical properties describe how wood responds under applied forces. To ensure accurate testing results, assessments of wood properties are typically conducted using clear, straight-grained samples to minimize the impact of defects. Additionally, the orthotropic nature of wood, combined with variable growth conditions, can result in differing properties among samples from the same species depending on their geographic origin. For instance, a white birch sample collected from Thunder Bay, Ontario, may exhibit distinct physical and mechanical characteristics compared to one from Toronto, Ontario. This variation also holds true for trees sourced from nearby locations that experienced differing environmental conditions, such as moisture levels in the soil. (McKay, 2021)

2.3.1. Physical Properties

The physical characteristics of wood encompass directional properties, moisture levels, dimensional stability, thermal expansion, pyrolysis behavior and specific gravity, electrical conductivity, resistance to decay, and chemical resilience. These physical attributes play a crucial role in influencing the strength properties of wood, particularly in structural applications. (Ali, 2011)

2.3.2. Directional Properties

The directional characteristics of wood are crucial due to its orthotropic and anisotropic nature, which distinguishes it from materials such as metals. Consequently, the physical properties of wood vary when assessed along its three principal axes. It is crucial to recognize that wood properties vary across different axes; however, the most significant differences are observed between the tangential and radial axes. This variation in dimensional strength is directly linked to the cellular arrangement within the wood. The cells are structured such that their long axes run parallel to the grain. In this configuration, there is minimal alteration in response to changes in moisture content along the longitudinal axis, while substantial changes occur in the lateral axis.(Ali, 2011; Yang et al., 2019)

2.3.3. Moisture Content

In structural applications, the moisture content of wood serves as a crucial indicator, as it directly influences the material's mechanical properties. Moisture content, defined as the weight of water in wood and expressed as a percentage, can be calculated using the formula MC = (wet weight - dry weight) / dry weight × 100%. Within trees, sapwood typically exhibits a higher moisture content than heartwood, with green wood moisture levels varying significantly across species, ranging from 30% to 200%. Water exists in wood either as free water in cell cavities or as bound water within cell walls. The term "fiber saturation point" refers to the state where all free water has been removed, leaving only a minimal amount of moisture in the cell walls. Wood is hygroscopic, meaning it can absorb and release moisture depending on environmental humidity levels. Moisture can enter wood through cell lumens as fluid or vapor, as well as via diffusion through cell walls. Given that fluctuations in moisture content can affect the strength properties of wood, it is essential to maintain stable moisture levels in structural lumber. To enhance durability and weather resistance, various sealants and treatments have been developed to reduce moisture absorption in wood products. (Ali, 2011; Leblon et al., 2013) see Figure 2.7 illustrated General relationship between strength and/or stiffness and moisture content.

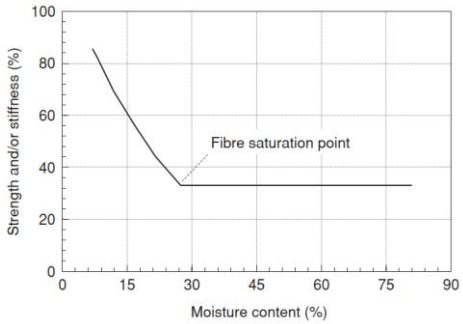


Figure 2.7. Overall correlation between moisture content and strength and/or stiffness (Porteous and Kermani, 2007)

2.3.4. Shrinkage and Swelling

The interaction between water and microfibrils in the cell wall of wood is crucial for its dimensional stability, as changes in moisture content cause microfibrils to move closer together, resulting in wood shrinkage. The S2 layer, which predominantly contains microfibrils oriented at a slight angle to the longitudinal axis, influences how wood behaves during shrinkage and swelling, with most shrinkage occurring in the transverse directions. Juvenile wood and compression wood, characterized by larger microfibril angles, experience more significant longitudinal shrinkage see Figure 2.9. Strain values indicate that a 1% change in moisture content results in longitudinal shrinkage of 0.0001, radial shrinkage of 0.0015, and tangential shrinkage of 0.0030, with tangential shrinkage being approximately twice that of radial shrinkage due to structural differences see Figure 2.8. Although longitudinal shrinkage is minimal, it can be significant over larger lengths, and the presence of compression wood or juvenile wood can increase this shrinkage dramatically, potentially making it up to a hundred times greater than in normal wood. (Swedish Wood, 2015)

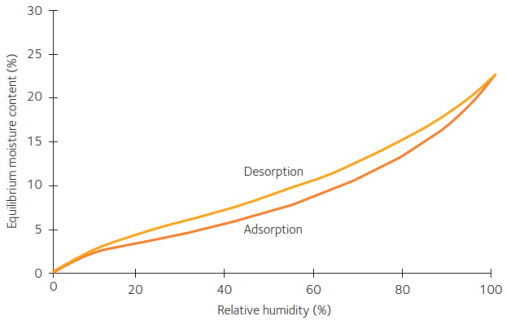


Figure 2.8. Relative humidity and the moisture content at equilibrium (Swedish, 2015)

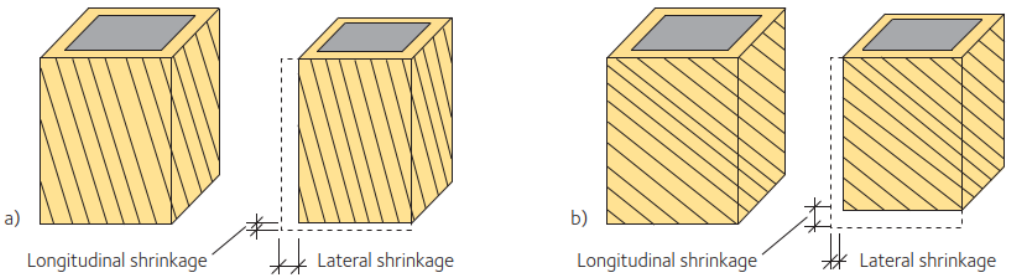


Figure 2.9. Diagrammatic representation of the arrangement of microfibrils and shrinkage in both compressed and normal wood (Swedish Wood, 2015)

2.3.5. Distortion of Timber

Variations in wood shrinkage can lead to geometric distortions in its cross-section, complicating its use, with four main forms of distortion identified: twist, spring, cup, and bow shown in Figure 2.10. Twist and spring create the most significant issues for construction timber, while moderate bow is usually acceptable, and cup primarily leads to material loss during planning. Twist arises from the interplay of annual ring orientation, spiral grain angle, and differential shrinkage, while cup distortion is mainly due to variations in radial and tangential shrinkage. Bow and spring result from differing longitudinal shrinkage and the release of growth stresses when a tree is milled. The extent of these distortions can be mitigated through optimal sawing techniques, careful drying processes, and the application of weights during drying, as well as by paying attention to the spiral grain angle of the wood. (Swedish Wood, 2015)

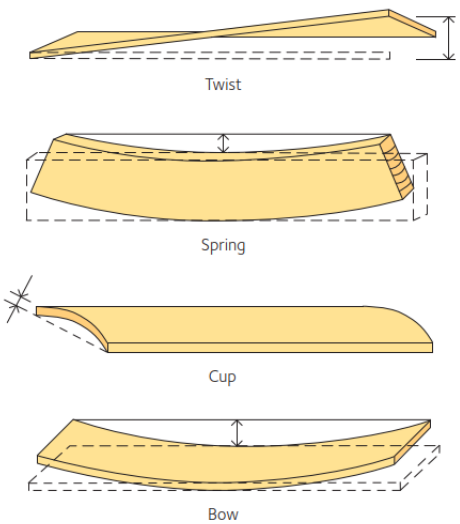


Figure 2.10. Definition of distortion/warp modes (Swedish, 2015)

2.4. Mechanical Properties

The mechanical properties of wood are evaluated through various stress and strain measurements. To ensure consistency and comparability in testing, wood samples must be free from defects and possess a straight grain structure. Such carefully selected samples allow for an accurate reflection of the inherent properties of each wood species without the adverse effects of any deformities.

The assessment of strength properties aims to determine the maximum load or capacity that a wood sample can endure. A variety of characteristics are examined, including as density, hardness, modulus of elasticity, shear modulus, modulus of rupture, and compression parallel to the grain. (Ali, 2011)

2.4.1. Modulus of Elasticity (MOE)

The modulus of elasticity (MOE) quantifies the extent to which a wood sample can bend under low stress and subsequently return to its original shape. While MOE can be assessed along all three axes, it is predominantly measured in the direction perpendicular to the grain (Ali, 2011). Accurate MOE measurements are crucial for applications such as floor joists, which must be capable of bending under load and returning to their initial form without incurring any defects. (Ali, 2011; Arriaga et al., 2023)

2.4.2. Shear Modulus

The shear modulus quantifies a material's resistance to deformation under applied shear stresses. When a load is exerted along the longitudinal axis of a wooden specimen, it may induce a slippage of the cellular structure within the wood, leading to deformation. The shear modulus can be evaluated through three different moduli: τ_{LR}, τ_{LT}, and τ_{RT}. τ_{LR} represents the shear modulus associated with shear strain in the longitudinal-radial (LR) plane, as well as the shear stresses occurring in the longitudinal-transverse (LT) and radial-transverse (RT) planes respectively. (Ali, 2011; Woodall et al., 2024)

The shear strength of timber is highest along the fiber direction, ranging from 5 to 8 MPa, while the shear strength perpendicular to the fiber direction, known as rolling shear (τ_{RT}), typically falls between 3 and 4 MPa—approximately half of the parallel strength. In

timber structures, shear forces in the τ_{LR} and τ_{LT} directions are most prevalent, with the τ_{LT} direction exhibiting lower sheasr strength due to failures occurring primarily through the weaker early wood layers as shown in Figure 2.12. Rolling shear failure occurs when the tubular-shaped fibers roll against one another rather than being severed longitudinally. (Swedish Wood, 2015) Figure 2.11 show Relationship between the failure strength and the angle of the shear.

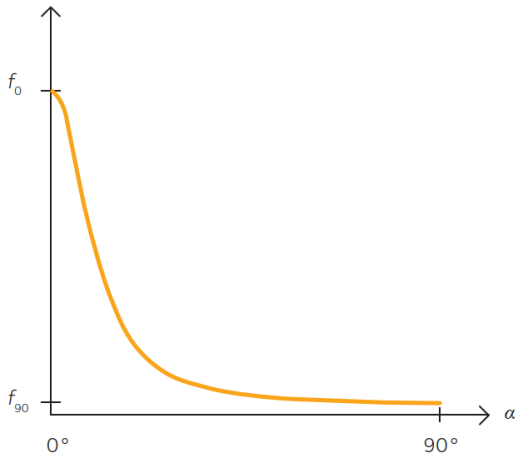


Figure 2.11. The relation between the ultimate strength of failure (Swedish, 2015)

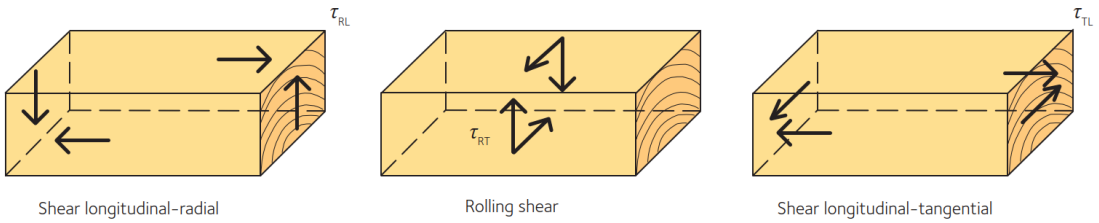


Figure 2.12. Shear in different directions (Swedish, 2015)

2.4.3. Modulus of Rupture (MOR)

The Modulus of Rupture (MOR) represents the maximum stress that a wood sample can withstand before failure. Testing for MOR is conducted similarly to testing for the Modulus of Elasticity (MOE) and is considered a direct measure of strength. According to the Forest Products Laboratory (2010), MOR is not classified as a true stress due to the specific formula employed in its determination. While the MOR value from a single test may not offer significant insights, comparing MOR values across different species can facilitate meaningful comparisons. This comparative analysis proves particularly

valuable for structural engineers in selecting appropriate wood species for construction projects. (Ali, 2011; Woodall et al., 2024; Leblon et al., 2013)

2.4.4. Hardness

Wood hardness is characterized by its resistance to denting, a crucial factor when selecting appropriate species for applications such as flooring and the construction of bowling alley lanes. The determination of hardness is commonly conducted through tests such as the Janka Ball Test or the Brinell Hardness Test, which assess the force needed to embed a metal sphere with a diameter of 11.28 mm to a depth equivalent to half its diameter. (Ali, 2011; Woodall et al., 2024)

2.4.5. Density

Wood density is influenced by a variety of factors, including wood type, environmental conditions, humidity, age, light exposure, and growth rates. Typically, older trees and those growing in competitive environments exhibit higher density. Variations in density can occur not only between species but also within individual trees, affected by soil fertility and light competition. wood density generally decreases from the center of the trunk outward, indicating that newer growth is less dense. Denser wood is often more resistant to environmental stresses, such as wind, which can affect growth rates and mortality. Accurate measurement of wood density is crucial, as it can vary with moisture content and the method of volume determination. Common measurement techniques include apparent density, green density, and basic density, each providing unique insights into wood properties. Drying conditions also significantly impact density readings; for example, drying wood at 80°C typically results in higher density measurements compared to 103°C due to the loss of chemically bound water and organic compounds at elevated temperatures. Additionally, hollows within trees can distort density measurements, potentially leading to overestimations if not adequately addressed. Understanding wood density is essential for grasping tree physiology and forest dynamics, highlighting the importance of carefully selecting measurement methods to ensure accurate and reliable data. Wood density is a critical factor affecting wood strength, stiffness, and market value, defined as the mass of wood per unit volume at a specific moisture content, typically expressed in kg/m3. To determine density, a wood sample is weighed at 12% moisture

following ASTM standards, and its volume is measured using the water displacement method. The formula D = M/V (where D is density, M is mass, and V is volume) is utilized for calculations. Density can be assessed at various moisture levels, including oven dry, 12%, fiber saturation point (FSP), and green. When wood is oven-dried, the cell wall material has a consistent density of about 1.5 grams per cubic centimetre, with minimal variation across species. However, as moisture is introduced, density changes for each species due to the filling of cell wall micro-cavities with water. Increased moisture content leads to alterations in strength properties, with the FSP varying among species but generally ranging from 25-30% moisture content. Higher moisture absorption results in decreased modulus of elasticity (MOE), modulus of rupture (MOR), and compression parallel to the grain, underscoring the importance of measuring these values when using wood as a construction material. (Ali, 2011; Woodall et al., 2024; Nogueira et al., 2005; Alfred, 2002) Figure 2.13 illustrate the relationship between the influence parameters of density.

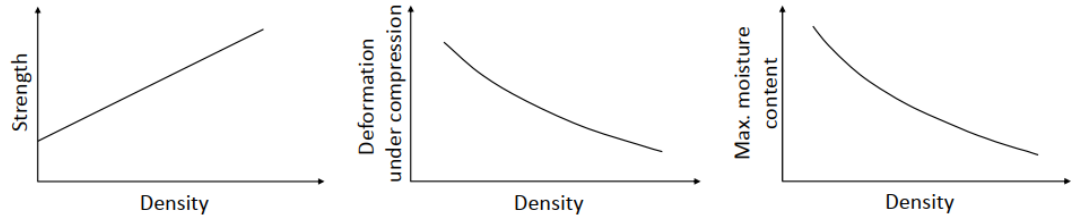


Figure 2.13. Schematic illustration of the influence of density (Blaß and Sandhaas, 2017)

2.5. Wood Products:

Timber has historically been one of the most prevalent materials employed in construction, attributed to its availability, adaptability, and user-friendliness. It has been integral in the development of various architectural styles, ranging from traditional log homes to renowned timber bridges, influencing building practices across diverse cultures. Timber has seen a revival in popularity in modern construction in recent years, primarily due to rising demand for environmentally friendly and sustainable building materials. The Engineered Timber also known as mass timber or composite timber, represents a significant advancement in timber construction. It encompasses a range of products manufactured by binding together wood strands, veneers, lumber, or other forms of wood

fibers. This process, often involving adhesives, heat, and pressure, results in products with enhanced structural properties and dimensional stability compared to traditional sawn timber.

2.5.1. Solid Timber

Sawn timber is produced through the longitudinal sawing of logs and encompasses various products from sawmills, categorized primarily by their cross-sectional dimensions into boards, planks, battens, and square timbers see Figure 2.14. Different sawing technologies, such as frame saws and band saws, optimize yields and manage industrial residual wood. Post-cutting, the timber undergoes visual pre-grading before being dried, either in kilns or naturally, although smaller sawmills may struggle with moisture control. Once dried to the appropriate moisture content, the timber is graded and assigned a strength class, accounting for potential shrinkage during drying. The processing of sawn timber may include finishing techniques, with rough-sawn structural timber and glued solid timber options available.(Blaß and Sandhaas, 2017)



Figure 2.14. Squared wood with knots, drying cracks, and pith (Blaß and Sandhaas, 2017)

2.5.2. Glulam

Glued laminated timber (glulam) is the earliest types of engineered wood products. The initial patent for a glue lamination technique involving sawn boards was granted to Otto Hetzer in 1906. Among engineered wood options, glulam distinguishes itself by delivering superior structural performance while retaining the ecological advantages of wood.



Figure 2.15. Glued laminated timber (Blaß and Sandhaas, 2017)

Glulam is manufactured by bonding together layers of dimensioned timber with durable (at least four) laminations (finger jointed sawn boards), moisture-resistant adhesives (Figure 2.15). This process allows for the creation of large, strong, and dimensionally stable structural elements, such as beams and columns compared to solid wood of similar dimensions. This manufacturing process permits the production of glulam beams and columns in varied shapes and sizes, facilitating architectural creativity in timber construction. The use of glulam is becoming increasingly prevalent in both residential and commercial sectors, particularly in the design of long-span structures such as bridges, beams, columns, and arches. Beyond their structural and aesthetic benefits, glulam components also provide environmental advantages, as wood captures and stores carbon

over its lifespan. With a rising focus on sustainable building methodologies, glulam structures are being more widely incorporated into low-rise buildings, multi-story developments, and even certain high-rise projects, thereby contributing to a reduced environmental impact.(Chrisp et al., 2003; Swedish Wood, 2015)

Production Process of Glulam:

The production process of glulam involves several key steps, which can be summarized as follows and shown in Figure 2.16:

1. Timber Selection: Choose suitable timber species, typically from fast-growing trees, ensuring they meet quality standards for strength and durability.
2. Drying: The selected timber is dried in a kiln to reduce moisture content, which helps prevent warping and ensures proper adhesive bonding.
3. Grading: Machine graders are used to assess dried timber pieces for strength, identifying and marking any flaws that could impact their structural performance.
4. Cutting: Areas with localized strength-reducing defects are cut off, and the remaining pieces are cut to the required lengths using a cross-cut saw.
5. Finger-Jointing: Shorter pieces of timber are joined together using finger joints to create longer lengths, which are essential for producing continuous glulam beams.
6. Adhesive Application: Adhesive is uniformly spread on the flat surfaces of the timber pieces that will be bonded together.
7. Lamination: The glued timber pieces are stacked and pressed together, allowing the adhesive to cure and bond the layers into a single structural unit.
8. Curing: The laminated timber is left to cure under pressure for a specified period to ensure a strong bond between the layers.
9. Planning and Finishing: After curing, the glulam is planned to remove any excess adhesive and to achieve the desired dimensions and surface finish.
10. Quality Inspections: The completed product is subjected to quality inspections to verify that it complies with the necessary standards for durability and performance prior to being dispatched for construction use. (Ong, 2015)

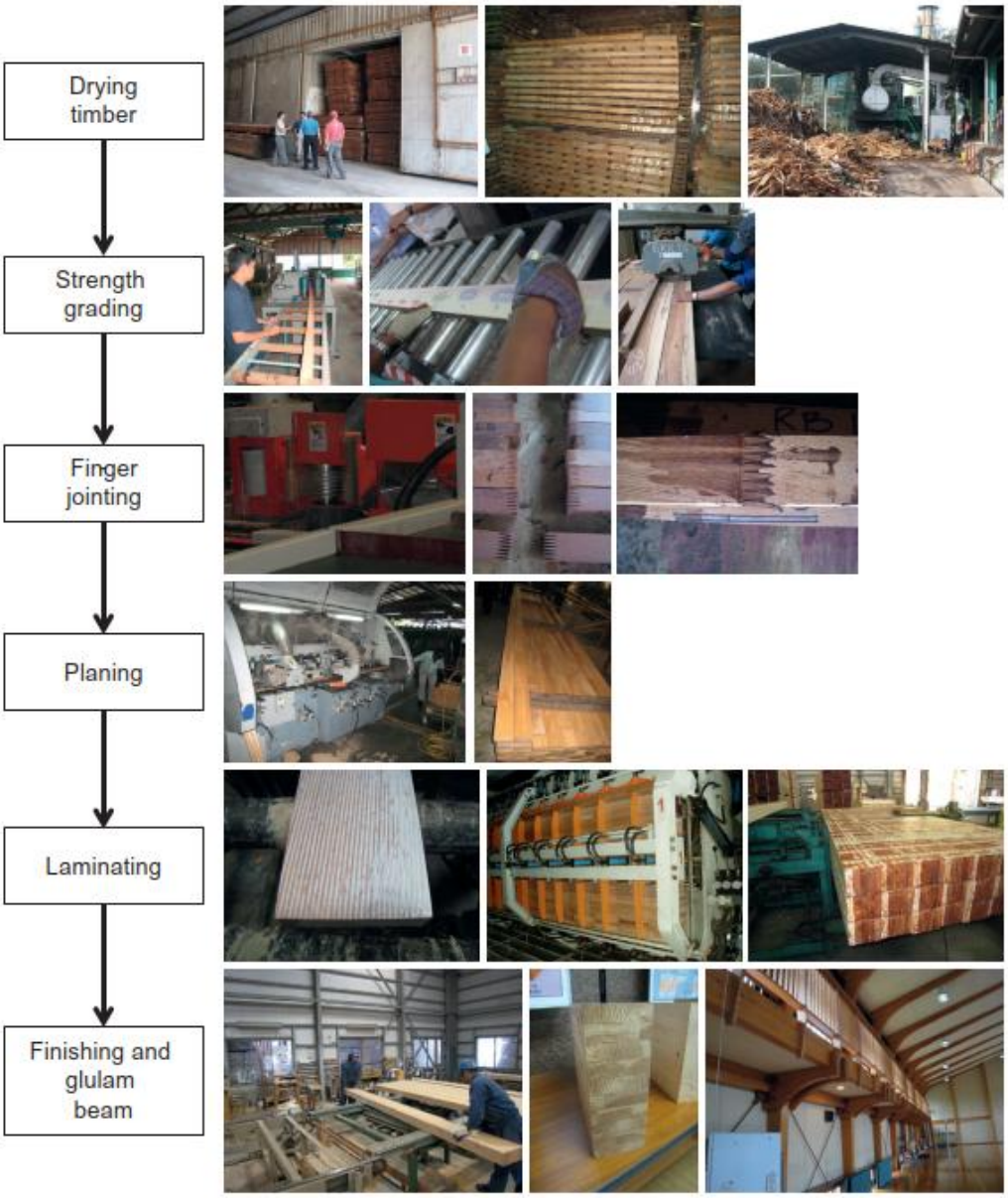


Figure 2.16. Typical stages of glulam production (Ong, 2015)

This systematic approach ensures that glulam is produced efficiently and meets the necessary structural requirements for various applications.

Advantages of Glulam:

Strength-to-Weight Ratio and Large Span Capabilities: Glulam is manufactured by gluing individual pieces of lumber together to form large-dimension beams. This gluing method enhances the structural strength of the material while maintaining its lightweight

properties, making it a suitable choice for large-span applications such as bridges and residential buildings. (Manninen, 2014)

Versatility in Design: Glulam can be manufactured in various sizes and complex shapes, allowing architects and engineers to create aesthetically pleasing structures, such as arches and large spans. (Chai et al., 2021)

Sustainability: Made from renewable timber resources, glulam is an environmentally friendly option. It can utilize smaller pieces of timber from fast-growing trees, promoting sustainable forestry practices. (Xu et al., 2024)

Disadvantages of Glulam:

Cost: The production of glulam can be more expensive than traditional timber due to the manufacturing processes involved, including drying, grading, and adhesive application. (Manninen, 2014)

Potential for Adhesive Failure: The performance of glulam is dependent on the quality of the adhesive used. Poor adhesive bonding can lead to structural failures. (Alam et al., 2009)

In summary, while glulam offers numerous advantages in terms of strength, design flexibility, and sustainability, it also presents challenges related to cost, moisture susceptibility, and manufacturing complexity.

2.5.3. Cross-Laminated Timber

CLT consists of layers of wood arranged in a crosswise pattern and glued together. as illustrate in Figure 2.17. This cross-lamination technique results in panels with strength, stiffness, and dimensional stability in both directions. (Raquel, 2019)

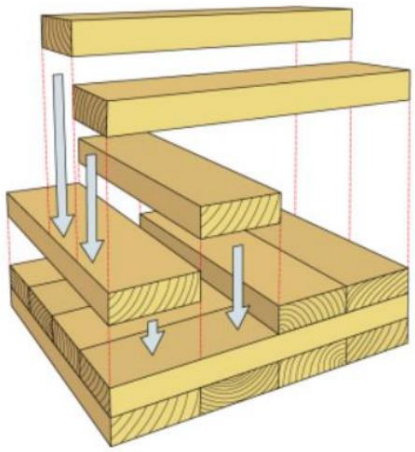


Figure 2.17. Cross-laminated timber layup (Raquel, 2019)

Production Process of CLT:

The production procedure for Cross Laminated Timber (CLT). involves several key steps to ensure the quality and performance of the final product. Here's an overview of the typical process(Mohammad et al., 2011):

Lumber Selection: High-quality lumber is selected based on specific criteria to ensure it meets the required standards for strength and durability.

Lumber Grouping and Planning: The selected lumber is grouped according to size and quality and then planned to achieve uniform thickness.

Adhesive Application: Adhesives are applied to the wide faces of the lumber boards in North America, adhesives utilized must adhere to the same standards as those employed in the production of glued-laminated timber, which encompasses approved polyurethane, melamine, and phenolic-based adhesives.

Panel Lay-Up: The lumber boards are stacked in layers, typically with each layer oriented at 90 degrees to the adjacent layers. This crosswise arrangement enhances the structural properties of the panel.

Pressing: Vacuum or hydraulic presses are used to press all of the layers together, depending on the panel thickness and adhesive used. This step ensures a strong bond between the layers.

Product Cutting: After the adhesive dries, the panels will be cut to size. Additionally, windows, doors, and service channels are constructed during this phase, frequently with the aid of Computer Numerically Controlled (CNC) routers for accuracy.

Marking and Packaging: Finally, the finished panels are marked for identification and packaged for transportation to the construction site.

Quality control: measures are implemented throughout the process to ensure that the final CLT products meet the necessary performance standards, such as bending strength and shear strength.

Advantages of CLT:

Dimensional Stability: The cross-laminating process enhances the dimensional stability of the panels, reducing the risk of warping and cracking, which is common in solid wood products.

Strength and Stiffness: CLT panels exhibit high in-plane and out-of-plane strength and stiffness, allowing them to perform well under various loads. This two-way action capability is similar to that of reinforced concrete slabs.

Rapid Construction: The prefabrication of CLT panels allows for quick assembly on-site, leading to faster construction times and reduced labor costs. This is particularly beneficial for mid-rise buildings.

Good Insulation Properties: CLT provides excellent thermal and sound insulation, contributing to energy efficiency and occupant comfort.(Mohammad et al., 2011)

Disadvantages of CLT:

Cost: While CLT can be cost-competitive, the initial investment may be higher than traditional materials, particularly in regions where CLT is not yet widely produced or available.

Limited Availability: In some areas, the availability of CLT may be limited, which can affect project timelines and costs. The market for CLT is still developing in North America compared to Europe.

Building Codes and Standards: The implementation of CLT in construction is still evolving, and there may be challenges related to building codes and standards that can complicate its use.

Moisture Sensitivity: Although CLT is engineered for stability, it can still be sensitive to moisture. Proper design and detailing are necessary to prevent moisture-related issues, such as mold or decay.

Connection Systems: Designing effective connection systems for CLT can be more complex than for traditional materials, requiring specialized knowledge and experience.

Fire Safety Concerns: While CLT has good fire resistance, there may still be concerns about its performance in high-rise buildings, necessitating careful design and engineering.

Overall, while CLT offers numerous benefits, it is essential to consider these disadvantages in the context of specific projects and local conditions.

2.5.4. Laminated Veneer Lumber (LVL)

LVL is produced by bonding multiple layers of wood veneer using an exterior-grade adhesive. see Figure 2.18. It is known for its high strength, dimensional stability, and uniformity. LVL is commonly used as beams, headers, and flanges for wood I-beams, as well as scaffolding planks. It is available in various thicknesses (19.1–89 mm), depths (63.5–1219 mm), and lengths (up to 24 m). (Lam, 2001; Chrisp et al., 2003)



Figure 2.18. Laminated Veneer Lumber (Weyerhaeuser, 2024)

The Production Process of LVL:

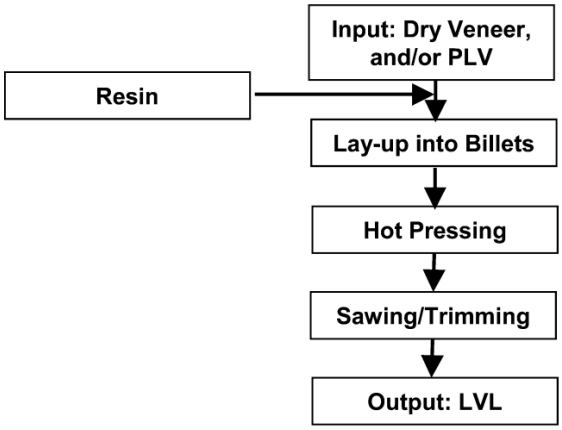


Figure 2.19. LVL production includes multiple steps, and if green veneer is used, it undergoes drying before resin application (Weyerhaeuser, 2024)

Lay-up of Billets: Dried veneers, generally at approximately 5% moisture content, are arranged with their grains aligned. They are then coated with phenol-formaldehyde resin and put together into billets for pressing. Waste veneer is generated as a co-product during this stage. In the case of Parallel Laminated Veneer (PLV), a comparable process is used, but the panels are finger-jointed and laminated to form the billets.

Pressing: The gathered LVL billets undergo heat and pressure treatment, reaching temperatures around 170°C and a pressure of 1.72 MPa (approximately 340°F and 250 lb/in^2). This process solidifies the resin, fusing the veneers to create LVL. Importantly, this step does not produce any by-products or waste.

Sawing/Trimming: The billets are sawed to the appropriate length and width after pressing. In addition to the final LVL product, this phase produces co-products such panel trim and sawdust.

Different manufacturing plants may employ various types of lay-up lines and pressing systems, with some utilizing automated processes for resin application and veneer alignment before pressing. (Wilson and Dancer, 2005)

Advantages and Disadvantages of Veneer Lumber:

Veneer lumber, particularly types like Laminated Veneer Lumber (LVL) offers significant advantages such as a high strength-to-weight ratio, uniform mechanical properties, and efficient use of smaller wood pieces, making it ideal for structural applications like beams and headers. (Grabner et al., 2016). Additionally, it offers enhanced strength and stability, significantly reducing the risks of warping, twisting, or shrinking when compared to solid wood. The manufacturing process ensures uniformity, which results in consistent quality and precise dimensions, thereby enhancing design flexibility. LVL also supports resource efficiency by using thin layers of veneer from smaller or lower-quality trees, thus minimizing waste. (Wilson and Dancer, 2005)

However, it also has disadvantages, including susceptibility to moisture-related issues like swelling and warping, which can compromise its integrity if not properly managed. Additionally, the reliance on adhesives raises concerns about long-term durability and environmental impact. Overall, while veneer lumber represents a modern and efficient alternative to traditional solid sawn timber, careful consideration of its limitations is essential for successful application in construction. (Grabner et al., 2016) Another notable disadvantage of veneer lumber is its cost, which is frequently higher than that of traditional solid wood due to the complex manufacturing processes involved. Additionally, there are aesthetic limitations, as laminated veneer lumber (LVL) generally does not possess the visual warmth and character of solid wood, making it less ideal for projects that prioritize appearance. Furthermore, despite being engineered to enhance dimensional stability, LVL remains sensitive to moisture, and inadequate protection can lead to delamination issues. This highlights the need for careful consideration of veneer lumber's limitations alongside its benefits for effective use in construction. (Wilson and Dancer, 2005)

2.5.5. Plywood

Plywood is a flat engineered wood product made by bonding multiple layers of thin veneer, known as plies, under pressure as seen in Figure 2.20. The manufacturing process begins with debarking and steaming logs before they are rotary-peeled into veneers typically ranging from 2 to 4 mm in thickness. These veneers are then kiln-dried, glued, and assembled with alternating grain directions in an odd number of layers, ensuring strength and stability. There are several types of plywood produced globally, including

American, Canadian, Finnish, and Swedish varieties, with specific structural plywood grades used in the UK. Sheet dimensions generally measure 1200 mm × 2400 mm or 1220 mm × 2440 mm, with face veneers oriented according to regional standards. Plywood's structural integrity is influenced by factors such as ply count, thickness, wood species, and stress direction, which are critical for its application in construction, whether subjected to bending in-plane or perpendicular to the panel. (Porteous and Kermani, 2007)

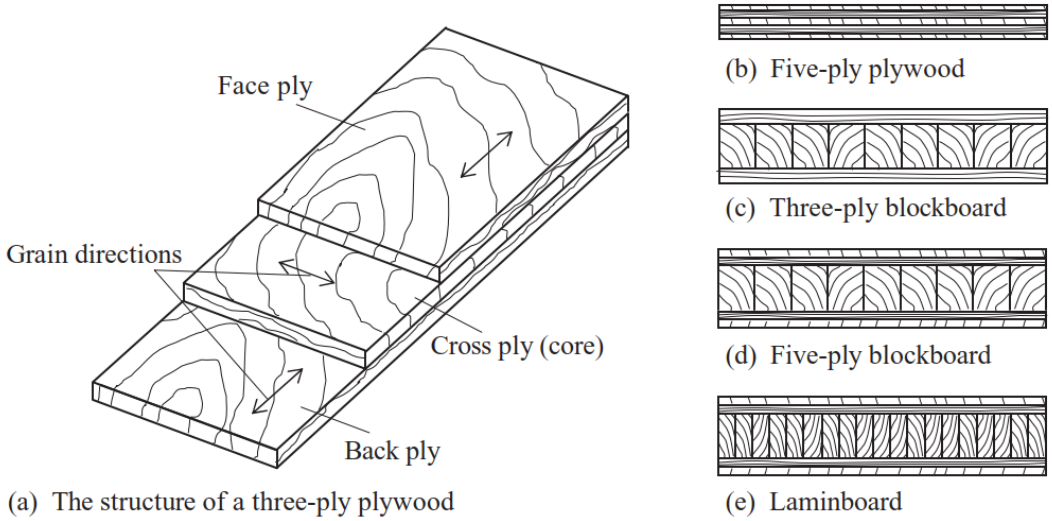


Figure 2.20. Examples of plywood and wood core plywood (Porteous and Kermani, 2007)

2.5.6. Oriented Strand Board (OSB)

Oriented Strand Board (OSB) is an engineered structural panel made from small wood pieces like strands, flakes, or wafers from small-diameter logs, which are combined with an exterior-grade adhesive consisting of 95% wood and 5% resin and wax, then subjected to heat and pressure see Figure 2.21. Its construction features surface layers with strands aligned along the panel's long direction and inner layers with strands arranged randomly, creating a multi-layer design that enhances strength through cross-orientation. The use of water-resistant and boil-proof adhesives adds to the durability, rigidity, and moisture resistance of the panels. Its advantages over plywood, such as cost-effectiveness, environmental sustainability, and dimensional stability, make it a popular choice for various applications. OSB is available in multiple thicknesses ranging from 8 to 25 mm and can be manufactured in sizes up to 2.4 m wide by 4.8 m long, making it suitable for

uses such as wall sheathing, roof cladding, floor decking and composite construction system like Structural Insulated Panels (SIPs).



Figure 2.21. Oriented Strand Board (URL-5)

2.5.7. Laminated Strand Lumber (LSL)

LSL is made from long strands of wood that are oriented and bonded together. It is designed to provide a strong and stable product, suitable for various structural applications see (figure 2-22). The manufacturing process involves drying, resinating, and pressing the strands to form solid panels(Lam, 2001).



Figure 2.22. Laminated Strand Lumber (Weyerhaeuser, 2024)

The Production Process of LSL:

The manufacturing process for LSL (laminated strand lumber) is characterized by a high level of automation, strict process control, and a relatively linear workflow, as depicted in Figure 2.23. The primary stages in the process include the storage of logs, a log pond, debarking, stranding, drying, screening, blending, forming, hot (steam) pressing, cutting,

trimming, sanding, and packaging. Once the logs arrive at the mill, the production of LSL commences with the debarking of the whole logs after they have been softened in a heated log pond. Following this, the logs are processed using the rotating knives of a stranding machine to create strands, which are subsequently screened, dried, and screened again to prepare for the bonding phase. In the bonding process, a waterproof adhesive is sprayed onto the strands while they are in a rotating drum. The resulting strand–resin–adhesive mat is then cured through the application of steam and pressure. Finally, the LSL panels are cut to specified dimensions and treated with a protective edge seal before being packaged and shipped. (Sahoo et al., 2021)

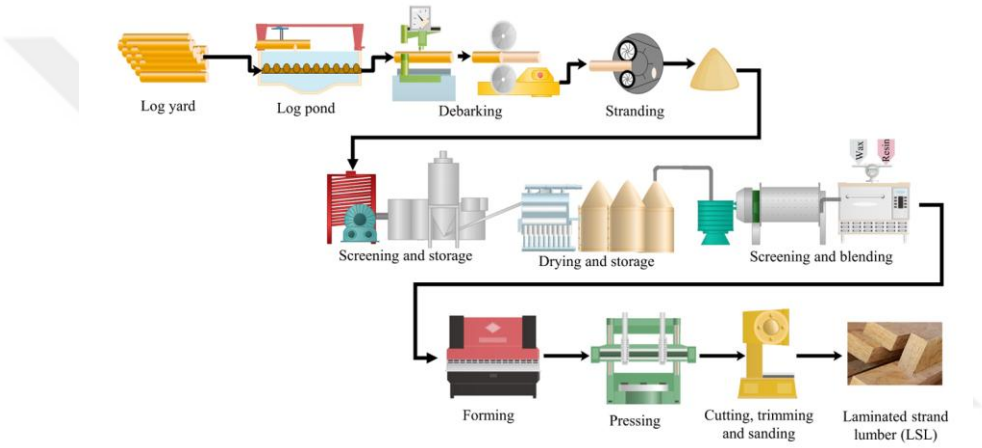


Figure 2.23. Flowchart illustrating the manufacturing procedure for laminated strand lumber (Sahoo et al., 2021)

Advantages of LSL:

1. Carbon Sequestration: LSL stores 1,150 kg CO2eq per cubic meter, significantly more than the 275 kg CO2eq emitted during its production. This makes it a net carbon sink.
2. Use of Low-Quality Wood: It utilizes smaller-diameter and lower-quality hardwood logs, promoting resource efficiency.
3. High Strength-to-Weight Ratio: LSL offers robust structural capabilities while being lightweight, making it versatile for headers, beams, roof rafters, and trusses.
4. Renewable Resource: Manufactured primarily from renewable hardwood species, it supports sustainable forestry practices.

5. Energy Recovery: Mill residues, such as bark and wood waste, are utilized for on-site energy production, reducing waste. (Sahoo et al., 2021)

Disadvantages of LSL

1. High Resin Emissions: Resin production contributes significantly to environmental impacts, accounting for 45% of greenhouse gas emissions.
2. Energy-Intensive Manufacturing: The production process consumes substantial energy, particularly from nonrenewable sources, which account for 56% of total energy use.
3. Limited Regional Manufacturing: Currently, only two mills in North America produce LSL, which could limit accessibility and increase transportation-related emissions.
4. Chemical Emissions: The manufacturing process releases hazardous air pollutants (HAPs), including volatile organic compounds (VOCs), which may pose environmental risks. (Sahoo et al., 2021)

2.5.8. Parallel Strand Lumber (PSL)

PSL is produced using strands of veneer that are clipped into smaller pieces and then glued together with adhesives as seen in Figure 2.24. This type of lumber is particularly useful for applications requiring high strength and stability. The production process allows for the use of veneers that may not be suitable for other products, thus maximizing material efficiency. (Lam, 2001)



Figure 2.24. Parallel Strand Lumber (Weyerhaeuser, 2024)

The Production Process of PSL:

1. Veneer Cutting: The production of veneer sheets employs rotary cutting techniques, which are subsequently segmented into narrower strips measuring approximately 25 mm in width. To ensure the structural integrity of the final product, any defective strips are systematically sorted out.
2. Drying and Preparation: Following cutting, the veneer strips undergo a drying process and are prepared for further processing. This stage may also incorporate by-products generated from the manufacturing of plywood or LVL.
3. Forming and Pressing: The prepared strips are aligned in parallel and subjected to continuous pressing to create a composite beam. The bonding of these strips is typically achieved using phenolic adhesives.
4. Finishing: Once the pressing phase is complete, the parallel strand lumber (PSL) beams are cut to specified dimensions and undergo a finishing process. (Bączek and Borysiuk, 2024)

Advantages and Disadvantages of PSL:

Advantages of this material include its efficient resource utilization, as it makes use of low-quality or smaller-diameter hardwood logs, thereby enhancing resource efficiency. Additionally, it serves as a carbon sink, storing more carbon dioxide than is produced during its manufacturing process, which contributes positively to carbon sequestration efforts. The material is characterized by a high strength-to-weight ratio, offering strong structural performance across various applications. Its durability and versatility allow it to be employed in the construction of beams, headers, and other structural elements. Moreover, the use of mill residues for energy recovery helps to minimize production waste. (Bączek and Borysiuk, 2024) On the downside, the production of this material has a high dependency on resin, which significantly impacts its environmental footprint. Furthermore, the manufacturing process is energy-intensive, relying heavily on nonrenewable sources, which contributes to substantial energy consumption. The limited number of production facilities restricts accessibility, resulting in increased emissions associated with transportation. Additionally, the manufacturing process emits hazardous

air pollutants and volatile organic compounds (VOCs), raising concerns about air quality. (Bączek and Borysiuk, 2024)

3. TIMBER STRUCTURAL ELEMENTS

Timber structural components play an essential role in the integrity and functionality of buildings, offering both aesthetic appeal and strength. This section delves into the various aspects of timber construction, focusing on critical elements such as beams, columns, the innovative use of timber shells as floor and wall systems and connections.

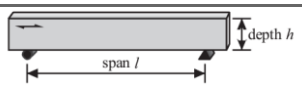
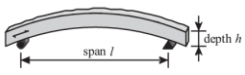
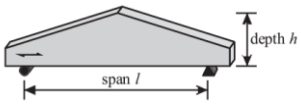
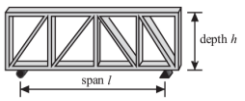
3.1. Beam

Timber structural beams are essential components in diverse construction projects such as public buildings, bridges, and large-span structures. Their high strength-to-weight ratio, visual attractiveness, and eco-friendliness make them a preferred option. Timber beams can be categorized according to factors such as span, shape, and type of material, with glued laminated timber (glulam) emerging as a leading choice for accommodating large open areas thanks to its capacity to achieve considerable spans while ensuring structural stability. (Franke et al., 2015)

Table 3.1. Classification of timber beams types (Franke et al., 2015)

Category	Representatives, options
Material/ Product	Solid timber; glulam; block glued glulam; LVL; plywood; OSB; LSL; CLT
Cross Sectional	Solid; box-beam; I-beam; T-beam; C-beam
Geometry	Straight beam; curved beam; tapered beam; truss

Table 3.2. According to Geometry (Franke et al., 2015)

Timber beam form		**Sectional cross**	**Depth to span ratio**
Straight beam			10m≤L≤40m h ≈L/17
curved beam			15m≤L≤35m h ≈L/17
tapered beam			12m≤L≤25m h ≈L/15
truss			20m≤L≤85m h ≈L/10

The Failure Modes of Timber Beams:

Understanding the failure modes of timber beams is essential for evaluating their structural integrity and durability. Several primary failure modes are important to consider. (Franke et al., 2015)

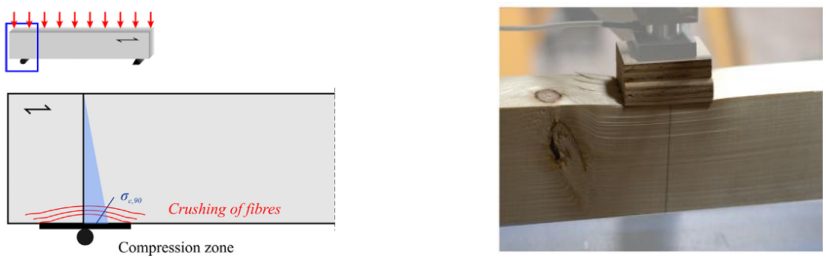
1. Bending Failure: This is the predominant failure mode, arising when excessive bending moments induce crack formation, especially along the grain direction. Fluctuations in moisture content can lead to shrinkage or expansion, resulting in internal stresses that surpass the material's strength threshold. (Franke et al., 2015)



a) b)

Figure 3.1. a) Principal drawing of bending failure, b) failure of tension during bending (Franke et al., 2015)

2. Compression Failure: This mode arises when compressive stresses exceed the timber's capacity, resulting in buckling or crushing. This is particularly relevant for members subjected to axial loads. (Franke et al., 2015)



(a) (b)

Figure 3.2. (a) Key design representation for compression failure at the support point, (b) compression failure (Franke et al., 2015)

3. Shear Failure: While bending stress is generally the primary concern in design, shear failure may become a critical issue in shorter or tapered beams, or under specific loading conditions as seen in Figure 3.2. This type of failure manifests as fiber sliding and cracking parallel to the grain, frequently occurring near supports or in notched sections of the beam. (Franke et al., 2015)



Figure 3.3. Shear failure (Schmid et al., 2010)

4. Cracking: Variations in moisture distribution can lead to the development of cracks, which in turn create internal stresses within the timber. These cracks can greatly diminish the load-bearing capacity of the beams.



Figure 3.4. Crack and split of timber beam. (inspectapedia.com)

5. Decay and Biological Damage: Timber beams are vulnerable to decay from fungi and insect infestations, particularly when moisture content exceeds certain limits. Fungal decay is especially probable when moisture content is at or above the fiber saturation point, while insect damage can occur at lower moisture levels conditions as seen in Figure 3.4. (Franke et al., 2015)

3.2. Column

Timber columns, including CLT and GLT, present a range of benefits in construction that make them increasingly popular. One of the primary advantages is their sustainability, as these materials are renewable and have a lower carbon footprint compared to conventional building materials like steel and concrete. Their lightweight nature contributes to reduced overall structural weight and lower foundation costs, while the natural aesthetic of timber adds warmth to architectural designs. Additionally, timber possesses excellent insulation properties, enhancing energy efficiency in buildings. The prefabrication of timber columns allows for improved quality control and minimized waste, which can lead to quicker construction timelines. Furthermore, timber's versatility enables its application in various structural contexts. While GLT columns are recognized for their high compressive strength, CLT columns excel in flexibility and resilience, positioning timber as a compelling option for contemporary construction projects. (Wei et al., 2019)

Solid timber columns are constructed from a singular piece of solid wood. These columns are typically employed in traditional architecture, smaller residential projects, and buildings that do not experience significant load demands. One of the primary benefits of solid timber columns is their aesthetic appeal and the straightforwardness of their production process. However, they do have limitations, including size constraints dictated by the natural dimensions of trees and a susceptibility to issues such as splitting and warping.

Glulam Columns are constructed by adhering multiple layers of wood laminates using adhesives. These columns are utilized in demanding structural applications, including bridges, expansive buildings, and tall structures. The benefits of Glulam include the ability to customize dimensions and configurations, a favorable strength-to-weight ratio, and minimized imperfections such as knots. However, it is important to note that the cost of Glulam is typically higher than that of solid timber materials. (Zahn and Rammer, 1995)

CLT Columns are a modern engineered wood product created by gluing layers of dimension lumber at right angles, resulting in a strong and stable structural element. This

cross-lamination enhances the columns' strength and stiffness, allowing them to bear significant loads while exhibiting greater ductility and energy absorption. (Wei et al., 2019)

Timber's versatility enables its application across various structural contexts. While GLT columns are recognized for their higher compressive strength, CLT columns excel in flexibility and resilience, positioning timber as a compelling option for contemporary building projects. (Wei et al., 2019)

Failure Modes of Timber Columns:

The failure mechanisms of timber columns can differ significantly based on various factors, including the nature of the loads applied, the condition of the timber, and environmental factors. Here are several critical failure modes associated with timber columns (Chang, 2015):

Buckling failure: Timber columns especially slender ones subjected to compressive loads are susceptible to buckling. Buckling can be increased by elements like low material strength, vertical fractures, or insufficient cross-sectional dimensions.

Compressive failure: Under high compressive stresses, particularly in engineered applications, timber columns may fail through crushing. Although this is less frequent, it can occur if the columns are overstressed or if biodeterioration is also present.

Cracking: Vertical cracks may form in timber columns due to various stresses, including shrinkage and fluctuations in environmental conditions as shown in Figure 3.5. These cracks can diminish the effective cross-section of the column, thereby reducing its load-carrying capacity.

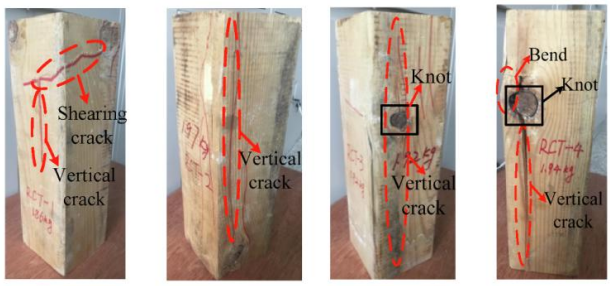


Figure 3.5. Images showing the failure modes (Qiao et al., 2020)

Combined Loading: Timber columns can experience combined loads, incorporating both axial compression and bending moments. This situation may lead to failure or splitting along the grain, which can further jeopardize the structural stability of the column.

Moisture-Related Issues: Variations in moisture content can induce dimensional changes in timber, creating stresses that may result in cracking or other failure modes. Additionally, the presence of moisture can promote biodeterioration, amplifying the risk of failure.

Biodeterioration:

1. Insect Infestation: Timber columns are vulnerable to damage from insects, notably termites, which can undermine the internal integrity of the wood. This form of biodeterioration often remains undetected until substantial damage has occurred, resulting in a reduction of the effective cross-sectional area and overall strength of the column.
2. Fungal Decay: High moisture levels can promote fungal growth, further compromising the timber's structural integrity. This issue is particularly prevalent in columns that are in contact with wet soil.(Alfieri et al., 2016)

4. FIBER REINFORCED POLYMER (FRP)

FRP materials are composite materials composed of fibers that provide stiffness and load-bearing capacity within a polymer resin that protects the fibers and transfers loads between the fibers. FRP comes in several forms, each with unique properties depending on fiber material, volume fraction, and orientation. FRP is primarily used as a reinforcement material and comes in two main forms: pultruded rod/plate and fabric. Pultruded rods/plates are used for internal reinforcement and FRP plates or fabrics for external reinforcement. (Schober et al., 2015b) FRPs such as glass (GFRP), carbon (CFRP), basalt (BFRP) and aramid (AFRP) are commonly used in civil engineering. GFRP is the most widely used type of FRP and is a proven composite material used in various industrial applications. Compared to wood and steel, FRP composites are significantly lighter and have a higher strength-to-weight ratio than steel. Basalt is a new eco-friendly FRP material, as it does not cause toxic reactions when in contact with water or air and is non-flammable. BFRP rods are used in the construction and road industries due to their stiffness and thermal performance. AFRP has the highest strength-to-weight ratio and lowest density, but it degrades rapidly under UV light and requires coating or painting. The CFRP composite used for structural reinforcement is made from polyacrylonitrile filaments, which improves material quality. However, CFRP types are significantly more expensive than his GFRP or BFRP. A Table 5.4.1 presents the usual characteristics of standard fibers and polymers. Carbon fiber is suitable because of its chemical resistance to alkaline environments, high modulus and tensile strength of composites. Using FRP instead of steel, significantly reduces weight increase and is more corrosion resistant, opening up new possibilities for designers and engineers. The polymer matrix, which binds the fibers in composites, is crucial for effective load transfer and provides protection against environmental degradation. Commonly used matrices include epoxy and polyester resins, known for their excellent bonding properties and chemical resistance. The mechanical performance of FRP materials is influenced significantly by factors such as fiber orientation, fiber type, and the composition of the matrix. As shown in Figure 4.1. (Günaslan, et al. 2014)

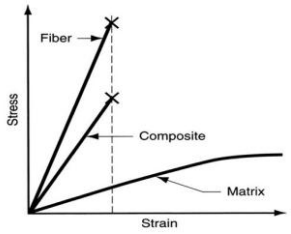


Figure 4.1. Stress Strain Diagram for Composite Phases (Günaslan et al., 2014)

Carbon Fibers (CFRP): Carbon fibers exhibit anisotropic properties and are manufactured at temperatures around 1300ºC see Figure 4.2 (a). They offer several advantages, including high strength, excellent resistance to creep, durability against chemical exposure, low electrical conductivity, lightweight characteristics, and a high elastic modulus. However, the drawbacks of carbon fibers include their high cost and their inherent anisotropy, which results in lower compressive strength. (Günaslan et al., 2014)

Glass Fibers (GFRP): Glass fibers, as illustrated in Figure 4.2 (b), possess isotropic properties and are among the most commonly utilized filaments in various applications. The predominant types of glass fibers include E-Glass, S-Glass, and C-Glass. Notable characteristics of glass fibers are their high tensile strength, affordability, and notable resistance to moisture and chemicals.

Aramid Fibers (AFRP): Aramid fibers, commonly known in the market as Kevlar, are depicted in Figure 4.2 (c). These fibers possess an anisotropic structure and typically exhibit a yellow coloration. Although aramid fibers are more costly than glass fibers, they offer moderate stiffness and are particularly effective in tension-related applications, such as cables and tendons; however, they demonstrate lower strength when subjected to compression. Aramids are characterized by high tensile strength, considerable stiffness, elevated modulus, and reduced weight and density.



a) b) c)

Figure 4.2. Typical FRPs (Günaslan et al., 2014)

Table 4.1. Fibre and Polymer properties (Günaslan et al., 2014)

Material	Modulus of elasticity (GPa)	Tensile strength (MPa)	Failure strain (%)	CTE (10^-6 °C^-1)	Density (g/cm3)
E-glass	70–80	2000–4800	3.5–4.5	5.0–5.4	2.5–2.6
Carbon (HM)	390–760	2400–3400	0.5–0.8	-1.45	1.85–1.90
Carbon (HS)	240–280	4100–5100	1.60–1.73 1	-0.6 to -0.9	1.75
Aramid	62–180	3600–3800	0.9–5.5	-2.0	1.44–1.47
Basalt	62–180	860–3450	5.5	3.15	1.52–2.7
Polymer	2.7–3.6	40–82	1.4–5.2	30–54	1.10–1.25

CTE refers to the coefficient of thermal expansion; HM stands for high modulus; HS indicates high strength.

The stress-strain curve illustrates the distinct mechanical properties of unidirectional FRPs-carbon (CFRP), aramid (AFRP), and glass (GFRP)-compared to mild steel as shown in Figure 4.3. CFRP has the highest tensile strength over 6 GPa but lower strain capacity, indicating brittleness. In contrast, AFRP and GFRP exhibit moderate strength (2 to 4 GPa) with higher ductility. Mild steel, while having lower tensile strength, shows significant ductility.

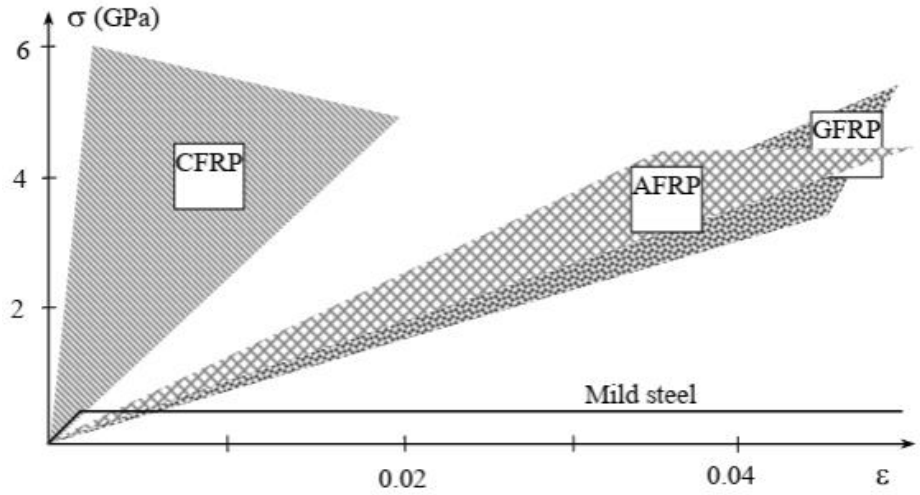


Figure 4.3. Stress-strain graphs for various unidirectional FRPs and steel under uniaxial tension (FIB 2001)

The stress-strain behavior of fiber-reinforced polymers (FRPs) varies significantly based on their composition, with carbon FRP (CFRP) exhibiting the highest tensile strength,

ranging from 2100 MPa to 6000 MPa, but with a lower ultimate tensile strain of 0.2% to 2.3%. In contrast, glass FRP (GFRP) and aramid FRP (AFRP) demonstrate higher ductility, with ultimate tensile strains of 3.0% to 5.5% and 2.5% to 5.0%, respectively, though they possess lower tensile strengths. The elastic modulus of CFRP is significantly higher, ranging from 215 GPa to 700 GPa, compared to 70 GPa to 90 GPa for GFRP and 70 GPa to 130 GPa for AFRP. These mechanical properties highlight the brittle nature of CFRP, whereas GFRP and AFRP offer more balanced strength and ductility characteristics. The stress-strain response of these materials follows the "rule of mixtures," where the overall mechanical behavior is dictated by the properties of the fiber and matrix. Given their anisotropic nature, FRP materials generally exhibit linear elastic behavior up to failure, unlike conventional ductile materials such as steel. Experimental tensile testing is often necessary to determine the precise stress-strain relationship of FRPs in structural applications. (FIB 2001)

Advantages of FRP:

1. Durability: Fiber-reinforced polymer (FRP) materials exhibit strong resistance to corrosion and degradation, making them ideal for application in harsh environments, such as marine settings where conventional timber is susceptible to damage from marine borers. (Iskander and Hassan, 1998; Günaslan et al., 2014)
2. Lightweight: FRP is lighter than steel and conventional materials, reducing overall structure weight and simplifying handling and installation processes. (Iskander and Hassan, 1998; FIB 2001)
3. Low Maintenance: Composite piling generally demands less upkeep than treated timber, which is prone to decay and damage from pests. (Iskander and Hassan, 1998)
4. Environmental Advantages: The incorporation of recycled plastics in FRP composites contributes to mitigating environmental disposal challenges associated with creosote-treated timber, which poses potential risks to marine ecosystems. (Iskander and Hassan, 1998)
5. Consistent Performance: FRP composites possess engineered characteristics that ensure predictable strength and stiffness, in contrast to timber, which can exhibit significant variability in its physical properties. (Iskander and Hassan, 1998; Günaslan et al., 2014)

Disadvantages of FRP:

1. High Initial Cost: The expense associated with fiber-reinforced polymer (FRP) composite materials can be significantly higher, often ranging from two to three times the cost of traditional creosote-treated timber piles. (Iskander and Hassan, 1998; Günaslan et al., 2003)
2. Reduced Installation Efficiency: The drivability of composite piling tends to be less effective compared to conventional materials, which can complicate the installation process. (Iskander and Hassan, 1998; Günaslan et al., 2003)
3. Creep Behavior: FRP materials demonstrate viscoelastic characteristics, resulting in creep under sustained loads. This behavior necessitates careful consideration and management in the design phase. (Iskander and Hassan, 1998; Günaslan et al., 2003)
4. Limited Historical Data: The use of FRP composites in civil engineering is relatively novel, which may lead to concerns regarding their long-term performance and reliability due to the lack of a comprehensive track record. (Iskander and Hassan, 1998)
5. Low Stiffness: Certain FRP composites exhibit low stiffness, presenting challenges during installation and handling. Consequently, they may not be suitable for all applications. (Iskander and Hassan, 1998; Günaslan et al., 2003).

5. APPLICATIONS OF FRP REINFORCEMENT IN TIMBER STRUCTURES IN THE PREVIOUS STUDIES

FRP reinforcement has emerged as a significant advancement in the enhancement of timber structures, providing an innovative approach to improving the mechanical properties of timber elements such as beams and columns. Previous studies have highlighted the effectiveness of FRP materials in addressing common challenges faced in timber construction, including limited load-carrying capacity, and susceptibility to shear and flexural failures. By integrating FRP reinforcement into various structural components, researchers have demonstrated the potential for increased strength, stiffness, and overall resilience of timber structures, while also promoting sustainability through the use of lightweight and corrosion-resistant materials. This section will explore the diverse applications of FRP reinforcement in timber beams and columns, providing insights into the methodologies, outcomes, and implications of these studies for contemporary engineering practices.

5.1. Beams

In previous studies, various reinforcement techniques have been explored to enhance the structural performance of timber beams using FRP. These reinforcement methods aim to improve the beams' load-carrying capacity and stiffness, addressing the inherent weaknesses of timber under bending and shear stresses. The effectiveness of FRP reinforcement largely depends on the application method, material type, and bonding quality. This section categorizes and examines different reinforcement configurations used in past research, including Side Face Reinforcement, which enhances shear resistance and lateral stability; Bottom Face Reinforcement, commonly employed to improve flexural strength; U-Wrap Configuration, which provides additional confinement and prevents premature failure; Near-Surface Mounted (NSM) Reinforcement, offering a more embedded strengthening approach with improved bond efficiency; and Pultruded FRP Bars, which integrate continuous fiber reinforcement within the timber matrix for enhanced performance. By analysing these reinforcement techniques, this section aims to highlight their advantages and limitations.

5.1.1. Side Face Reinforcement

FRP is utilized on the lateral surfaces of the beam and is frequently paired with additional methods to enhance shear strength.

Triantafillou (1997) investigates the mechanical properties of timber beams enhanced with carbon-fiber-reinforced plastic (CFRP) fabrics, focusing on their application in shear-critical regions. The study analyses seven distinct glulam beam configurations, with three identical specimens for each, totalling 21 beams tested under a four-point bending setup with a span of 500 mm and a shear span of 110 mm as shown in Figure 5.1 of these, six designs were reinforced with epoxy-bonded CFRP, while one served as an unreinforced control. The findings reveal that the most effective FRP configuration involves longitudinal fiber orientation and the bonded sheet height exceeding a critical value. Results demonstrated a substantial increase in ultimate bearing capacity, with a strong correlation between actual and predicted shear capacities. The study emphasizes that even minimal FRP reinforcement is effective in mitigating shear stresses, highlighting both cost-effectiveness and aesthetic advantages while urging further research into long-term performance. Overall, the reinforcement significantly improved both strength and stiffness in the timber specimens, underscoring the potential benefits of FRP in timber construction. The research concludes that its efficiency varies with configuration and area fraction, optimal shear capacity increase requires minimal FRP area fraction with longitudinal fiber placement and experimental results align closely with analytical predictions, which slightly overestimate shear failure loads. Ultimately, the study shows that a small amount of FRP reinforcement can effectively relieve shear stresses in timber structures, and despite the need to explore the long-term behavior of the FRP-wood system, previous experience suggests no significant issues will arise.(Triantafillou, 1997)

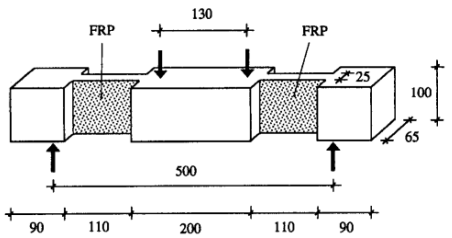


Figure 5.1. Shape and structure of wood beams that have been tested (Triantafillou, 1997)

Table 5.1. summary of the results (Triantafillou, 1997)

Beam design	CFRP Application	Experimental Shear Capacity (KN)
C	-	14.5
L1/1	one ply at 0°	17.6
L2/1	two plies at 0°	20.7
LV2/1	two plies at 0°/90°	17.7
V1/1	one ply at 90°	15.2
L1/0.6	one ply at 0°	17.2
L2/0.6	two plies at 0°	18.7

5.1.2. Bottom Face Reinforcement

FRP strips or sheets are attached to the tensile side (bottom) of the beam to improve its flexural strength.

Andor et al. (2015) performed a study to assess the structural performance of Norway spruce timber beams (Picea abies) reinforced with CFRP, focusing on enhancing their load-bearing capacity and stiffness. The team conducted a series of four-point bending tests Figure 5.2 on 44 timber specimens, which were categorized into unreinforced beams and three groups of reinforced beams utilizing different CFRP configurations. The solid timber beams, measuring 95 mm by 95 mm, were carefully prepared to have a moisture content of 12% and were permitting the presence of natural knots. The CFRP was applied on the tensile side using a unidirectional carbon fiber fabric (300 g/m²) with a two-component epoxy, allowing for a practical application process without mechanical pressure. The results demonstrated that CFRP reinforcement led to an increase in load-bearing capacity of 18–33% and stiffness improvements of 9–16% in comparison to unreinforced beams see table 5.5. Notably, the presence of natural defects impacted the performance, with reinforcement proving particularly beneficial for defective specimens, while the effects were less significant for homogeneous beams. The Figure 5.3 and 5.4 illustrates the failure modes observed during the experimental tests. The specimens exhibited a variety of failure modes influenced by the timber quality and reinforcement configuration. The most frequently observed failure was tensile failure of the timber, often accompanied by horizontal splits near the midpoint, which could lead to

delamination or rupture of the CFRP. In specimens with lower performance, additional failure modes such as cross-graining, compression failure, and shearing were noted, typically associated with defects like knots or inconsistencies in the material. Rare occurrences included CFRP rupture and torsional buckling in unreinforced specimens. Generally, reinforced specimens showed improved structural integrity, with higher-performance examples primarily failing in tension, while those with lower performance were more likely to experience mixed-mode failures. (Andor et al., 2015)

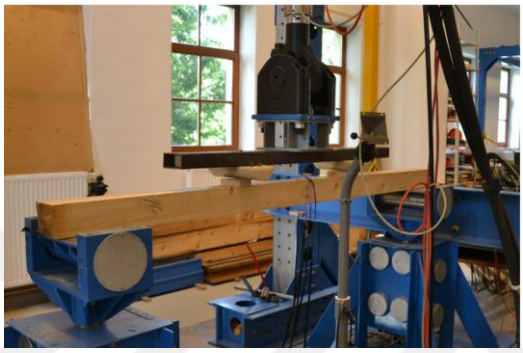


Figure 5.2. The MTS testing apparatus alongside one of the specimens prepared for the bending test (Andor et al., 2015)



Figure 5.3. The test specimen is positioned upside down after the experiment, revealing the CFRP strip bonded to the beam's tensile face across its full width (Andor et al., 2015)



Figure 5.4. The failure mechanisms of the samples are shown in a grid, featuring images of different failures such as tension, compression, shearing, cross-graining, and CFRP (Andor et al., 2015)

Table 5.2. Increases in average values compared to the reference group S0 (Andor et al., 2015)

Test group	Ultimate load (KN)	Maximum deflection (mm)	Stiffness (KN/mm)
S0	-	-	-
S1	+31.47	+18.87	+15.22
S2	+33.33	+29.21	+16.32
SN	+18.21	+8.58	+9.12

Where + stand for Increase

Al-Katib et al. (2022) conducted an investigation into the structural performance of standard timber beams reinforced with CFRP sheets under flexural loading. The research involved high-quality timber obtained from Russia and comprised tests on ten timber beam specimens, which included one control beam without reinforcement and nine beams strengthened with CFRP sheets. The specimens were categorized into 3 groups based on variations in CFRP strip width and length, with the strips applied to the tension face of the beams Figure 5.5. Flexural testing was executed using a four-point bending setup, revealing that CFRP reinforcement significantly enhanced the ultimate load-bearing capacity, stiffness, and toughness of the timber beams, with ultimate load increases ranging from 5% to 76% contingent upon the specific strengthening configuration showing in Figure 5.7. The optimal performance was observed when the CFRP strips were as long as twice the shear span and matched the beam's width. Conversely, extending the strip length beyond this optimal point or utilizing widths greater than the beam width resulted in minimal benefits. Additionally, the failure modes observed in the tested timber beams were influenced by the different configurations of reinforcement. The control beam (B1) failed in simple tension due to the rupture of wood fibers on the underside, typical of flexural failure. Similarly, beams B2, B3, B4, B5, and B8 also displayed simple tension failures, but they had stiffer load–deflection responses and could withstand greater loads compared to the control beam. However, when CFRP sheets were used with an area ratio below 0.186% or a length less than 900 mm (which is double the shear span length), were insufficient to change the failure mode, even though they increased stiffness. Beams B3 and B4 showed CFRP sheet debonding due to insufficient width (30 mm), while beams B6, B7, B9, and B10 failed in splintering tension, a flexural failure mode associated with tougher timber beams see Figure 5.6. This change in failure mode

was due to an adequate area ratio (≥0.186%) and bonding length (≥900 mm), which helped reduce the tensile stresses in the timber fibers. In beams B6 and B7, the CFRP sheets, which were 60 mm wide, ruptured, demonstrating they were sufficiently wide to counteract bond forces and support higher tensile stresses. All of the strengthened beams failed in the tension zone without showing any signs of failure in the compression zone, confirming that they were under-reinforced. (Al-Katib et al., 2022)

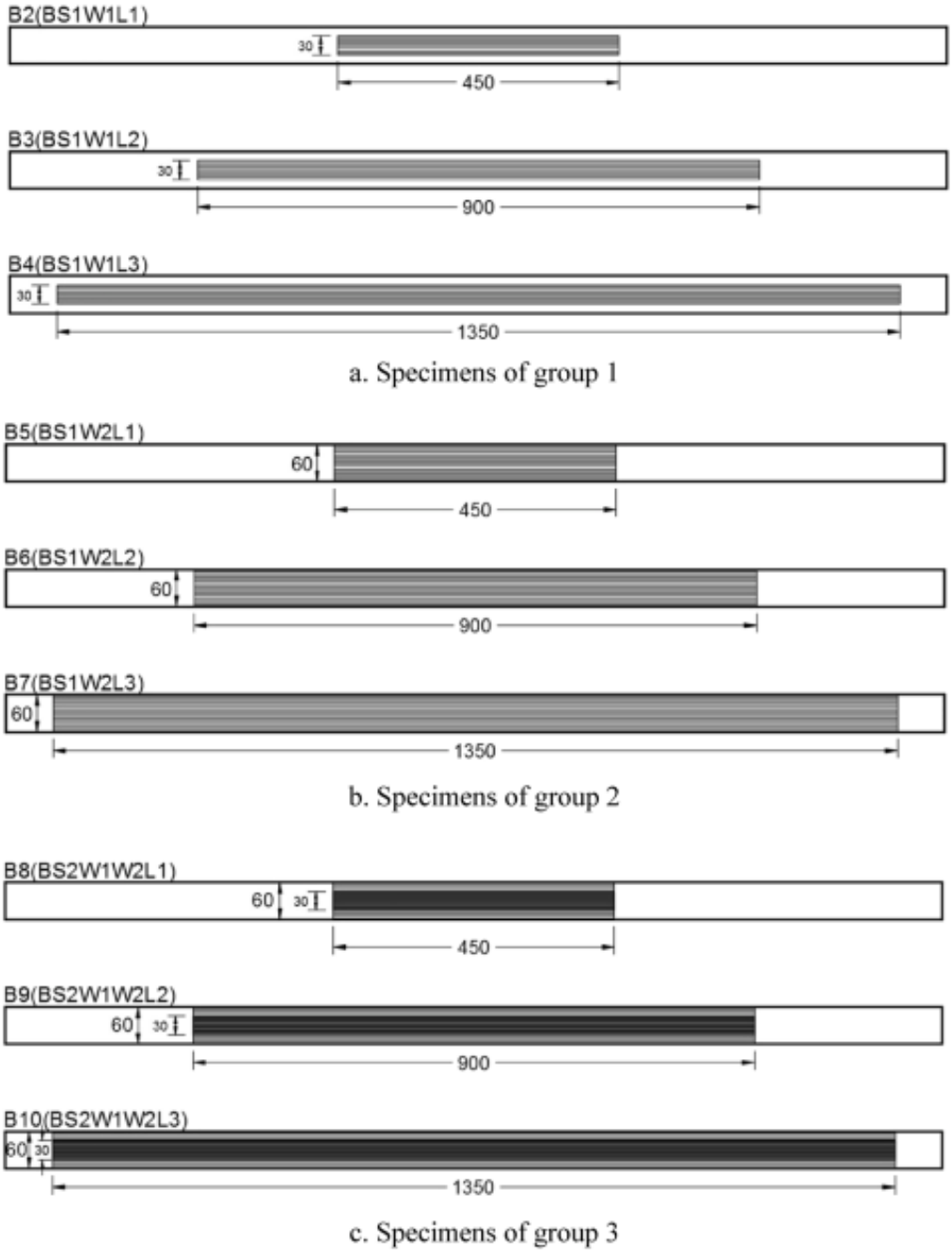


Figure 5.5. All Specimens (Al-Katib et al., 2022)



Figure 5.6. Crack formations for timber beams (B1, B3, B6, and B9) (Al-Katib, et al. 2022)

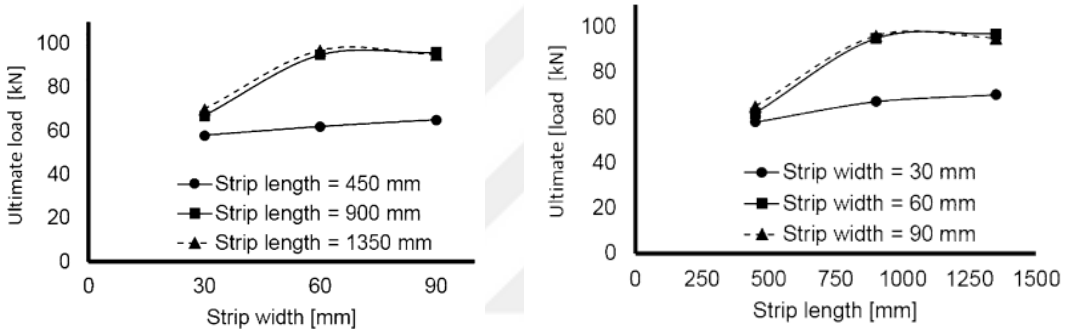


Figure 5.7. Analyzing how varying the widths/ lengths of CFRP strips influence the maximum load capacity of timber beams with different widths of CFRP strips (Al-Katib, et al. 2022)

Vahedian et al. (2019) carried out an extensive investigation into how bond geometries affect the flexural capacity, stiffness, and failure modes of CFRP-strengthened glulam beams. This research involved testing eight full-scale Pine GL10 beams under four-point bending conditions with monotonic loading. Figure 5.8. The researchers tested two unstrengthened control beams, B1 and B2, which experienced brittle failure with mid-span deflections of 29 mm and 26 mm, respectively. In contrast, the CFRP-strengthened specimens exhibited marked enhancements: B3, with 2 layers of CFRP bonded over a 1000 mm length and 30 mm width, showed a 31% increase in stiffness and a 43% increase in ultimate load over B2; B4, featuring 4 layers with the same bond dimensions, achieved a 52% increase in ultimate load and an 18% reduction in mid-span deflection compared to B3. B5, which maintained the bond length and layers as B3 but increased the bond width to 45 mm, demonstrated a 43% stiffness improvement. The full-width B6 beam,

also with 2 layers and a 1000 mm bond length, revealed a dramatic ultimate load increase of approximately 90% compared to B3. Beam B7, leveraging an extended bond length of 1300 mm while using 2 layers, attained an ultimate load of 18.29 KN. Lastly, B8, integrating all enhancements with 4 layers, a 1300 mm bond length, and a 45 mm width, registered the maximum ultimate load of 19.48 KN and a 64% increase in stiffness. The Figure 5.9 illustrates the failure modes which exhibited various failure modes depending on their reinforcement status. Unstrengthened specimens primarily failed due to brittle tension in the tension zone, showing no signs of compressive failure. In contrast, the failure mechanisms of the strengthened beams were influenced by the bond configurations. Beams with inadequate bond length displayed cracks that began at the ends of the FRP reinforcement, resulting in a brittle failure attributed to stress concentrations. Conversely, beams with sufficient bond length and width experienced a transition to a more ductile failure mode, characterized by partial plasticization in the compression zone followed by tension failure in the timber. Notably, there was no occurrence of delamination between the timber and FRP, and the CFRP sheets remained intact, with the maximum strain in the FRP recorded at approximately 0.6%.In some cases, natural defects such as knots initiated cracks, underscoring the importance of addressing these weaknesses in strengthened beams. (Vahedian et al., 2019)

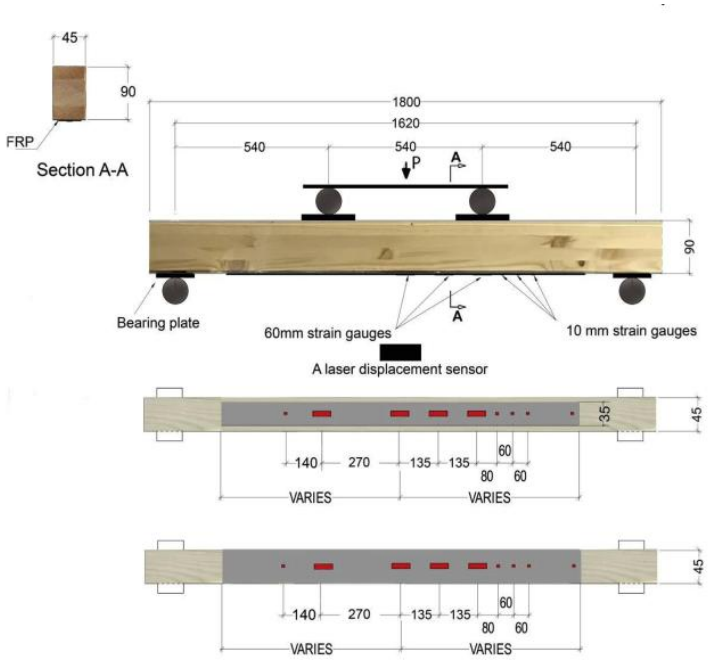


Figure 5.8. Illustration of the test configuration; a schematic representation, (a) bond width of 45 mm, (b) bond width of 30 mm (Vahedian et al., 2019)

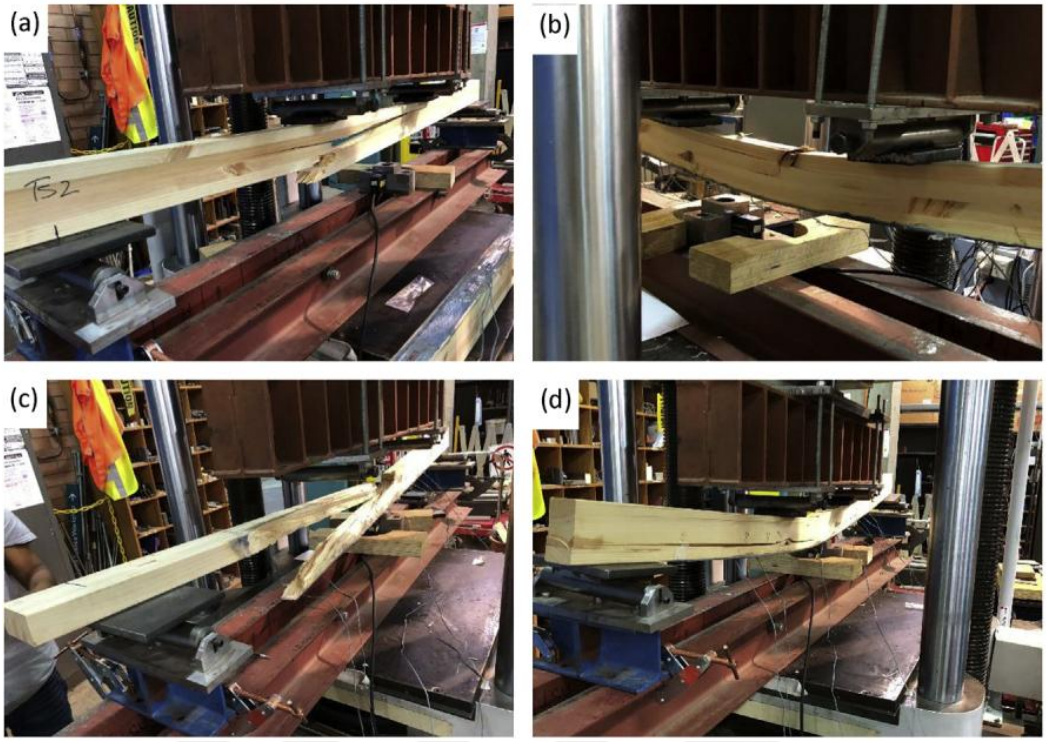


Figure 5.9. Failure mode of timber beams (Vahedian et al., 2019)

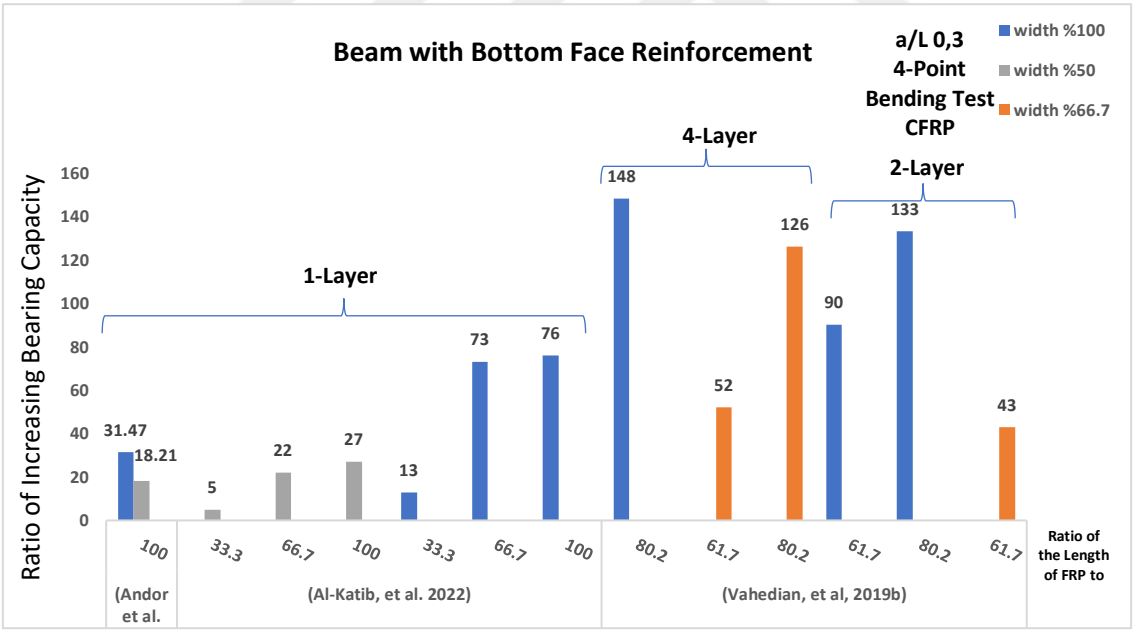


Figure 5.10. Comparison of Load-Bearing Capacity and Width and length Utilization in Timber Beams Reinforced with CFRP

This graph compares the ratio of increased bearing capacity for beams reinforced with CFRP under a 4-point bending test, varying the number of layers, CFRP width, and length-to-beam ratio. Results show that full-width CFRP application (100%) consistently achieves the highest reinforcement efficiency across all studies, with reduced widths

(50%, 66.7%) significantly lowering performance. Increasing the number of CFRP layers improves bearing capacity, as seen in Vahedian et al.'s 4-layer setup (148% improvement) outperforming the 2-layer (133%) and 1-layer configurations. Additionally, longer CFRP-to-beam length ratios (80.2%) yield greater benefits compared to shorter ratios (33.3%, 61.7%). Based on these results, it is advised to pick longer CFRP lengths in relation to beam size, maximise the CFRP width (ideally 100%), and take into account multi-layer reinforcement (e.g., 2 or more layers) for the best results in terms of boosting bearing capacity.

Corradi et al. (2017) carried out an experimental investigation to evaluate the mechanical properties of timber beams reinforced with FRP sheets. The study encompassed a total of 221 timber beams made from firwood (softwood) and oakwood (hardwood), featuring various dimensions. The beams were reinforced on their tension side with CFRP and GFRP sheets using epoxy resin Figure 5.11, subjected to four-point bending tests Figure 5.12. The results indicated a remarkable enhancement in structural performance, with the ultimate bearing capacity increasing by as much as 122% for CFRP and 81.9% for GFRP. Flexural stiffness improvements ranged from 5% to 15%, depending on the size of the beams and the type of reinforcement used. The observed failure mechanisms in unreinforced timber beams included tensile failure occurring on the tension side for straight-grained timber and cross-grained tension failure resulting from grain deviations or the presence of knots, which frequently initiated crack formation. While compression failure was noted on the compression side, it seldom resulted in structural collapse due to the material's plasticity under compressive loading. Horizontal shear rupture was relatively rare; however, it did occur in beams that exhibited significant defects or openings. In the case of timber beams reinforced with FRP, failure predominantly originated in the timber rather than the reinforcement itself. This failure often began with localized plastic deformation in the compression zone, coupled with tensile failure on the tension side see Figure 5.13. The use of FRP reinforcement enhanced the bending capacity of the beams, mitigated the impact of local defects, prolonged the onset of crack development, and diminished variability in strength. Nevertheless, the failure mode consistently remained dominated by tensile stresses. (Corradi et al., 2017)

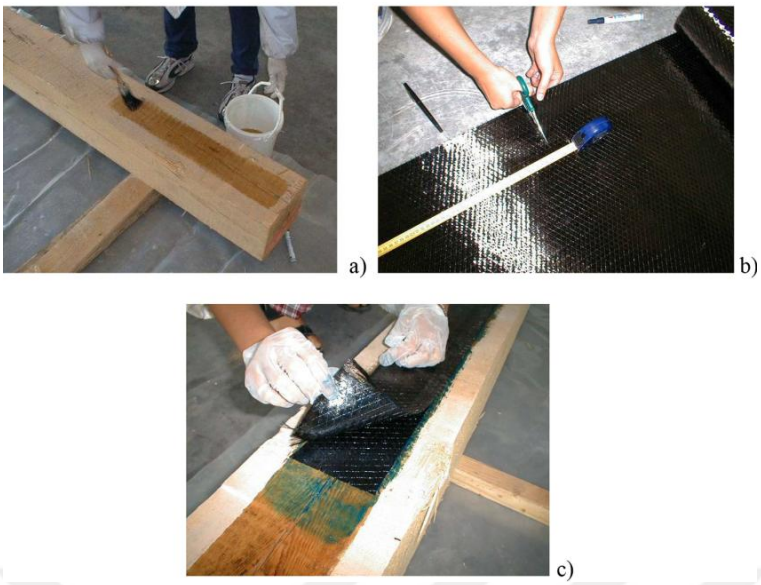


Figure 5.11. Reinforcement method: a) apply an initial layer of epoxy resin, b) fibers can be easily trimmed with scissors, c) several layers of fibers can be applied in succession and interchanged (Corradi et al., 2017)

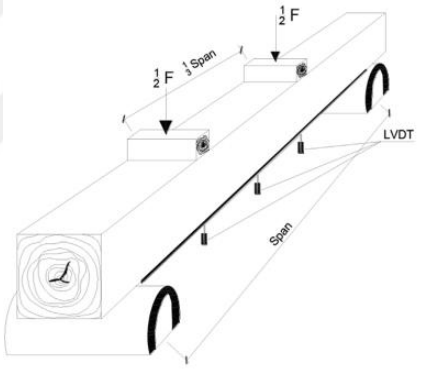


Figure 5.12. Test setup, with LVDT placements at one-quarter and three-quarters of the span, as well as at the midpoint (Corradi et al., 2017)

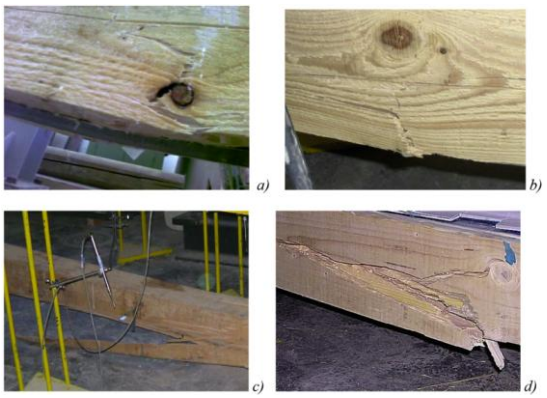


Figure 5.13. Tension failure types include: a) failure caused by a knot on the tension side, b) standard tension failure in a straight-grained beam, and c) and d) tension failure in cross-grained scenarios (Corradi et al., 2017)

Corradi et al. (2021) conducted a study to evaluate the reinforcement of firwood (Abies alba) beams, focusing on restoring the mechanical performance of defective beams affected by knots or artificial cuts. The research analyzed a total of 36 specimens, which included both small and large timber beams, subjected to four-point bending tests Figure 5.15 to examine the efficacy of applying (CFRP sheets to localized defective areas Figure 5.14. The findings revealed that the use of CFRP reinforcement enhanced the ultimate load capacity by 35.5% for large beams and 47.6% for small beams when compared to unreinforced defective beams Figure 5.17. Additionally, flexural stiffness demonstrated an improvement of 22.7%, and the localized reinforcement technique effectively contained defects, thereby preventing localized cracking and deformation. This approach not only minimized material consumption and costs but also provided a viable solution for strengthening timber elements while maintaining both structural integrity and aesthetic appeal. (Corradi et al., 2021)



Figure 5.14. Various retrofitting techniques utilizing FRP) include: (a) applying FRP sheets; (b) positioning FRP pultruded elements on the compression side; and (c) using CFR) laminae (Corradi et al., 2021)

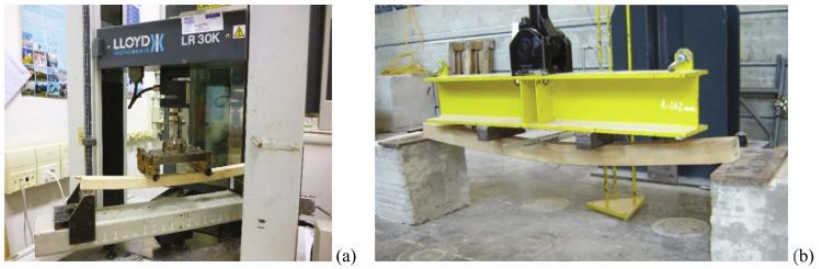


Figure 5.15. Experimental test configuration: (a) small beams; (b) large beams. (rafters) (Corradi et al., 2021)

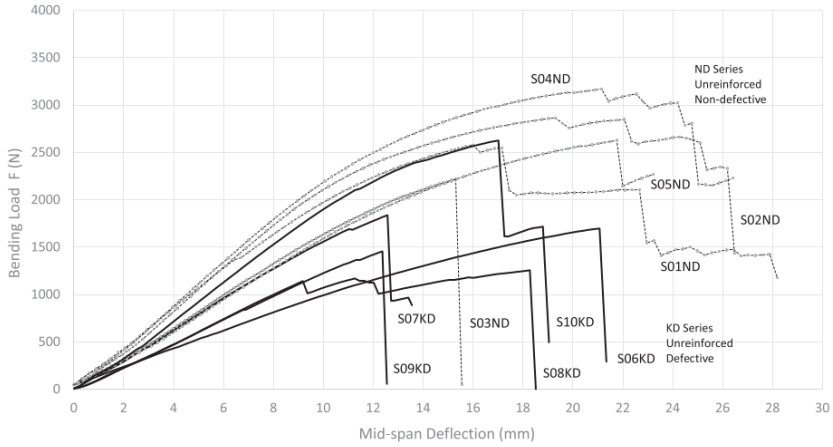


Figure 5.16. The four-point bending tests, with simply supported ends, measure the relationship between load and mid-span deflection for both unreinforced non-defective (ND Series) and defective samples. (KD Series) (Corradi et al., 2021)

Śliwa-Wieczorek et al. (2021) conducted a study to investigate the impact of CFRP sheets on the bending performance of GLT beams. The research involved testing 32 specimens, which included both unreinforced beams and those reinforced with 1, 3, and 5 layers of CFRP. The CFRP sheets were applied in the tension zones of the beams using the dry lay-up method Figure 5.17, and all specimens underwent four-point bending tests. The findings indicated that the one-layer CFRP reinforcement provided the most balanced performance, resulting in a 41.07% increase in ultimate load-bearing capacity and improved ductility without negatively affecting stiffness. In contrast, reinforcements with three and five layers yielded increases in load capacity of 28.46% and 31.29%, respectively, but did not correspondingly enhance stiffness, underscoring the importance of reinforcement configuration and material quality in influencing performance outcomes. The failure modes as showing in Figure 5.18 of the tested beams varied based on reinforcement. For the unreinforced beams, the dominant failure was tension failure in the bottom fibers, occasionally accompanied by shear. Knots in the tensile zone significantly affected stiffness and initiated cracks, reducing the beam's strength. In CFRP-reinforced beams, failure typically occurred through shear, often in the support zone, with cracks propagating horizontally or diagonally across the section. Beams with one layer of reinforcement experienced shear-dominated failures, with occasional tension-shear or compression-shear combinations. Beams reinforced with three or five CFRP layers primarily failed by shear, starting at the interface between the wood and adhesive in the support zone due to stress concentrations. The CFRP reinforcement

increased the beams' load-bearing capacity, while maintaining linear elasticity until failure, with no breakage or detachment of the CFRP laminate. However, interfacial shear and pull-off stresses at the adhesive layer were observed, especially in beams with three and five layers, potentially impacting the final strength. (Śliwa-Wieczorek et al., 2021)

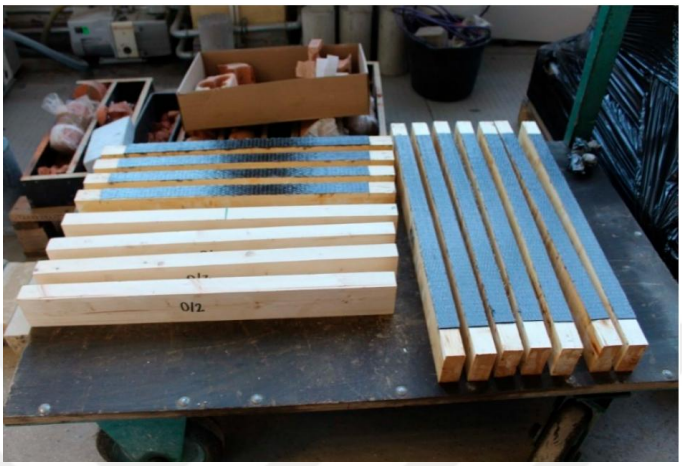
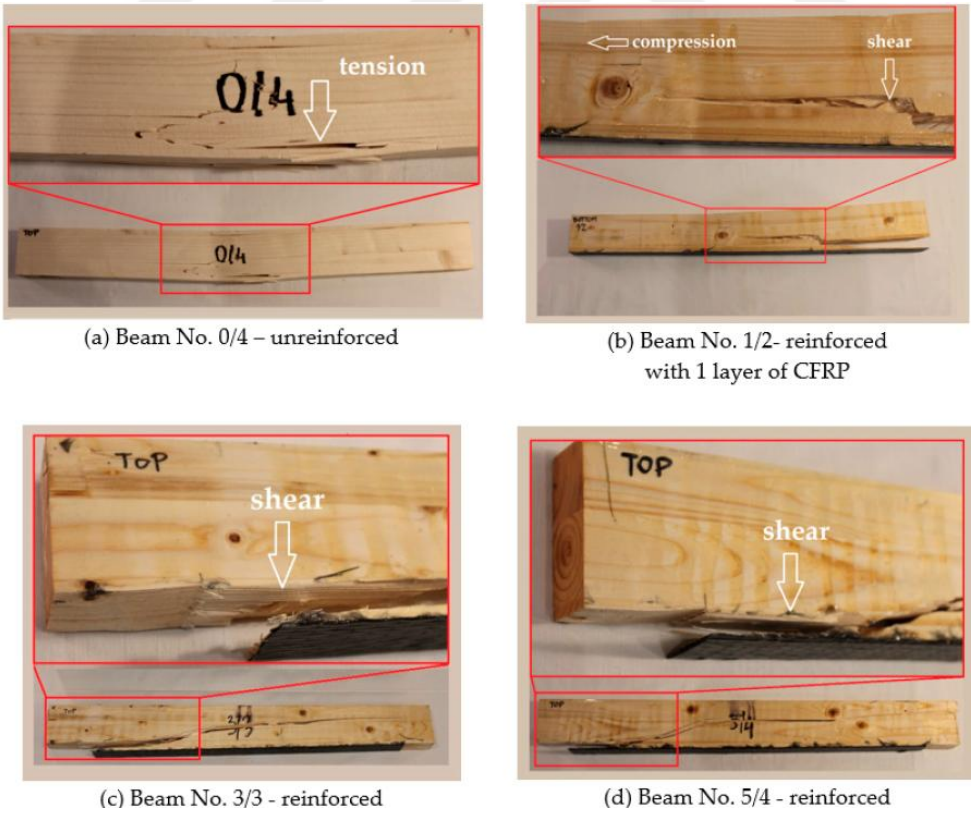


Figure 5.17. Beams set up for destructive evaluation: unreinforced beams and those reinforced with CFRP Glued Laminated Timber (Śliwa-Wieczorek et al., 2021)



(a) Beam No. 0/4 – unreinforced

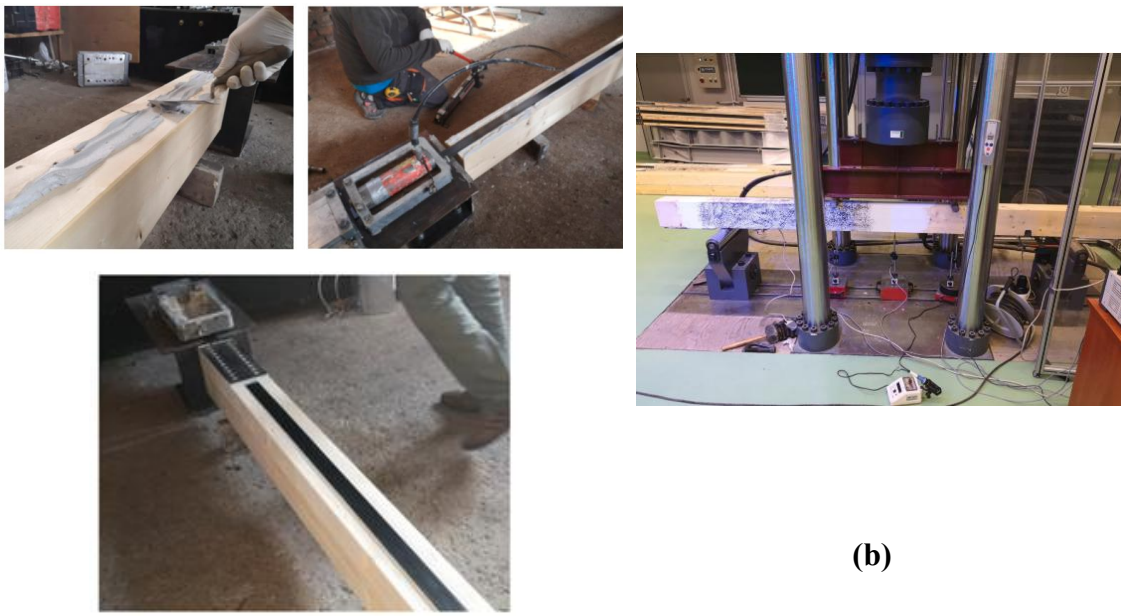
(b) Beam No. 1/2- reinforced with 1 layer of CFRP

(c) Beam No. 3/3 - reinforced

(d) Beam No. 5/4 - reinforced

Figure 5.18. Examples of failures for each group of analysed samples are shown: Beam No. 0/4 (a), Beam No. 1/2 (b), Beam No. 3/3 (c), and Beam No. 5/4 (d) (Śliwa-Wieczorek et al., 2021)

Halicka and Ślósarz (2021) conducted an experimental study to evaluate the reinforcement of timber beams using pretensioned CFRP strips. They tested twelve C24 wood beams with dimensions of 140 × 200 mm see Figure 5.19 (a) under four point bending test as showing in Figure 5.19 (b) average increase of 13.9% in ultimate load capacity compared to the reference beams, with ultimate forces ranging from 94.3 kN to 138.9 kN. Additionally, under a 70 kN load, the prestressed beams exhibited significant reductions in deflection, with decreases of approximately 23.4% (30 kN), 26.7% (60 kN), 44.4% (75 kN), and 36% (90 kN). The force needed to produce a 30 mm deflection increased by 20.9% for beams prestressed at 30 kN, 11.43% at 60 kN, 36.8% at 75 kN, and 14.3% at 90 kN, indicating a clear relationship between prestressing levels and enhanced stiffness. The failure modes differed significantly, with reference beams failing due to bending, while the strengthened beams primarily experienced delamination of timber fibers Figure 5.20. Notably, one beam (75/1) exhibited a unique failure mechanism involving the breakage of bottom timber fibers, longitudinal cutting of the CFRP strip near the support, and slippage of the strip from its anchorage. The study also highlighted the influence of natural defects in timber, such as knots, on the effectiveness of the prestressing force. (Halicka & Ślósarz, 2021)



(a) **(b)**

Figure 5.19. (a) Production of prestressed beams, (b) Test set-up (Halicka & Ślósarz, 2021)



Figure 5.20. View of the damaged prestressed beam (Halicka and Ślósarz 2021)

Li et al. (2023) investigated the out-of-plane bending performance of CLT beams reinforced with various FRP fabrics, focusing on CFRP and BFRP. The study involved eight Western hemlock CLT beams, which were reinforced with one to three layers of CFRP, BFRP, or a hybrid of both and subjected to four-point bending tests. The findings indicated that the bending strength and stiffness of the CLT beams improved with an increased FRP volumetric ratio. Notably, three layers of CFRP provided the most significant enhancements, increasing bending strength by 23.8% and stiffness by 18.4%. In contrast, BFRP resulted in smaller increases of 10.0% in strength and 14.1% in stiffness when using three layers. With a single layer, improvements were minimal, with BFRP and CFRP achieving strength increases of 1.4% and 3.0% and stiffness enhancements of 2.5% and 6.7%, respectively. For two layers, the enhancements were more considerable, with BFRP and CFRP showing increases of 8.8% and 10.5% in strength and 11.7% and 13.5% in stiffness. Hybrid configurations, combining both CFRP and BFRP, offered a cost-effective solution, yielding enhancements of 13.1% in bending strength and 8.2% in stiffness, particularly at lower FRP volumetric ratios. The study underscored the importance of utilizing at least two layers of FRP for effective reinforcement, while hybrid configurations presented an economical alternative to full CFRP reinforcement. Despite its relatively lower performance, BFRP's inclusion in hybrid setups with CFRP emerged as a cost-efficient strategy. Moreover, the shift in failure mechanisms from tensile rupture to rolling shear and delamination in transverse layers pointed to the need for additional strengthening in these areas Figure 5.21. (Li et al., 2023)

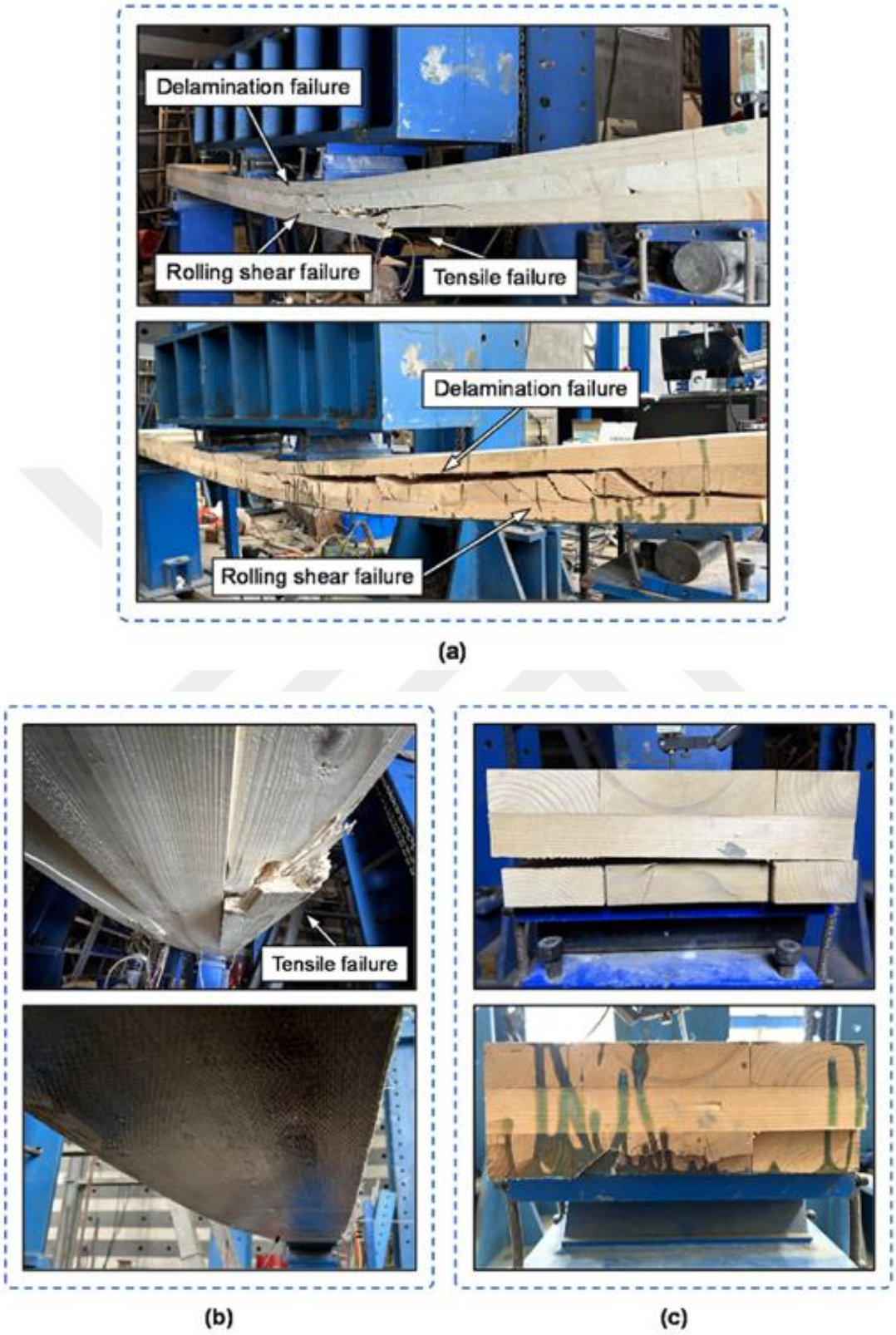


Figure 5.21. Failure mechanisms for specimens without FRP (above) and those reinforced with FRP (below): (a) side surface, (b) bottom surface, and (c) end surface (Li et al., 2023)

Table 5.3. Summary of studies on timber beams reinforced with frp on the bottom face

eam With Bottom Face Reinforcement																	
BFRP		**GFRP**		**CFRP**		**Loading Method**	**Reinforcement Method**					**Beam Dim, (mm)**				**Wood Type**	**REFERENCE**
ST +%*	**BC +%***	**ST +%***	**BC +%***	**ST +%***	**BC +%***		**%W_{frp}/**	**W_{frp}**	**%L_{frp}**	**L_{frp}**	**Num.**	**w**	**a/L**	**a***	**L (clear**		
				15.2	31.5		100	95	100	1800	1	95	0.3	600	1800	spruce (Soild timber)	(Andor et al. 2015)
				9.1	18.2		50	47.50	100	1800	1	95	0.3	600	1800		
				16.3	33.3		100	95	100	1800	2	95	0.3	600	1800		
				31	43		66.7	30	61.7	1000	2	45	0.3	540	1620	Pine GL10 (soild timber)	(Vahedian, et al, 2019b)
				39	52		66.7	30	61.7	1000	4	45	0.3	540	1620		
				43	126		66.7	30	80.2	1300	4	45	0.3	540	1620		
				31	90		100	45	61.7	1000	2	45	0.3	540	1620		
				45	133		100	45	80.2	1300	2	45	0.3	540	1620		
				64	148		100	45	80.2	1300	4	45	0.3	540	1620		
		11.6	82			4- point bending	100	20	100	380	1	20	0.3	127	380	Oakwood	Corradi et al. 2017)
		13.3	65				100	20	100	380	1	20	0.3	127	380	Firwood	
				15.1	122		100	20	100	380	1	20	0.3	127	380	Firwood	
		7.8	47				100	67	100	1320	1	67	0.3	436	1320	Oakwood	
				9.4	36.4		100	67	100	1320	1	67	0.3	436	1320	Oakwood	
		9.1	38				100	100	100	1950	1	100	0.3	644	1950	Firwood	
				11.2	65.6		100	100	100	1950	1	100	0.3	644	1950	Firwood	
				4.7	43.5		50	100	100	4000	2	200	0.3	1200	4000	Oakwood	
		7.9	51				50	100	100	4000	2	200	0.3	1200	4000	Firwood	
				11.9	59		50	100	100	4000	2	200	0.3	1200	4000	Firwood	
					-		0		0			100	0.3	630	1900	Firwood (non-defective)	(Corradi et al. 2021)
				-18	-41		0		0			100	0.3	630	1900	Knot Defect, KD	
				-21	-20		50	50	100	1900	1	100	0.3	630	1900	Knot Defect-Reinforced	

Table 5.3. (Continuous) Summary of studies on timber beams reinforced with frp on the bottom face

Beam With Bottom Face Reinforcement																	
BFRP		GFRP		CFRP		loading method	Reinforcement Method					Beam Dim, (mm)				Wood Type	REFERENCE
ST +%*	BC +%*	ST +%*	BC +%*	ST +%*	BC +%*		%Wf_{rp} /W	W_{frp}	% L_{frp}	L_{frp}	Num. Layer	W	a/L	a*	L (clear		
					41.1	4- point bending	100	38	95.6	650	1	38	0.3	204	680	Glued Laminated Timber (GLT)	(Śliwa-Wieczorek et al. 2021)
					28.5		100	39	95.7	651	3	39	0.3	204	680		
					31.3		100	40	95.9	652	5	40	0.3	204	680		
					5		50	30	33.3	450	1	60	0.3	450	1350	Solid Timber	(Al-Katib, et al. 2022)
					22		50	30	66.7	900	1	60	0.3	450	1350		
					27		50	30	100	1350	1	60	0.3	450	1350		
					13		100	60	33.3	450	1	60	0.3	450	1350		
					73		100	60	66.7	900	1	60	0.3	450	1350		
					76		100	60	100	1350	1	60	0.3	450	1350		
					18		150	30+6	33.3	450	2	60	0.3	450	1350		
					75		150	30+6	66.7	900	2	60	0.3	450	1350		
					73		150	30+6	100	1350	2	60	0.3	450	1350		
2.2	3.1						100	105	100	2940	1	105	0.4	1050	2940	Western Hemlock CLT	(Hao Li et al. 2023)
11.5	9.1						100	105	100	2940	2	105	0.4	1050	2940		
14.1	10.4						100	105	100	2940	3	105	0.4	1050	2940		
				6.7	1.6		100	105	100	2940	1	105	0.4	1050	2940		
				13.4	10.9		100	105	100	2940	2	105	0.4	1050	2940		
				18.2	24.4		100	105	100	2940	3	105	0.4	1050	2940		
		CFRP+BFRP(HYBIRD)		8.2	11.1		100	105	100	2940	2	105	0.4	1050	2940		
				38.9	97.6		60	60	100	1800	1	100	0.3	600	1800	Douglas Fir (Solid	(Song et al. 2024)
				3.6	9.2	3- Point bending	100	45	71.4	1500	1	45	1	1050	2100	LVL	(Globa et al.
					18.00	4-Point Loading	100	100	100	1800	1	100	0.3	500	1800	Cunninghamia lanceolata	(C. Zhang et al. 2022b)
					39.00		100	100	100	1800	2	100	0.3	500	1800		

The provided tables summarize studies on timber beams reinforced with FRPs on their bottom face, focusing on various wood types, beam dimensions, reinforcement materials (CFRP, GFRP, BFRP), and their performance under different loading methods, such as 3-point and 4-point bending and comparing their performance in terms of bearing capacity (BC) and stiffness (ST) relative to control specimens, with results expressed as a +% (ratio increase). The parameter (a) represents the distance between the load and the support. W_{frp} and L_{frp} stand for width and length of FRP respectively. Results show that CFRP consistently provides the highest improvements in stiffness and load-carrying capacity, particularly with multiple reinforcement layers.

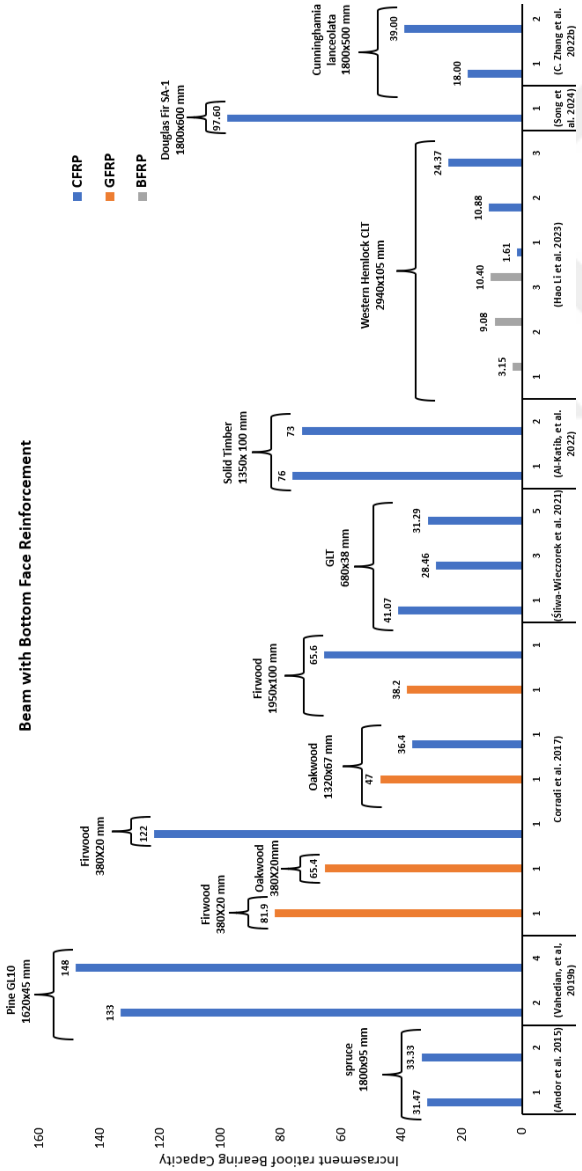


Figure 5.22. Beam with Bottom Face Reinforcement

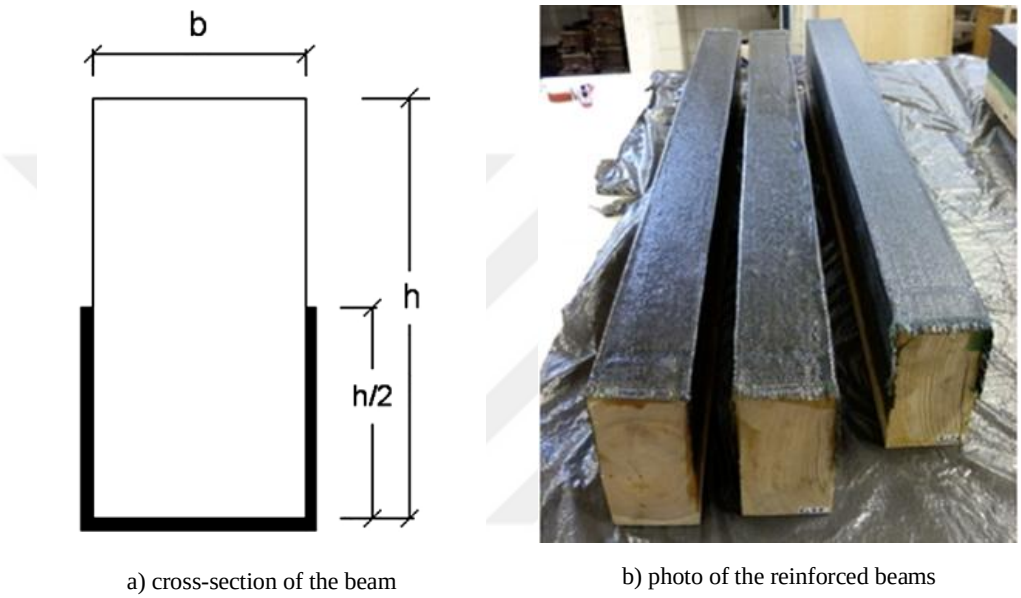
The bar chart illustrates the ratio of bearing capacity increase for timber beams reinforced with CFRP, GFRP, and BFRP, with the x-axis representing different studies and number of layers, and the y-axis showing the percentage increase in bearing capacity as ratio. The parameters analysed include the type of FRP, the number of reinforcement layers, and the type of wood (hardwood vs. softwood). The results reveal that increasing the number of reinforcement layers generally enhances bearing capacity, except in the case of Śliwa-Wieczorek et al. (2021), where using a single layer gave the highest improvement (41.07%). Hardwood, such as Oakwood, demonstrated better performance compared to softwood; for example, Oakwood (1320x67 mm) reinforced with GFRP achieved an 81.9% increase, whereas Firwood (380x20 mm) reinforced with GFRP reached 65.6%, showing a difference of approximately 16.3%. The type of FRP also significantly impacts results: Oakwood (1320x67 mm) with GFRP resulted in a 47% increase, whereas the same specimen with CFRP achieved only 36.2%. This highlights the importance of material selection, where GFRP may outperform CFRP in certain hardwood applications. Overall, the chart emphasizes that both the reinforcement configuration and wood type are critical in maximizing structural performance.

5.1.3. U-Wrap Configuration

FRP sheets are installed on three sides of the beam, creating a U-shaped configuration that usually encompasses the tensile face as well as both lateral faces of the beam.

De La Rosa García et al. (2013) conducted a study on the reinforcement of pine timber beams utilizing carbon (CFRP) and basalt fiber composites (BFRP). They tested a total of 26 beams, including 9 unreinforced and 17 reinforced, employing BFRP (unidirectional 280 g/m² and 600 g/m²) and CFRP (unidirectional 300 g/m² and bidirectional 160 g/m² and 210 g/m²) arranged in a unique “U” configuration for all specimens as illustrate in Figure 5.23 and tests conducted through four-point bending as shown in Figure 5.4. The findings revealed that bidirectional CFRP (160 g/m²) significantly enhanced the ultimate load capacity, with increases of 41.1% for single layers and 43.5% for double layers, on the contrary of unidirectional CFRP with the increase of 3.5%. Meanwhile, unidirectional BFRP (280 g/m²) improved load capacity by 24.6%, surpassing the 15% increase derived from the heavier BFRP (600 g/m²). All reinforced beams exhibited enhanced stiffness, particularly those reinforced with

bidirectional carbon fabrics, while the cost-effectiveness of basalt fibers was highlighted. The Figure 5.25 illustrates the failure modes observed during the experimental tests. The study noted that double-layer reinforcement provided marginal additional advantages over single layers. In conclusion, although CFRP excel in optimizing stress due to their high elastic modulus, BFRP present economic benefits, illustrating that FRP reinforcements significantly improve both load-bearing capacity and stiffness. Table 5.5 summarize failure modes of tested beams. (De La Rosa García, et al. 2013)



a) cross-section of the beam

b) photo of the reinforced beams

Figure 5.23. FRP reinforced beams in the De La Rosa García, et al. 2013 research

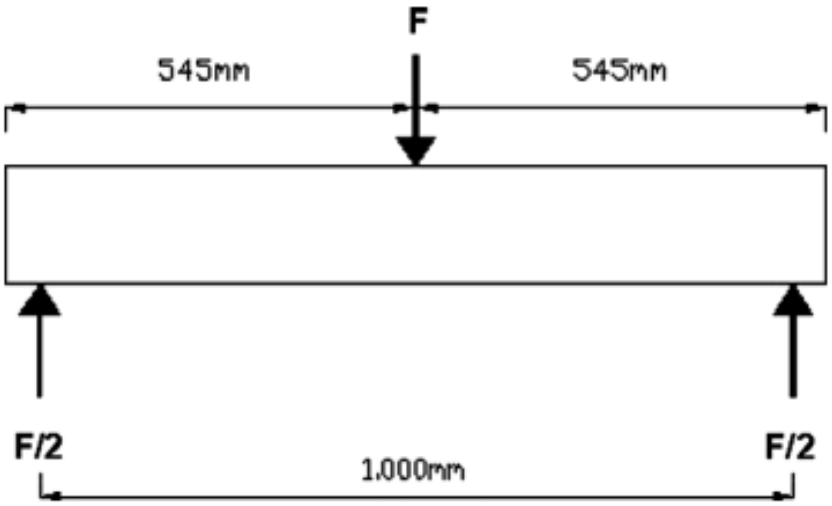
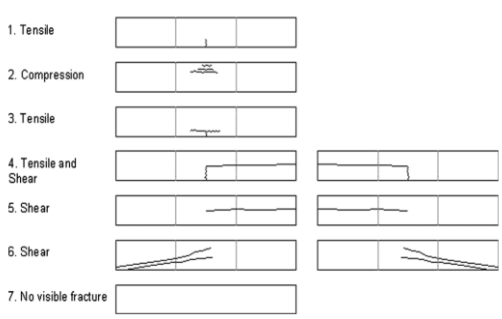


Figure 5.24. Test schème. (De La Rosa García, et al. 2013)



a) failure mechanism of analysed beams



b) beam 45, before and after the test

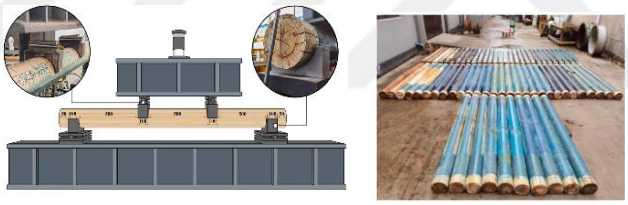
Figure 5.25. Failure mode of tested beams (De La Rosa García, et al. 2013)

Table 5.4. Failure mechanism of tested beams (De La Rosa García, et al. 2013)

Failure mode	Lower fibers tensile stress	Upper fiber compression	Shear	Span center	Influence of drying splits	Influence of fiber inclination	Influence of nodes	Reinforcement detachment	Failure scheme
3SRC	x			x					3
7SRC	x			x			x		3
17SRC	x			x					1
27SRC	x		X			x	x		1
28SRC	x			x					3
32SRC			X						6
45SRC			X		x				5
97SRC	x		X						4
93SRC	x			x					1
56FC300	x						x		3
69FC300	x		X		x				4
72FC300	x			x			x		1
34FB280	x			x				x	7
63FB280			X		x				5
65FB280	x						x		3
40FB600	x						x		1
60FB600	x							x	7
73FB600		x		x					2
89FC160#1			X		x				5
48FC160#1	x		X			x	x		4
15FC160#2	x			x					1
22FC160#2	x								1
8FC210C#1	x			x					1
13FC210#1	x			x			x		1
23FC210#2	x			x					3
83FC210#2	x		X				x		4

Zhang, et al. (2022) conducted a study aimed at creating hybrid fiber-reinforced polymer (HFRP) sheets that are both economically feasible and exhibit high ductility for the reinforcement of timber beams with square and round cross-sections. The research involved testing 68 timber beams see Figure 5.26 (b) made from Cunninghamia lanceolata through a four-point bending method Figure 5.26 (a), exploring various reinforcement configurations, including both single-layer and double-layer HFRP sheets, unidirectional and bidirectional hybrids, and differing reinforcement angles for round beams (such as 45° and 60°). The reinforcing materials used were a blend of carbon fiber, aramid fiber, and glass fiber, optimized in specific ratios. The HFRP sheets were affixed with epoxy resin, with their placement either on the bottom or applied circumferentially, depending on the beam geometry. Results indicated significant improvements in performance, with the reinforcement leading to increases in ultimate bearing capacity by

as much as 106.7%, strength enhancements ranging from 41.9% to 72.6%, and stiffness improvements between 31% and 64%. The most effective reinforcement configuration found was the use of unidirectional sheets with a carbon fiber to aramid fiber to glass fiber ratio of 2:1:1, applied at angles of 45° to 60° for round beams, achieving an optimal balance of strength, ductility, and cost efficiency. The Figures 5.27 and 5.28 illustrate the failure modes observed during the experimental tests. Which can be summarized as follows: Unreinforced timber beams typically exhibited vertical or oblique cracks, with crack initiation influenced by the presence of knots. Cracks in square beams maintained a rectangular surface, while the width of cracks in round beams varied with section height. Reinforced beams showed similar crack patterns but also experienced fiber fractures. Low-toughness sheets (e.g., CFRP) exhibited neat fractures, whereas high-toughness sheets (e.g., C2A1G1) had unbroken fibers contributing to stiffness post-failure. A unique failure mode, debonding, was observed in round beams with bidirectional fiber sheets, attributed to insufficient adhesion and complex stress distributions in round sections. (Zhang et al., 2022)



(a) (b)

Figure 5.26. (a) Test Setup; (b) Diagram illustrating the structure of a device used for bending tests (Zhang et al., 2022)

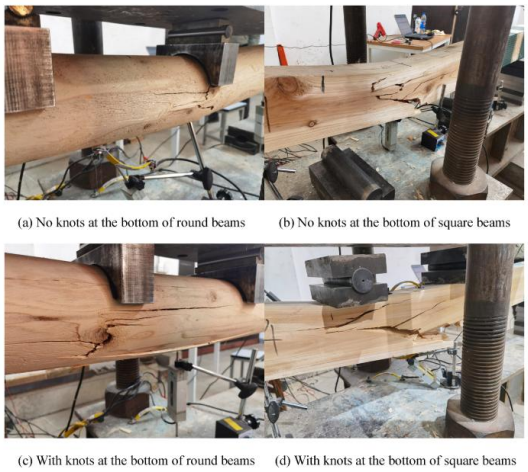


Figure 5.27. Common failure types in unreinforced timber beams (Zhang et al., 2022)



Figure 5.28. Common failure types in unreinforced timber beams (Zhang et al., 2022)

Globa et al. 2018 conducted a study examining the structural performance of laminated veneer lumber (LVL) beams that were reinforced with CFRP in both positive and negative bending moments. The research focused on assessing the impacts of unidirectional and bidirectional CFRP reinforcement on various performance metrics such as load-carrying capacity, stiffness, ductility, and modes of failure, with the goal of enhancing timber applications in multi-story and long-span constructions. The investigation involved testing 21 specimens under three-point bending showing in Figure 5.29, including control beams and those reinforced with different CFRP configurations, such as strips, U-wraps, and combinations of unidirectional and bidirectional CFRP. The results indicated that for positive bending, U-wrap reinforcement resulted in a 25% increase in load capacity, a 20% enhancement in stiffness, and a 30% improvement in ductility, leading to a shift from abrupt to progressive failure modes. In negative bending scenarios, the combination of bidirectional and U-wrap CFRP increased load capacity by 22% compared to unidirectional-only configurations and ensured structural integrity in beam-column joints. Observed failure modes see Figures 5.30 and Table 5.6 included splintering tensile

failure, which was predominant in the control group and characterized by fibrous fractures typical of tough wood. Beams reinforced with CFRP strips exhibited a combination of splintering tensile and cross-grain tensile failures, while those with unidirectional CFRP U-wrap consistently showed cross-grain tensile failure due to the CFRP being applied parallel to the timber grain. Additionally, CFRP fractures were observed in both strengthening schemes, often induced by the failure of the wood fibers, with some instances of CFRP delamination occurring at the point of timber failure. This study highlights the potential of CFRP-timber composites to reduce beam depth, enhance mechanical properties, and postpone catastrophic failures, underscoring their viability for sustainable construction practices.(Globa et al., 2018)

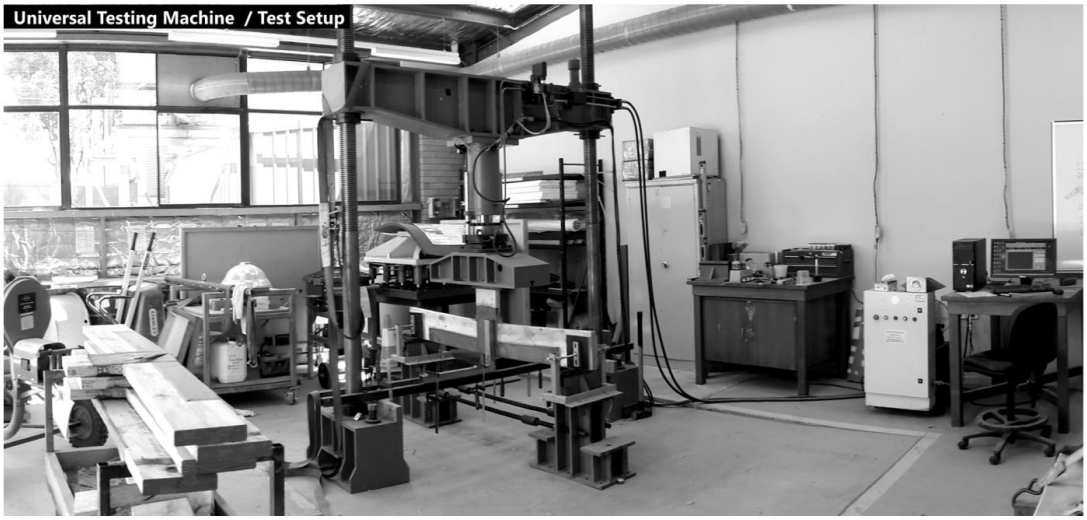
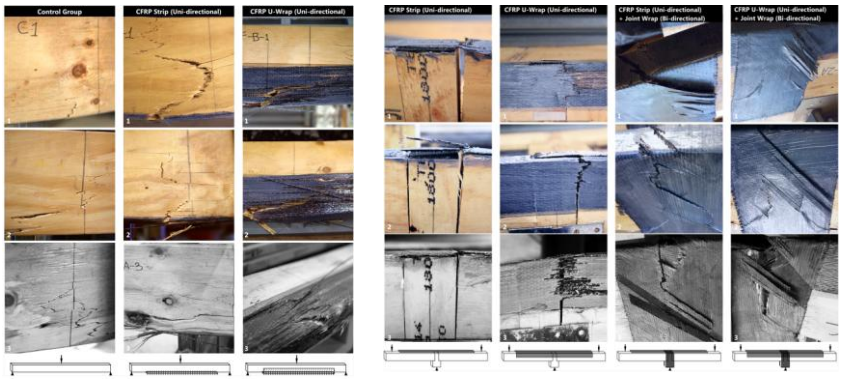


Figure 5.29. Test set-up (Globa et al., 2018)



(a) (b)

Figure 5.30. (a) modes of failure for (+M) bending group; (b) for (-M) bending group (Globa et al., 2018)

Table 5.5. modes of failure. Bending tests (+M) (Globa et al., 2018)

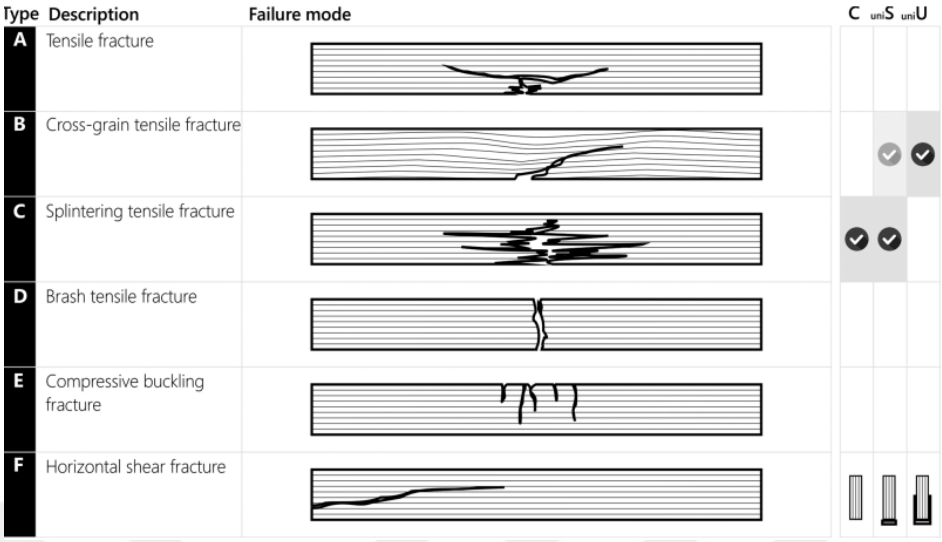


Table 5.6. Summary of Studies on Timber Beams Reinforced with FRP on U-Configuration

Beams Reinforced with U- Configuration													
Reference	**Wood Type**	**L (clear span)**	**Beam Dimension (mm)**				**FRP Dimension (mm)**				**Loading Method**	**BC+%***	
			a	**a/L**	**w**	**D**	**Layer**	**%Lfrp/L**	**%Wfrp/W**	**%Dfrp/D**		**CFRP**	**BFRP**
(De La Rosa García, et al. 2013)	Pinus Sylvestris	1000	500	0.5	78	155	280gm	100	100	50	3-Point Loading		24.6
		1000	500	0.5	78	155	600gm	100	100	50			15
		1000	500	0.5	78	155	300gm	100	100	50		3.5	
		1000	500	0.5	78	155	160gm	100	100	50		41.1	
		1000	500	0.5	78	155	160gm X2*	100	100	50		43.5	
		1000	500	0.5	78	155	210gm	100	100	50		10	
		1000	500	0.5	78	155	210gm X2	100	100	50		1.1	
(Globa et al. 2018)	LVL	2100	1050	0.5	45	230	1	71.4	100	50		25.1	

This table summarizes studies on timber beams reinforced with FRP on the bottom face, comparing their performance in terms of bearing capacity (BC) relative to control specimens, with results expressed as a +% (ratio increase). The parameter (a) represents the distance between the load and the support. Wfrp and Lfrp stand for wwidth and length of FRP respectively. X2 means two layers.

5.1.4. Near-Surface Mounted

Yeboah and Gkantou 2021 conducted an experimental investigation into the flexural behavior of white spruce timber beams reinforced through the Near-Surface Mounted

(NSM) technique using (BFRP) and (GFRP) bars Figure 5.31. The study involved a total of 20 beams, including unreinforced control specimens, subjected to four-point bending Figure 5.32 with two reinforcement configurations: one featuring two bars in the tensile zone and another with bars in both tensile and compression zones. The results revealed substantial enhancements in flexural performance, with reinforced beams exhibiting an increase in ultimate load capacity ranging from 33% to 69% (51.90 kN to 65.80 kN) compared to the unreinforced average capacity of 38.97 kN. Additionally, flexural stiffness improved by 22% to 39% (EI between 4.51E+11 and 4.91E+11 Nmm²), while the average mid-span displacements at failure increased by 34%, suggesting enhanced ductility. The predominant failure mode observed was brittle tensile failure of the timber in the tensile zone for both reinforced and unreinforced specimens. The introduction of NSM BFRP and GFRP bars decreased variability in ultimate performance, demonstrating their efficacy in counteracting timber defects, although the inclusion of reinforcement in the compression zone provided only marginal additional benefits compared to reinforcement solely in the tensile zone. The Figures 5.33 illustrates the failure modes observed during the experimental tests. (Yeboah & Gkantou, 2021)

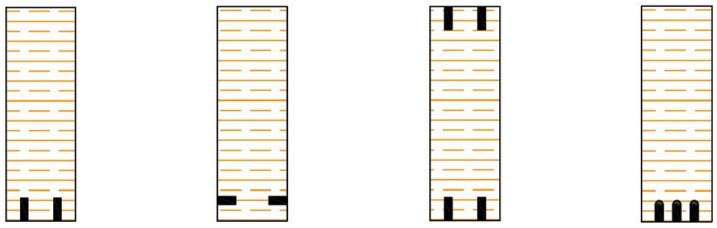


Figure 5.31. NSM reinforcement configurations: Bottom single reinforcement with 2, 3 bars in rectangular grooves, with in the lateral side and double bottom and top (Yeboah and Gkantou 2021)

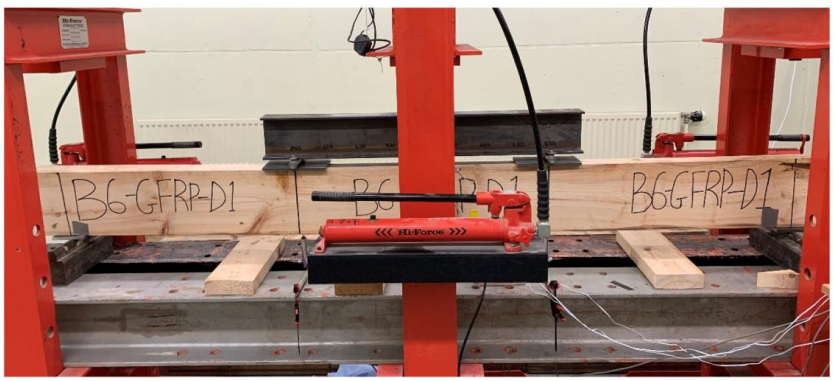


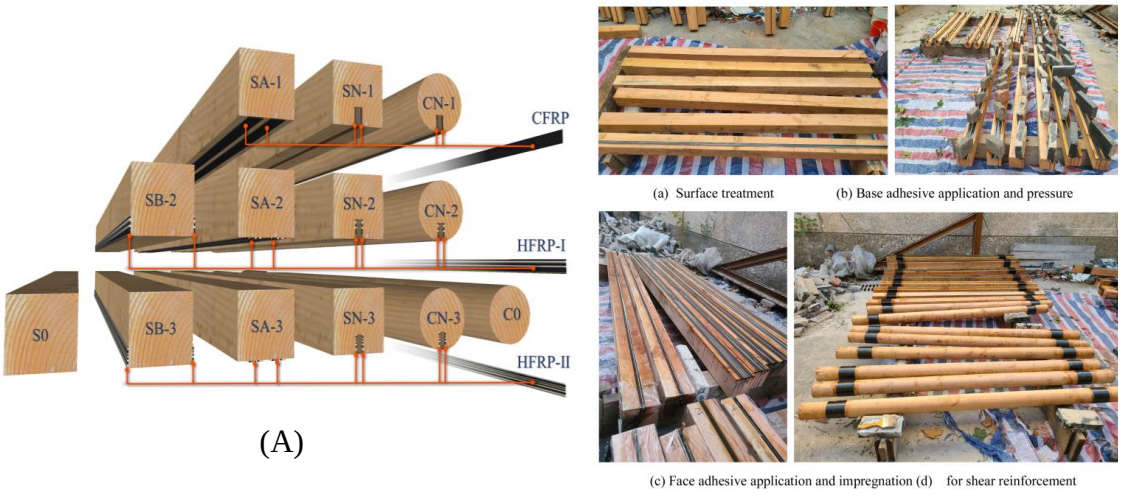
Figure 5.32. Experimental set-up (Yeboah and Gkantou 2021)



Figure 5.33. Typical failure modes (Yeboah and Gkantou 2021)

Song et al. (2024) conducted an experimental analysis focused on the flexural performance of Douglas Fir timber beams featuring both circular and square cross-sections, which were reinforced using Hybrid Fiber Reinforced Polymer (HFRP) plates made from varying ratios of carbon, aramid, and glass fibers. The study included 26 specimens categorized by cross-section geometry, reinforcement strategies (Near-Surface Mounted (NSM) and externally bonded plates), and fiber compositions (HFRP-I, HFRP-II, CFRP) Figure 5.34. A three-point bending test was performed to assess their flexural characteristics. The findings revealed that circular beams reinforced with NSM plates exhibited the most substantial enhancements, achieving a 39.2% to 60.4% increase in ultimate bearing capacity and a 21.8% to 33.3% improvement in stiffness, whereas square beams showed increases of 14.7% to 39.1% in capacity and 1% to 9.7% in stiffness. Notably, bottom bonding of FRP plates outperformed side bonding, leading to a

remarkable 77.65% rise in bearing capacity. Among the reinforcement options tested, HFRP-I plates, composed of a carbon-aramid-glass fiber ratio of 2:1:1, resulted in the most significant overall enhancements, with bearing capacity increases ranging from 39.1% to 104.5% alongside balanced improvements in stiffness and ductility. These results underscore the effectiveness of HFRP plates, particularly in NSM configurations, to significantly improve the flexural performance of timber beams. Figure 5.35 illustrates the failure modes observed during the experimental tests. Which could be summarized as follows: All specimens primarily failed due to bottom tensile damage. Unreinforced beams exhibited brittle failure, while those with externally bonded FRP reinforcement also showed brittle characteristics but included signs of interfacial separation and delamination at the FRP-wood interface. In contrast, near-surface-mounted (NSM) FRP-reinforced beams exhibited more gradual failure due to improved bonding and mechanical anchorage, leading to slower crack propagation and better energy dissipation. For circular beams, top compression wrinkling was also observed, reflecting plastic deformation. Fiber delamination occurred in side-bonded FRP reinforcements, highlighting the influence of shear forces and interlayer strength on failure mechanisms. (Song et al., 2024)



(A)

(B)

Figure 5.34. (A) Specimen number and characteristics, (B) Reinforcing process of test specimens. (Song et al. 2024)

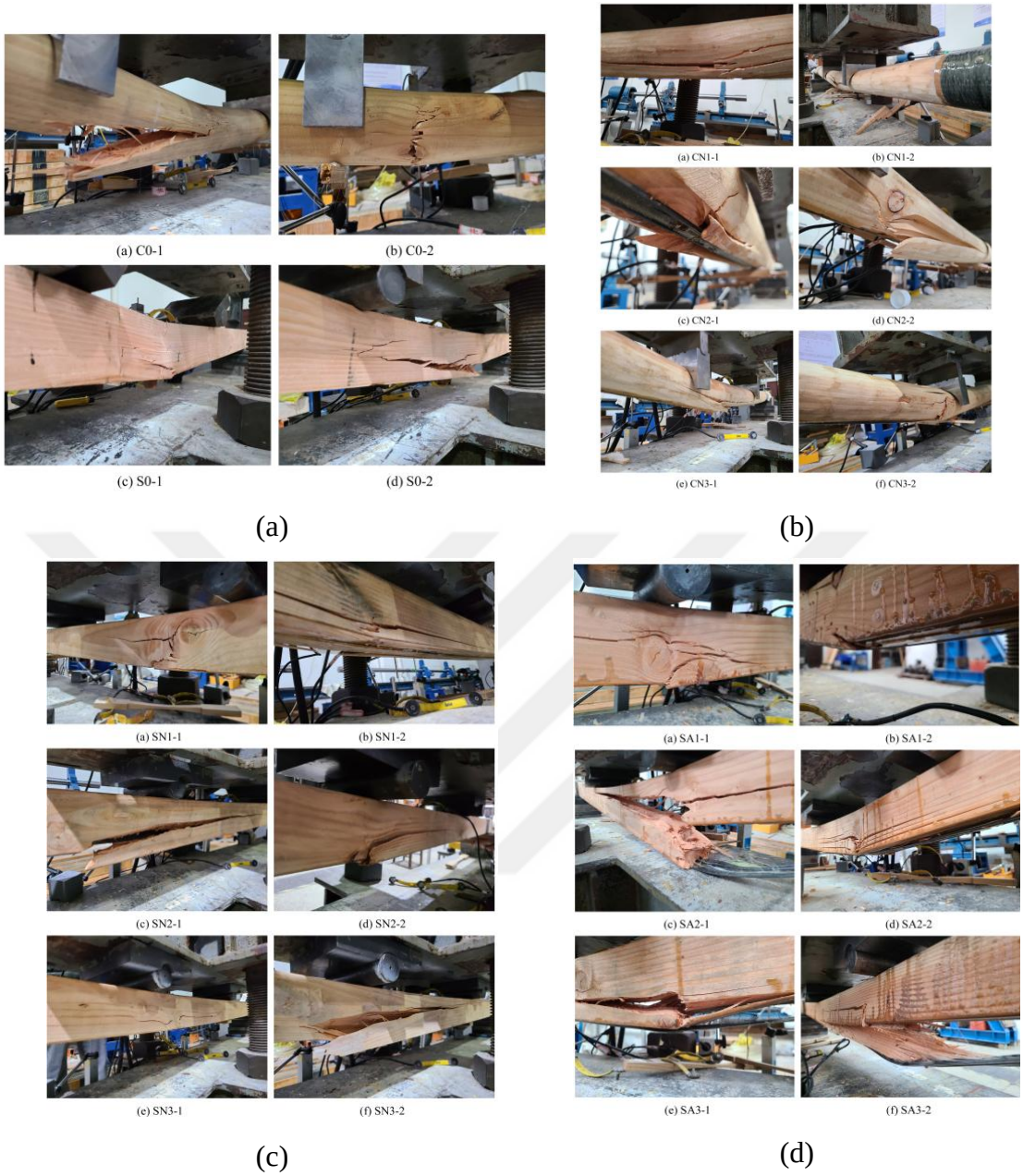


Figure 5.35. (a) Failure modes of unreinforced specimens; (b) NSM reinforcement circular specimens, (c) NSM reinforcement square specimens, (d) Bottom external bonding reinforcement (Song et al. 2024)

5.1.5. Pultruded FRP Bars

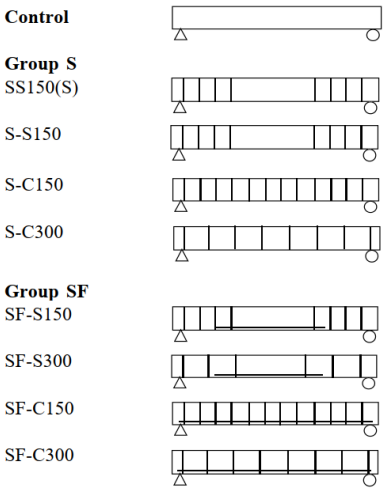
FRP bars can either be integrated into the timber or attached to the outside surface to provide reinforcement.

Svecova and Eden (2004) conducted a study at the University of Manitoba to evaluate the efficacy of GFRP reinforcement in salvaged Douglas Fir timber stringers. They tested 50 timber beams using two reinforcement strategies: shear dowels for 21 beams (group S)

and a combination of shear and flexural reinforcements for 20 beams (group SF) see Figure 5.36 (b). Through four-point bending tests see Figure 5.36 (a), group S exhibited a 17% to 35% increase in modulus of rupture (MOR), while group SF achieved an increase of 47% to 52%. The findings demonstrated that GFRP reinforcement not only enhanced stiffness but also reduced strength variability, with group SF displaying semi-ductile behavior and distinct failure modes compared to the control beams. Among the tested specimens, most failures occurred due to simple tension, with some experiencing cross-grain tension or horizontal shear failures. The introduction of flexural reinforcement aimed to mitigate weaknesses in the beam's tension zone to prevent tension failure Figure 5.37. Out of 50 specimens, 12 (24%) failed in cross-grain tension, 4 (8%) in horizontal shear, 5 (10%) in compression, while 29 (58%) failed in simple tension. The initial cracking in most specimens was found to originate from defects or discontinuities in the tension zone near mid-span. The study concluded that the most effective reinforcement strategy combined continuous shear dowels with flexural reinforcement, leading to compression failure instead of tension failure and enabling efficient load transfer after cracking. The load-deflection curves of beams in group SF became pseudo-ductile see Figure 5.40, with 60% of the tested beams displaying twice the deflection of the control beams. Despite some localized debonding of the GFRP reinforcement, the overall bond strength between the GFRP, timber, and epoxy remained robust. (Svecova and Eden, 2004)

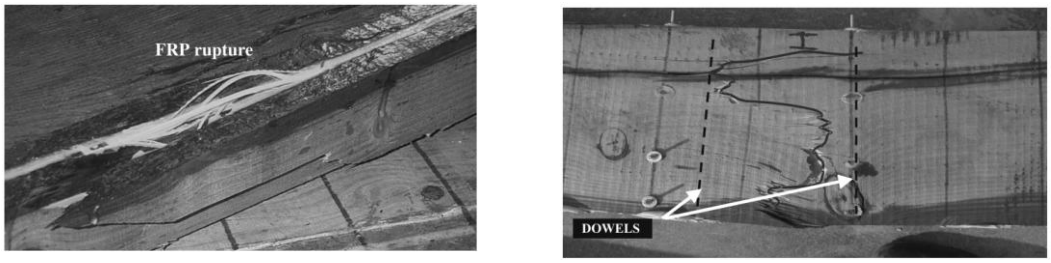


(a)



(b)

Figure 5.36. (a) Test setup, (b) Specimens configuration (Svecova and Eden, 2004)



(a) (b)

Figure 5.37. Tension failure (a) GFRP flexural reinforcement, (b) beams reinforced with dowels (Svecova and Eden, 2004)

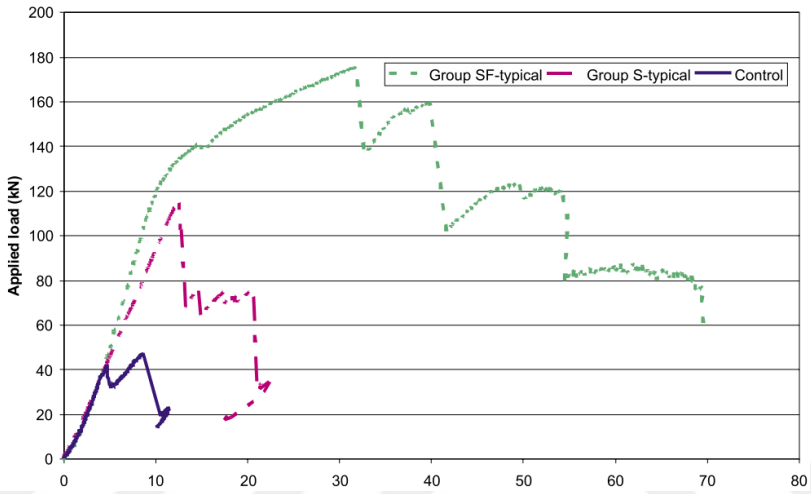


Figure 5.38. The effect of strengthening on load–deflection behaviour (Svecova and Eden, 2004)

Kliger et al. (2008) conducted a comprehensive experimental and analytical investigation into the performance of glulam timber beams reinforced with CFRP laminates and steel plates, emphasizing both short- and long-term behavior. The study encompassed 33 specimens, consisting of 9 beams shown in Figure 5.39 (a) featuring various reinforcement configurations for short-term bending assessments and 24 beams depiction in Figure 5.39 (b) designated for long-term creep analysis. The glulam beams measured 115 × 200 × 4000 mm, with the reinforcements installed in grooves along their length and bonded using epoxy adhesive. The configurations examined included reinforcement solely on the tension side, on both sides, and different reinforcement percentages utilizing high-strength or high-stiffness CFRP and steel. In the short-term tests conducted through four-point bending, the reinforced beams exhibited significant enhancements, with ultimate moment capacities increasing between 57% and 95.8% and stiffness improvements reaching up to 100%. The failure modes differentiated between

unreinforced beams, which failed in tension, and heavily reinforced beams, which experienced shear failure. Long-term creep assessments on smaller pinewood specimens (45 × 70 × 1100 mm) indicated that the reinforced beams showed diminished initial deflections and mechano-sorptive creep in contrast to unreinforced counterparts. However, substantial moisture fluctuations led to increased deflection changes in reinforced beams, particularly those with tension-only reinforcement. The findings concluded that reinforcing both the tension and compression sides effectively alleviated moisture-related challenges and permitted increases in span by up to 20% or reductions in beam size by 25%, without compromising overall performance. The research demonstrated that reinforcement strategies substantially improved strength, stiffness, and moisture-induced stability, highlighting the potential of CFRP and steel for the enhancement of timber beams. (Kliger et al., 2008)

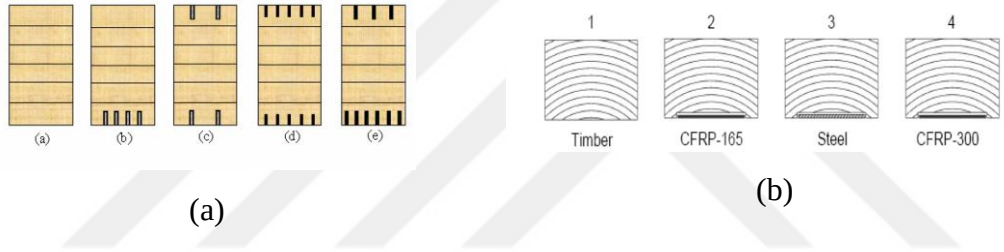
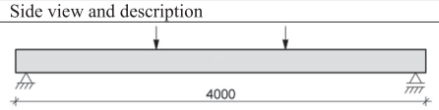
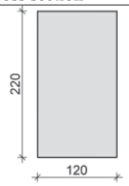
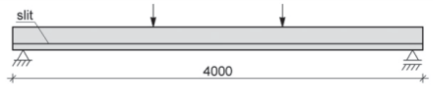
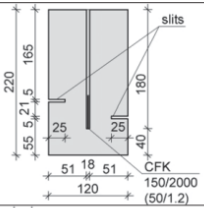
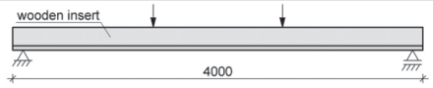
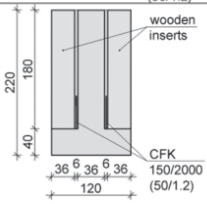
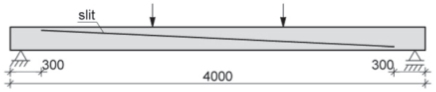
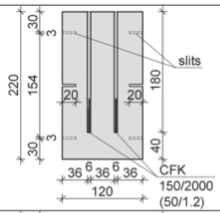
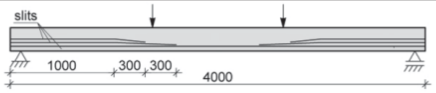
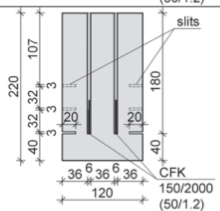
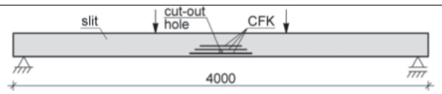
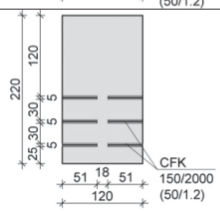


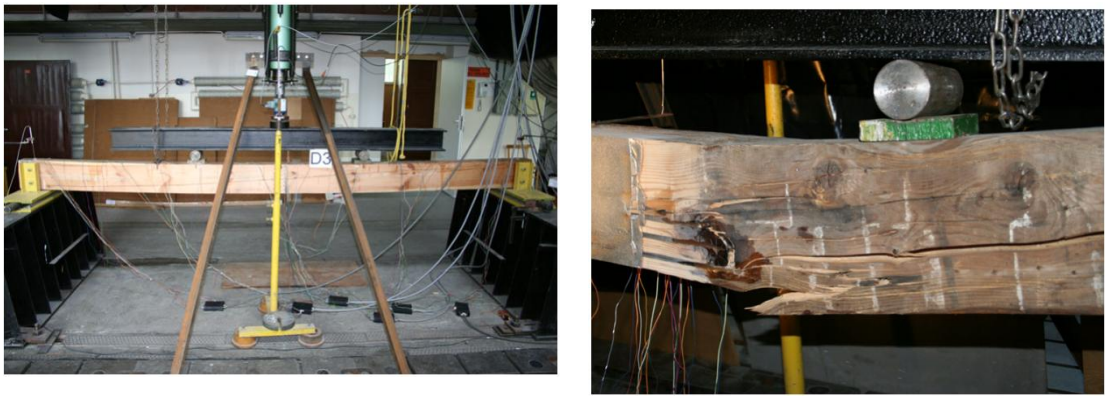
Figure 5.39. Reinforcement configurations (a) for short term; (b) for creep test specimens (Kliger et al. 2008)

Nowak et al. 2013 conducted a study to evaluate the effectiveness of CFRP strips in restoring and improving the structural integrity of historic timber beams that have suffered from defects such as biological decay, inclusions, and cracks. The research involved 21 specimens see table 5.8, comprising 18 century-old pinewood (Pinus sylvestris L.) beams alongside 3 newly fabricated beams. CFRP strips were bonded vertically into the cross-section of the beams using epoxy resin. The beams underwent four-point bending tests as shown in Figure 5.40 (a). The results indicated that CFRP-reinforced beams exhibited an increase in load-bearing capacity between 21% and 79%, contingent upon the specific reinforcement configuration employed. Stiffness enhancements were observed within a range of 14% to 32%, with significant reductions in the adverse effects of wood defects on failure modes see Figure 5.40 (b). The failure modes observed in the specimens could be summarized as follows: All tested beams primarily failed in the tension zone, particularly in areas with defects such as knots, grain

slopes, or biological corrosion. In beams reinforced with CFRP strips, failure occurred outside the reinforced regions, suggesting effective reinforcement in the strengthened zones. There were no instances of failure due to delamination at the strip-wood interface, indicating strong adhesion. However, the reinforcement method's efficacy was somewhat limited by the placement of strips away from the extreme tension fibers. Brittle cracking dominated in unreinforced beams, while reinforced specimens exhibited better load distribution and higher resistance before failure. (Nowak et al., 2013)

Table 5.7. Beam Configurations (Nowak, et al. 2013)

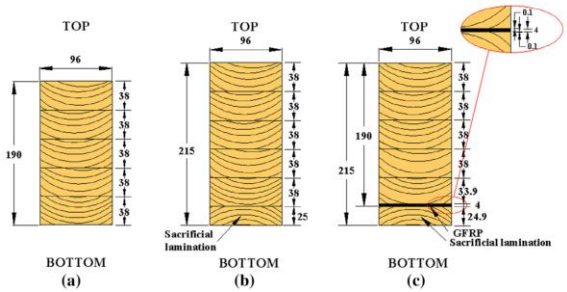
Beam series	Side view and description	Cross section
A, G	 Series A – reference beams, unreinforced, made of hundred-year-old timber; Series G – reference beams, unreinforced , made of new timber.	
B	 Beams reinforced with a single CFRP strip, wood cracking simulated by 4 mm wide and 25 mm deep slits along the whole length.	
C	 Beams with their corroded sides removed and replaced with wooden inserts. Two vertically arranged CFRP strips bonded in along the whole beam length.	
D	 Beams reinforced with two bonded-in CFRP strips vertically arranged along the whole length. Nonuniform wood grain simulated by 3 mm wide and 20 mm deep bilateral slits.	
E	 Beams reinforced with two bonded-in CFRP strips vertically arranged along the whole length. Wood grain simulated by a pattern of three 3 mm wide and 20 mm deep slits nonparallel to the beam's longitudinal edge.	
F	 Beams reinforced with three respectively 400, 500 and 600 mm long CFRP strips horizontally arranged in the maximum bending moment zone. The weakening of the tensioned zone is simulated by round hole 25 mm in diameter.	



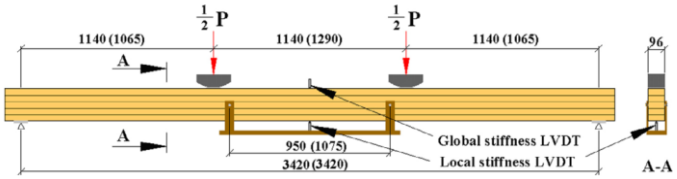
(a) **(b)**

Figure 5.40. (a) Test rig with beam D3 subjected to bending test, (b) Mechanism of failure of beam (Nowak et al., 2013)

Raftery and Rodd (2015) conducted research aimed at improving the structural performance of low-grade GLT beams by utilizing pultruded GFRP plates bonded with phenol resorcinol formaldehyde (PRF) adhesive. The study involved 21 specimens of Irish-grown Sitka spruce, which were divided into three categories: A (unreinforced-190), B (unreinforced-215), and C (reinforced-215) see Figure 5.41 (A) under four-point test as showing in Figure 5.41 (B). Implementing a reinforcement percentage of 1.86% of the cross-sectional area resulted in a notable performance enhancement, as testing with applied moments revealed a 31% increase in ultimate moment capacity and an 18% improvement in stiffness for the reinforced beams. Specifically, the performance of Phase C beams showed a 41.7% enhancement compared to Phase A, attributed to the addition of the GFRP plate and sacrificial lamination. Furthermore, predictions based on mechanical properties indicated a mean stiffness increase of 14%, while ultimate moment capacity enhancements exceeding 60% were observed, along with improved compressive strain behavior in the reinforced beams, underscoring the efficiency of FRP reinforcement in mitigating timber defects. The unreinforced control beams demonstrated linear elastic load–deflection behavior until failure, which occurred at defects in the bottom tension zone due to the low-grade timber, resulting in catastrophic failures. The Figure 5.42 illustrate the failure modes observed during the experimental tests. (Raftery and Rodd, 2015)



(a)



(b)

Figure 5.41. (a) Beam arrangements, (b) Stiffness test arrangement (Raftery and Rodd, 2015)



(a)



(b)



(c)



(d)

Figure 5.42. (a) Tension failure at defect in the Beam, (b) Compression wrinkling, (c) GF attached to sacrificial lamination demonstrating quality of bond, (d) Failure initiated from knot (Raftery and Rodd, 2015)

Fossetti et al. (2015) performed an experimental and analytical study to assess the short-term flexural performance of glulam beams made of GL24h spruce timber that were reinforced with FRP cords, positioning this approach as an alternative to traditional pultruded bars. The research included 15 small-scale specimens and 8 large-scale

specimens, utilizing CFRP, GFRP cords and Basalt rods that were adhered into rectangular grooves with either epoxy resin or melamine glue. The testing involved four-point bending Figure 5.43 to evaluate the effect of the reinforcement on the beams' load capacity and stiffness. The findings revealed that CFRP-reinforced beams experienced up to a 25% increase in strength and a stiffness improvement ranging from 10% to 19%. Additionally, specimens reinforced with basalt exhibited superior ductility and post-failure behavior, achieving an ultimate strain increase of around 40%. While challenges such as excessive resin application adversely affected elastic modulus and reinforcement efficiency were noted, the proposed reinforcement method successfully modified failure modes, thereby enhancing the overall performance and safety of the beams. Figures 5.44, 5.45 and 5.46 illustrate the failure modes observed during the experimental tests, which include brittle tension cracking in unreinforced beams, typically initiated at knots or weak zones and propagating longitudinally along the timber layers. In beams with low shear span-to-depth ratios, failure was a combination of bending and shear effects, often resulting in delamination between layers and occasional crushing at supports. Reinforced specimens exhibited a shift in failure mode, with compressive crushing of the upper timber layer occurring after tensile cracks, particularly in beams reinforced with basalt rods or FRP cords. However, reinforcement effectiveness was compromised in some cases by weak bonding between adhesives and wood, insufficient soaking of FRP cords, and damage caused by grooves introduced for reinforcement installation. Basalt-reinforced beams showed the best performance, with enhanced ductility and strength, while GFRP and CFRP reinforcements were less effective due to bonding and material limitations. (Fossetti et al., 2015)

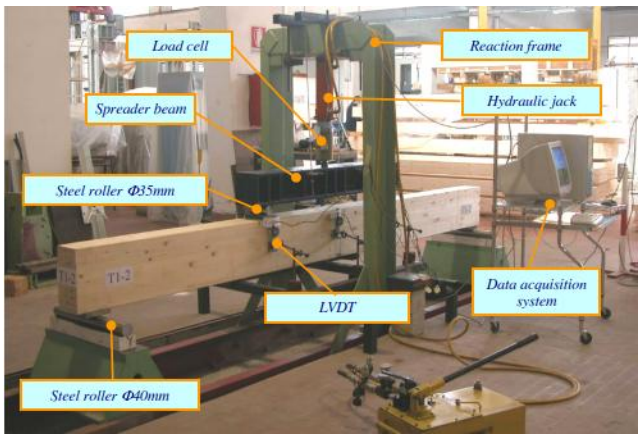


Figure 5.43. Test setup of tested specimens (Fossetti et al., 2015)



Figure 5.44. Failure modes for control specimens (Fossetti et al., 2015)

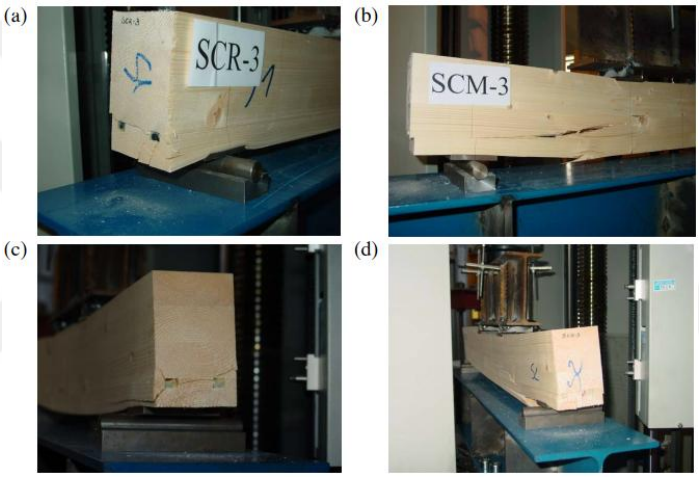


Figure 5.45. (a) SCR (CFRP + epoxy resin), (b) SCM (CFRP + melamine glue), (c) SVR (GFRP + epoxy resin), (d) SVM (GFRP + melamine (Fossetti et al., 2015)



Figure 5.46. (a) specimens HV (GFRP + epoxy resin), (b) specimens (basalt rods + epoxy resin) (Fossetti et al., 2015)

Yang et al. (2016) conducted a comprehensive investigation into the flexural performance of homogeneous glulam beams reinforced with (FRP) and steel. Testing included 46 Douglas fir specimens, organized into 16 series shown in Figure 5.47, subjected to monotonic four-point bending until failure. Each beam, measuring 6.0 m in length and with dimensions of 75 mm × 300 mm and a lamination thickness of 31 mm, underwent conditioning for 7 days prior to testing, which adhered to BS EN 408:2010 standards. Reinforcement configurations varied, including longitudinally slotted steel or FRP bars and bonded FRP plates, with lateral restraints to mitigate buckling. The results indicated that reinforced beams showed marked enhancements in structural performance, with ultimate load-bearing capacities increasing by up to 56.3%, while moderate reinforcement achieved an average failure load of 68.2 kN. Improvements in tensile strain at failure were noted, particularly in vertical plate-reinforced beams, where increases averaged 49.4%. Although steel-reinforced beams exhibited a maximum stiffness increase of 27.5%, FRP-reinforced beams showed more modest gains. Failure modes differed based on reinforcement type: unreinforced beams failed in brittle tension, while moderately reinforced beams displayed ductile compression failure. The study concluded that tensile reinforcement with high-modulus materials significantly improves glulam beams' structural performance, whereas compressive reinforcement offered limited benefits. The Figure 5.48 and Table 5.9 illustrates the failure modes observed during the experimental tests. (Yang et al., 2016)

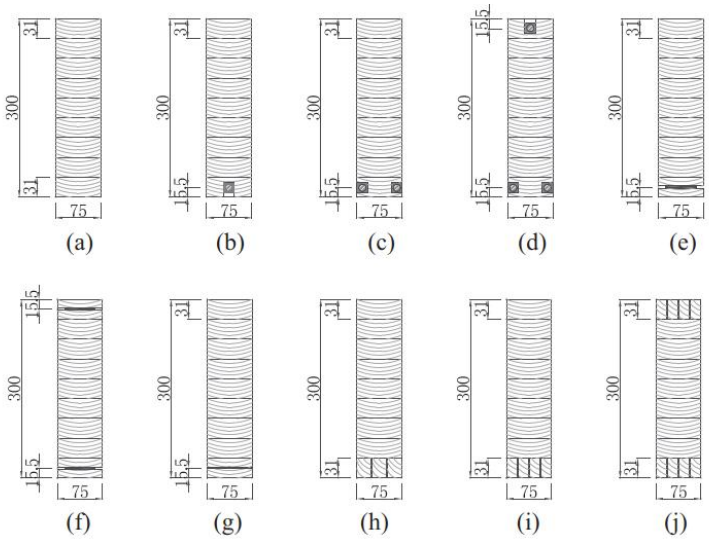


Figure 5.47. Beam configurations (Yang et al., 2016)

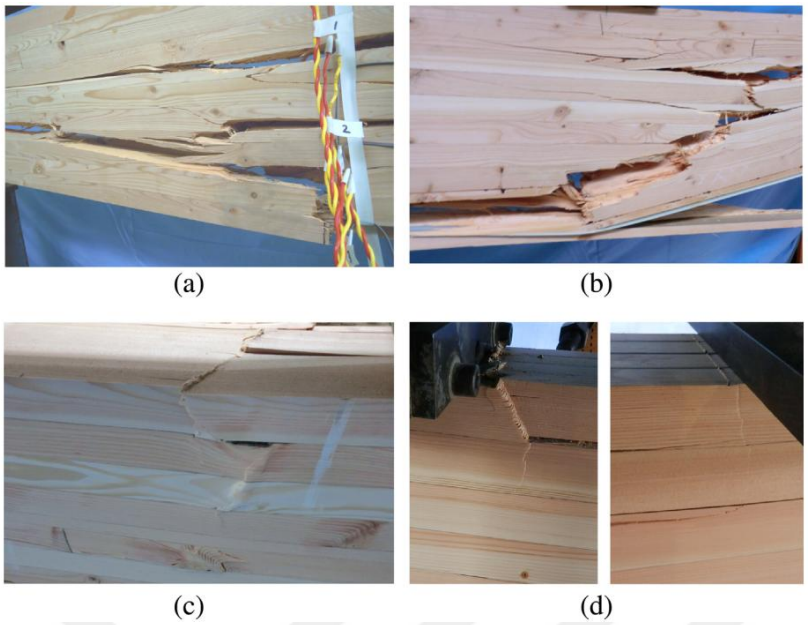


Figure 5.48. Typical beam failure modes include (a) unreinforced beams failing under tension; (b) weakly reinforced beams failing under tension; (c) moderately reinforced beams failing under compression; (d) compression failure of moderately reinforced beams by vertically CFRP plate reinforced beams (Yang et al., 2016)

Table 5.8. Comparison of experimentally obtained results (Yang et al., 2016)

Group no.	Series type	Failure moment M_u (kN m)	Stiffness $E_{mg}I$ (10^{12} N mm^2)	Mid-span deflection at ultimate load Δ_u (mm)	Failure modes
1	C	48.3	2.06	84.0	Tension[b]
2	GR0.5	53.8	2.12	97.0	Tension[b]
	% Increase[a]	11.3	3.1	15.5	–
3	GR1.0	54.5	2.10	97.4	Tension[b]
	% Increase[a]	12.7	2.0	16.0	–
4	GR1.8	61.8	2.16	119.9	Tension[b]
	% Increase[a]	27.8	4.9	42.7	–
5	GR1.8 + 0.5	64.8	2.19	112.7	Tension[b]
	% Increase[a]	34.1	6.6	34.2	–
6	SR1.0	64.0	2.43	100.3	Tension[b]
	% Increase[a]	32.4	18.0	19.5	–
7	SR1.8	69.8	2.62	112.7	Compression
	% Increase[a]	44.5	27.5	34.1	–
8	GP0.27	47.4	1.94	101.0	Tension[b]
	% Increase[a]	−1.8	−5.6	20.3	–
9	GP0.53	55.0	2.01	121.1	Tension[b]
	% Increase[a]	13.7	−2.3	44.2	–
10	GP0.80	53.6	2.10	106.6	Tension[b]
	% Increase[a]	11.0	2.0	26.9	–
11	GP0.53 + 0.27	54.3	2.06	100.1	Tension[b]
	% Increase[a]	12.3	0.5	19.2	–
12	CP0.67	58.4	2.08	108.1	Tension[b]
	% Increase[a]	20.8	1.3	28.6	–
13	CP-V0.33	64.6	2.18	127.4	Tension[b]
	% Increase[a]	33.7	6.2	51.7	–
14	CP-V0.66	75.5	2.13	139.5	Tension[b], Compression
	% Increase[a]	56.3	3.7	66.1	–
15	CP-V0.99	71.4	2.17	153.9	Compression
	% Increase[a]	47.7	5.8	83.2	–
16	CP-V0.66 + 0.66	73.3	2.44	129.3	Tension[b], Compression
	% Increase[a]	51.6	18.5	53.9	–

[a] Improvement compared to the unreinforced control beam based on average values.
[b] Tensile failure of wood in tension zone of glulam beams.

Shekarchi et al. (2020) investigated the flexural performance of beech timber beams (Fagus orientalis) reinforced with pultruded (GFRP) profiles through an experimental study that included 24 beams, consisting of 4 unreinforced control samples and 20 reinforced specimens with varying GFRP configurations as shown in Figure 5.49. The

beams underwent three-point bending tests while their load-deflection responses were monitored until failure occurred. The findings revealed that GFRP reinforcement significantly enhanced both the load-bearing capacity and stiffness of the beams, with improvements of 15.94%, 22.01%, 28.59%, 47.56%, and 60.68% in ultimate bearing capacity for the different reinforcement phases compared to control beams, alongside stiffness increases of 16.47%, 26.16%, 32.01%, 48.36%, and 58.88%. The load versus mid-span displacement diagram for timber beams in phases A to F shows that all beams initially exhibit linear behavior followed by nonlinear responses. As the loading increases, the slope of the diagrams decreases, indicating a change in flexural response. A comparison of the typical flexural response across all phases is provided in Figure 5.50. The failure mechanisms observed varied among the configurations, with control beams experiencing sudden tensile rupture, whereas reinforced beams demonstrated progressive failure modes shown in Figure 5.51, including GFRP debonding, tensile rupture, and localized buckling. Phase F, featuring GFRP channels on both surfaces, exhibited the most significant enhancements in mechanical performance and predictable flexural behavior due to reduced variance. Furthermore, the study highlighted a remarkable increase in energy absorption capacity, which improved by up to 209.32%, emphasizing the efficacy of pultruded GFRP profiles in enhancing the strength and ductility of timber beams for structural applications. (Shekarchi et al., 2020)

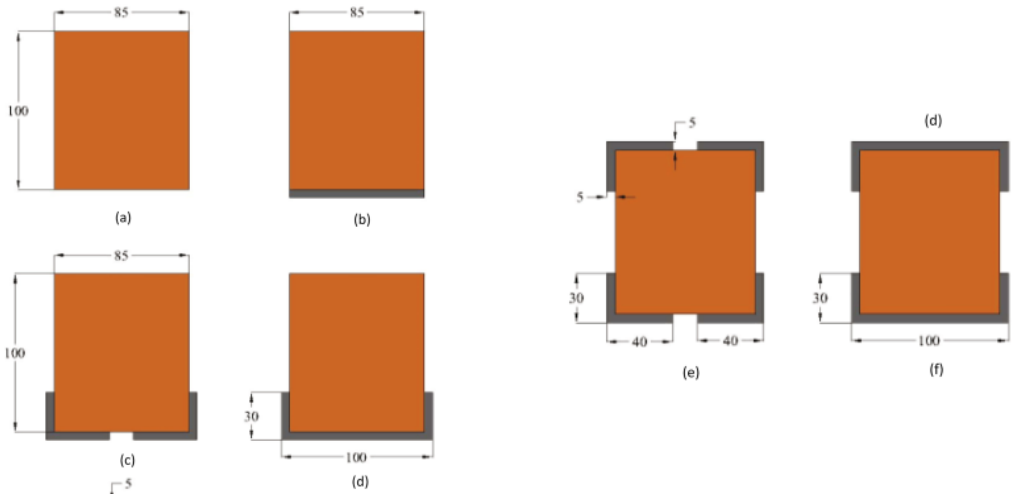


Figure 5.49. Configurations of strengthened beams: (a) Phase A, (b) Phase B, (c) Phase C, (d) Phase D, (e) Phase E, and (f) Phase F (mm) (Shekarchi et al., 2020)

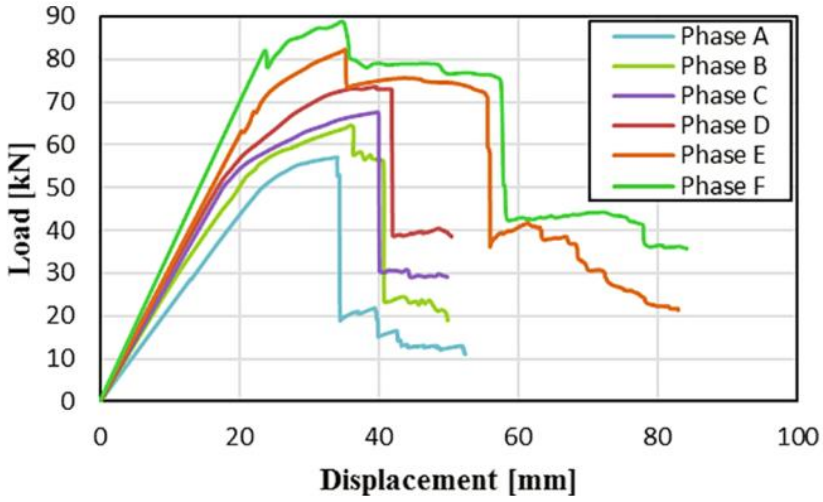


Figure 5.50. Each phase's typical load-deflection behaviour (Shekarchi et al., 2020)



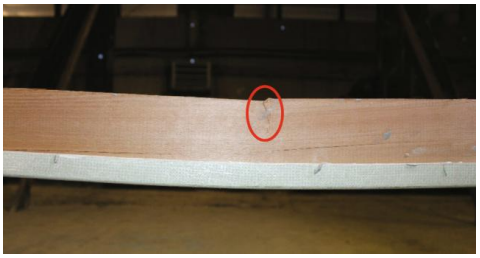
Phase A



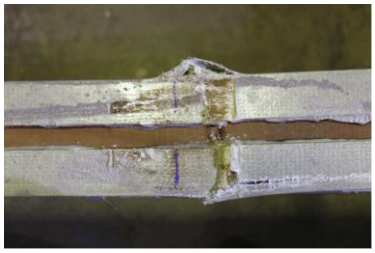
Phase B



Phase C (Rupture)



Phase D (compression buckling)



Phase E (Localised top GFRP failure)



Phase F (Timber tensile failure)

Figure 5.51. Typical failure modes for all phases (Shekarchi et al., 2020)

İşleyen et al. (2021) conducted a comprehensive experimental investigation into the flexural performance of glulam timber beams reinforced with (CFRP) strips, focusing on three key factors: the number of lamellas in the glulam beams, the quantity of CFRP strips employed, and the incorporation of fan-type CFRP anchors see Figure 5.52. The glulam beams were subjected to three-point bending tests to evaluate their load-displacement behavior, ultimate load capacity, initial stiffness, energy dissipation, and failure mechanisms. The findings revealed that increasing the number of lamellas from three to four led to average enhancements of 11% in ultimate load capacity, 24% in initial stiffness, and 13% in energy dissipation, with similar improvements observed when moving from four to five lamellas. The implementation of CFRP fan-type anchors resulted in increases of 30%, 20%, and 26% in ultimate load capacity, stiffness, and energy dissipation, respectively, when compared to specimens without anchors, although ductility ratios did not change. The addition of one CFRP strip on the tensile surface improved ultimate load capacity, stiffness, and energy dissipation by 35%, 43%, and 60%, respectively, relative to unreinforced beams. When two strips were added, these metrics rose by 16%, 20%, and 49% over the one-strip condition, while the introduction of a third strip further increased the gains by 12%, 8%, and 24%. However, the rate of improvement diminished with the addition of more strips. The study concluded that while elevating both the number of lamellas and CFRP strips significantly enhances structural performance, the diminishing returns at higher levels, along with cost considerations, should inform design choices. The Figure 5.53 and Table 5.10 illustrate the failure modes observed during the experimental tests, which included tensile cracking at the bottom face of the beams, which was the primary mode of failure in both reinforced and unreinforced specimens. Unreinforced glulam beams typically failed due to tension-induced fractures at weak points such as knots or defects. Reinforced specimens exhibited additional failure modes, including delamination or debonding of carbon fiber reinforced polymer (CFRP) strips from the timber surface. For beams with CFRP strips, rupture of the CFRP material was noted in some cases. Specimens with CFRP fan-type anchors demonstrated delayed debonding and enhanced ductility compared to non-anchored specimens. Other failure modes included flexural bending failure and combined tension face fractures and delamination, highlighting the interaction between reinforcement materials and the wooden substrate. (İşleyen et al., 2021)

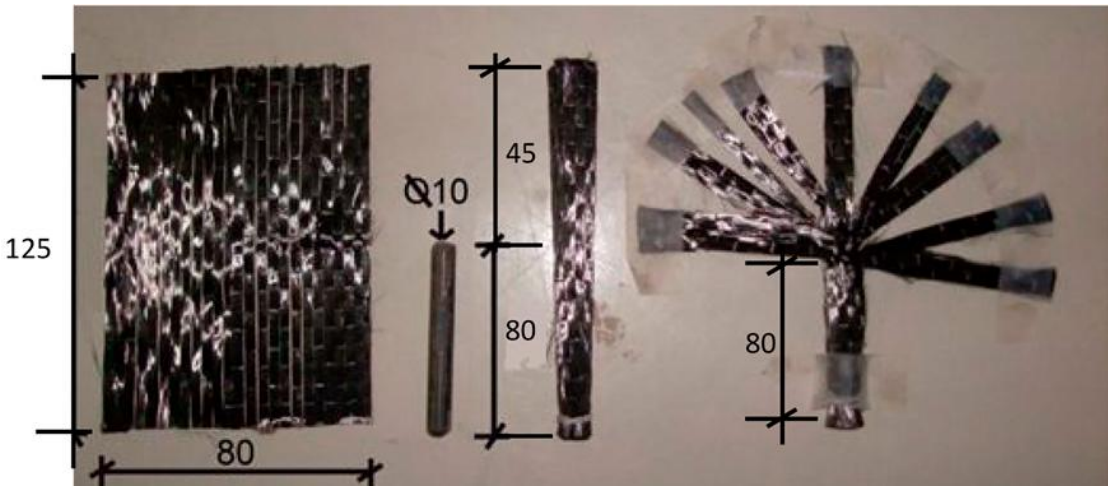


Figure 5.52. Properties of carbon FRP fan-type anchors (İşleyen et al. 2021)

Table 5.9. Specimens details and failure modes (İşleyen et al., 2021)

Spec. No	No. of glulam layers	No. of CFRP strips	Anchor usage	Failure mode
1	3	0	No	Tension face glulam fracture
2		1		Tension face glulam debonding
3		2		Tension face CFRP strip rupture
4	4	0		Tension face glulam fracture
5		1		Tension face CFRP strip rupture
6		2		Tension face glulam fracture
7		3		Tension face CFRP strip rupture
8	5	0		Tension face glulam debonding and fracture
9		1		Second glulam debonding
10		2		Tension face glulam fracture
11		3		Tension face glulam fracture
12	3	0	Yes	Flexural bending failure of beam
13		1		Tension face glulam fracture
14		2		Flexural bending failure of beam
15	4	0		Tension face and second glulam fracture
16		1		Tension face CFRP strip rupture and glulam fracture
17		2		Tension face CFRP strip rupture and glulam fracture
18		3		Tension face glulam fracture
19	5	0		Tension face glulam fracture
20		1		Tension face glulam fracture
21		2		Tension face glulam fracture
22		3		Tension face glulam fracture

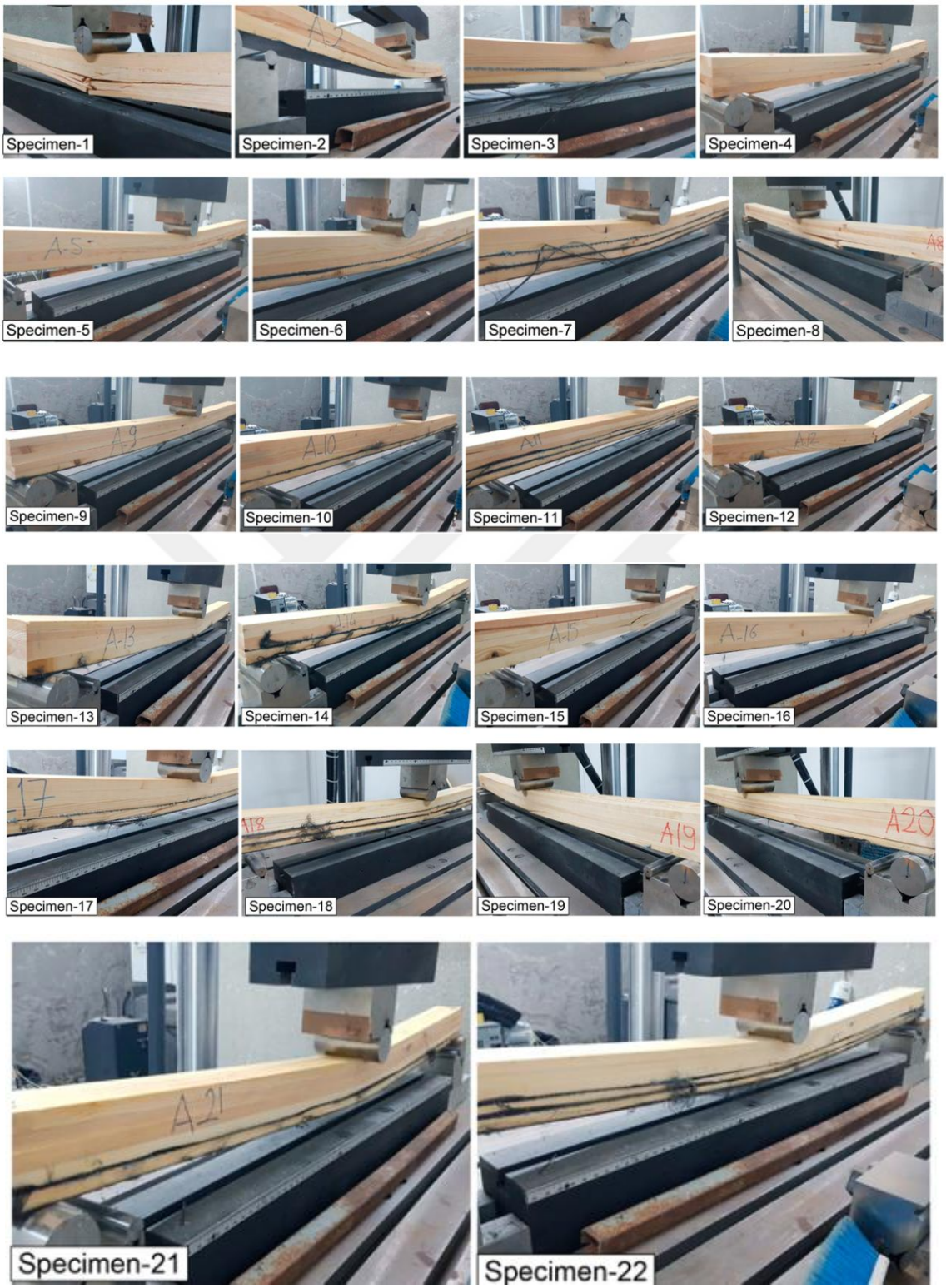


Figure 5.53. Specimen failure modes (İşleyen et al. 2021)

Table 5.10. Summary of Key Findings on FRP-Reinforced Timber Beams

Authors	Wood Type	Reinforcing Material	Loading Method	Increase In Ultimate Flexural Bearing Capacity	Increase In Flexural Stiffness
(Svecova & Eden, 2004)	Douglas Fir (Solid Timber)	GFRP	Four-point bending test	shear dowels beams increase up to 33% in modulus of rupture, shear and flexural reinforcements beams increase up to 47% to 52%	group SF became pseudo-ductile, with 60% of the tested beams displaying twice the deflection of the control beams
(Kliger et al., 2008b)	Glulam	CFRP laminates, Steel plates	Four-point bending tests	Up to 57%- 95.8%	Up to 100%
(Nowak, et al. 2013)	Century-Old Pinewood	CFRP	Four-Point Bending Test	21% to 79%, depending on reinforcement configuration	Stiffness increased by 14% to 32%, depending on the load level
(Raftery & Rodd, 2015)	Low-grade glued	GFRP plate	Four-point bending	31%	18%
(Fossetti, et al. 2015)	Glulam GL24h Spruce Timber	(CFRP) (GFRP)	Four-point bending test	CFRP increased load capacity by ~25%; GFRP and CFRP cords showed minor improvements. Enhanced ductility with ultimate strain increased by 40% (basalt reinforcement)	CFRP improved stiffness by ~10%-19%
(H. Yang et al., 2016)	North American Douglas fir (Pseudotsuga menziesii) (Solid Timber)	(CFRP) and Steel	Four-point bending test	Up to 56.3% compared to unreinforced control beams	49.4% increase in timber tensile strain at failure. 5% increase in flexural stiffness
(Shekarchi, et al. 2020)	Beechwood (Solid Timber)	Pultruded (GFRP) Profiles	Three-point bending	Up to 60.68%	Improved energy absorption capacity by up to 209.32%, with stiffness increasing by 59%
(İşleyen et al., 2021)	Glulam Timber	CFRP Strips	Three-point bending tests	11% (3 to 4 lamellas), 30% (with anchors), 35% (1 strip)	strength: 24% (3 to 4 lamellas), 20% (with anchors), 43% (1 strip) Stiffness: 13% (3 to 4 lamellas), 26% (with anchors), 60% (1 strip)

Table 5.10. (Continuous) Summary of Key Findings on FRP-Reinforced Timber Beams

Authors	Wood Type	Reinforcing Material	Loading Method	Increase In Ultimate Flexural Bearing Capacity	Increase In Flexural Stiffness
(Yeboah & Gkantou, 2021)	White Spruce Timber (Solid Timber)	GFRP and BFRP	Four-Point Bending Test	33% to 69% improvement depending on the reinforcement configuration	22% to 33% enhancement compared to unreinforced beams
(Al-Hayek & Svecova, 2014)	Poplar in Xinjiang, China (Solid Timber)	Draped CFRP tendons	Three point bending tests	70%	10%
(Alhayek & Svecova, 2012)	Creosote-treated Douglas Fir (Solid Timber)	GFRP	Three-point bending tests	Group T (tension-side reinforcement): 36%; Group TC (tension and compression sides): 31%	Group T: 3%; Group TC: 3.5%
(Gilfillan, et al. 2003)	Sitka spruce (Solid Timber) and LVL	pultruded strip of (CFRP), (GFRP), and steel	Four-Point Bending Test	10% to 150% depending on reinforcement type and configuration	10%–55% depending on the reinforcement ratio and material used
(Qi et al., 2015)`	Paulownia wood (Solid Timber)	GFRP	Three-point bending	17.4 times of the unreinforced pipe, and 4.1 times of the GFRP hollow pipe	12.8 times of the unreinforced pipe, and 1.7 times of the GFRP hollow pipe
(Kilinçarslan, et al. 2023)	Spruce Timber (Solid and Glulam Beams)	CFRP in U-shaped Bottom Configuration	Three-Point Bending Test	Glulam beams' capacity 76.96% higher than solid beams; CFRP reinforcement increased modulus of rupture by 39.60% in solid beams and 24.15% in glulam beams	Modulus of Elasticity increased by 16% in solid beams and 17.04% in glulam beams
(Ling et al., 2020)	Pinus sylvestris (Scots Pine) (Solid Timber)	CFRP and GFRP	Four-Point Bending Test	Longitudinal CFRP: 32.9% (1 layer), 68.6% (2 layers); GFRP: 21.2% (1 layer), 40.3% (2 layers).	Not explicitly addressed, but longitudinal CFRP showed significantly higher strengthening efficiency compared to GFRP.
(O'Ceallaigh et al., 2020)	Sitka spruce (glued laminated timber beams)	BFRP	Four-point bending tests under constant and variable climate conditions	On creep: Reduction in creep deflection by 16.4% and tensile strain by approximately 30%.	

5.2. Columns

5.2.1. Studies Conduct Full Wrapping Method

FRP sheets are applied to encompass the entire perimeter of the column, ensuring uniform confinement throughout.

O'Callaghan (2021) examines the impact of (GFRP) reinforcement on the compressive behavior of square Spruce-Pine-Fir (SPF) timber columns subjected to axial compression. A total of 36 specimens, including unreinforced control samples, were tested to evaluate the influence of different GFRP configurations, such as unidirectional at 90°(U), bidirectional at ±45°(X), and bidirectional at 0°/90° (B) relative to the wood grain were investigated with either one or three layers applied and layer thickness (1 layer versus 3 layers) Figure 5.54. The findings indicated that GFRP reinforcement substantially improved the peak compressive strength, stiffness, and post-peak performance of the timber columns. The reinforced specimens showed a reduction in longitudinal splitting, with damage primarily concentrated in areas of wood crushing beneath the FRP. It was observed that while the thinnest GFRP layers offered limited enhancements, increasing layer thickness and modifying fiber orientation did not produce a straightforward increase in performance. The findings indicated that GFRP wrapping considerably enhanced the post-peak performance, with the wrapped specimens retaining up to 61% of their peak compressive strength, in contrast to 41% for the control specimens. Additionally, the GFRP-wrapped columns demonstrated a capacity to dissipate 1.35 to 1.68 times more energy. The failure modes of GFRP-reinforced specimens varied by reinforcement type and layer configuration see Figure 5.55, with GFRP effectively localizing damage to the rupture plane and minimizing longitudinal damage. In the unidirectional groups (U and U3), GFRP failure aligned with the wood failure plane, and three-layer reinforcement (U3) showed less glass fiber rupture and better containment of damage compared to single-layer specimens (U). While specimens like U–1 and U3–1 displayed wood crushing similar to control specimens, longitudinal splitting was mitigated. The bidirectional groups (X and X3) demonstrated superior FRP integrity, especially in the three-layer X3 specimens, which resisted damage propagation from knots, voids, and grain flaws. Specimens X–1 and X3–3 highlighted the effect of defects on failure, while X–4 and X3–5 showed localized crushing in defect-free regions. Similarly, in the

bidirectional perpendicular groups (B and B3), three-layer reinforcement (B3) improved FRP intactness under high strains, arresting crack growth from defects and promoting adjacent fiber crushing. Specimens B3–2 and B3–4 displayed crushing failures controlled by reinforcement, with localized damage even in the presence of knots or cross-grain flaws. Across all configurations, the reinforcement effectively constrained damage and maintained structural integrity until large strains, particularly with three-layer wraps. Ultimately, GFRP reinforcement proved effective in alleviating the effects of wood defects, thereby enhancing the structural performance of the columns under compression. (O'Callaghan, 2021)

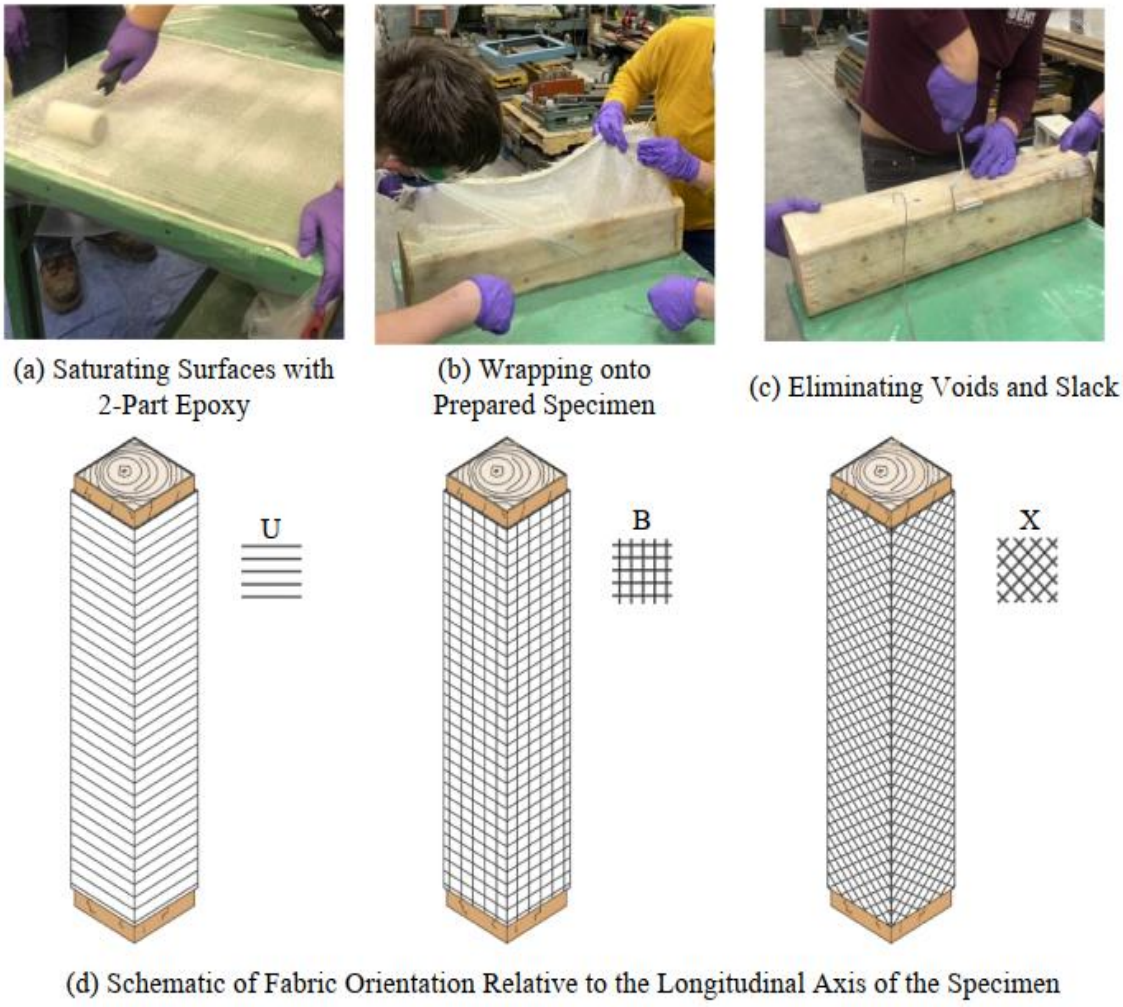


Figure 5.54. Epoxy and FRP application (O'Callaghan, 2021)



(a) (b)

Figure 5.55. Specimens strengthened with (a) three, (b) one layers of GFRP showed representative failure mechanisms (O'Callaghan, 2021)

Shi et al. (2022) conducted research on the compressive properties of (FRP)-confined (GLT) and (CLT) columns as showing in Figure 5.56 subjected to cyclic axial loading. The primary goal of their study was to evaluate the impact of (BFRP and CFRP) on the hysteretic behavior and load-carrying capacity of laminated timber columns. The investigation involved testing a total of 60 specimens, with variations in FRP type, thickness, and column height (200 mm and 400 mm). The application of FRP sheets adhered with epoxy resin was performed using a wrapping technique. The results under cyclic loading demonstrated an average increase in ultimate load-bearing capacity of 29% for CLT specimens and 24% for GLT specimens, with CFRP showing significantly greater enhancements in both strength and ductility. Furthermore, CFRP exhibited more substantial improvements in performance compared to BFRP. Corresponding stiffness enhancements indicated initial increases of 29% for CLT and 24% for GLT specimens. The observed failure modes included timber crushing, longitudinal buckling, and FRP cracking, highlighting the critical influence of FRP on failure mechanisms and overall column performance under cyclic loading conditions. See Figure 5.57 and 5.58. (Shi et al., 2022)



(a) (b)

Figure 5.56. (a) GLT and CLT column specimen dimensions, (b) Manufacturing process (Shi et al., 2022)

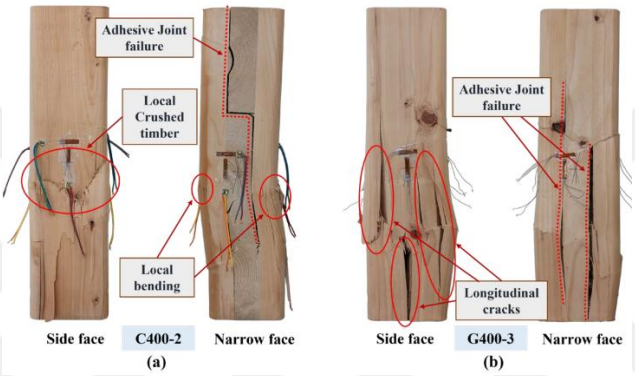


Figure 5.57. Common failure patterns observed in unconfined specimens (Shi et al. 2022)

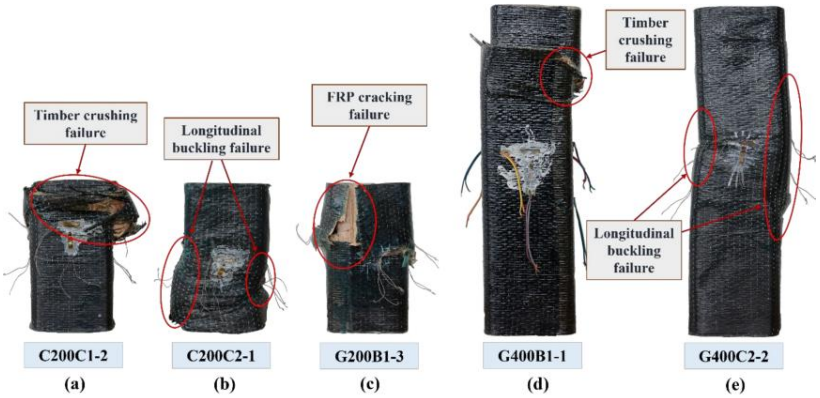


Figure 5.58. Common failure characteristics of the confined specimens (Shi et al., 2022)

Shi et al. (2024) investigated the axial compressive behavior of GLT and CLT columns confined with FRP sheets, focusing primarily on how confinement using BFRP and CFRP could enhance structural performance under monotonic axial compression. This study involved analyzing 80 specimens, including both unconfined and FRP-confined columns, with configurations that varied between one or two layers of FRP and column heights of 200 mm and 400 mm. They applied FRP sheets to the columns utilizing a two-component

epoxy resin. Their findings revealed that the ultimate load-bearing capacity of confined columns increased between 6.35% and 36.19%, with CFRP outperforming BFRP. Additionally, initial stiffness improvements were noted, reflecting enhancements of 29% for CLT specimens and 24% for GLT specimens. The observed failure modes in this study included timber crushing, FRP cracking, and longitudinal buckling, with FRP confinement shown to effectively delay structural failure and increase ductility see Figure 5.59. (Shi et al., 2024)

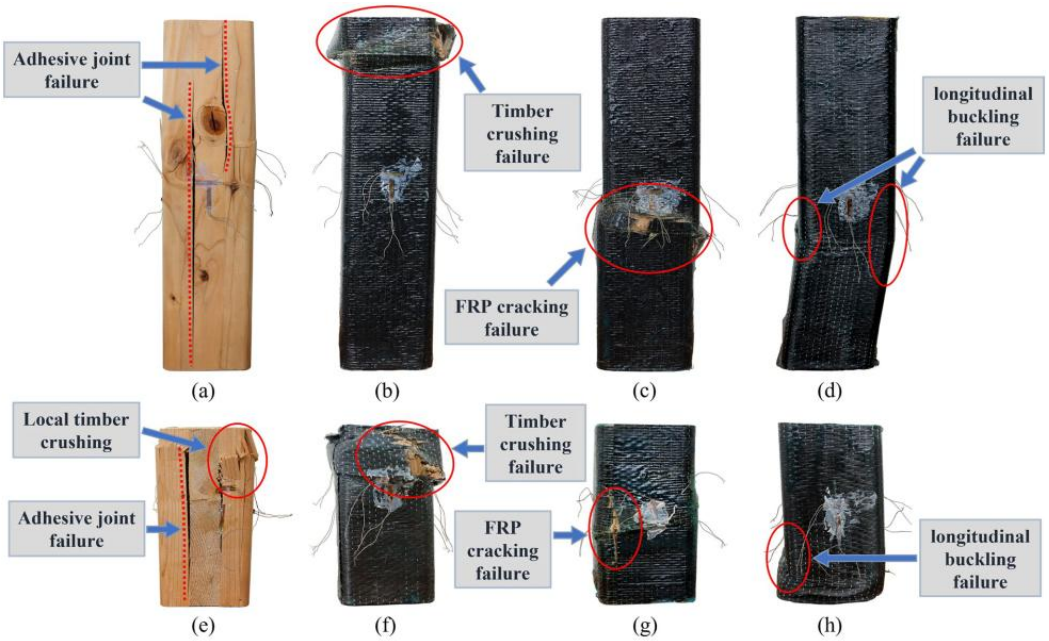


Figure 5.59. Typical examples of failure modes (Shi et al., 2024)

Hong et al. (2022) investigate the compressive behavior of Layered Bamboo Laminate (LBL) stub columns reinforced with Aramid Fiber Reinforced Polymer (AFRP), focusing on addressing the structural shortcomings of engineered bamboo materials. A total of 18 specimens were tested under axial compression test see Figure 5.60, with varying ratios of AFRP cloth ranging from 0% to 3.69% shown in Table 5.12. The findings indicate that AFRP effectively mitigates lateral deformation, thereby enhancing the mechanical properties of the columns. The ultimate compressive strength exhibited a linear increase with the AFRP cloth ratio, achieving a 24% enhancement, while the reduced modulus during the elastoplastic phase showed a significant increase of 161% see Figure 5.61. Although the initial stiffness remained largely unchanged, AFRP reinforcement led to notable improvements in ductility, a decrease in Poisson's ratio, and better confinement of deformation. Figure 5.62 illustrate the failure modes observed during the experimental

tests. Which varied between unreinforced and FRP-reinforced specimens. Unreinforced specimens were characterized by end crushing, local adhesive damage, and cracking of bamboo strips. Initially, there were no visible deformations, but as loading progressed, bamboo fibers at the ends became wrinkled. During the plastic flow stage, cracking occurred in the bamboo strips and adhesive layers, intensifying with increased deformation, eventually leading to the loss of ultimate bearing capacity. For FRP-confined specimens, the failure process in the elastic and elastic–plastic stages resembled that of unreinforced columns. However, during the plastic flow stage, the AFRP cloth folded in the perpendicular-to-fiber direction and tore as deformation increased. Unlike the unreinforced specimens, FRP-reinforced columns showed no visible crushing at the ends, with failure primarily occurring through cracking of bamboo strips. The FRP effectively constrained outward expansion at the ends under compression, mitigating damage and improving confinement. (Hong et al., 2022)

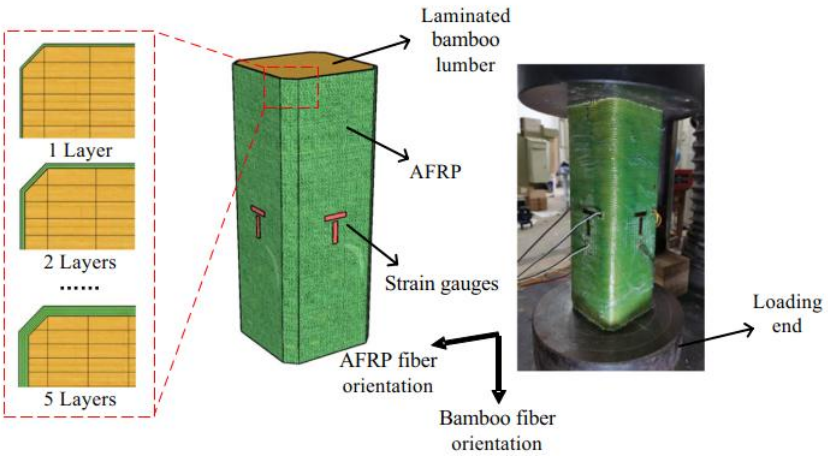


Figure 5.60. Test setup (Hong et al. 2022)

Table 5.11. Specimens' parameters (Hong et al. 2022)

Group	Length	Number of specimens	Number of AFRP layer	ρ
A300	300 mm	3	0	0%
SA1A300		3	1	0.74%
SA2A300		3	2	1.48%
SA3A300		3	3	2.21%
SA4A300		3	4	2.95%
SA5A300		3	5	3.69%

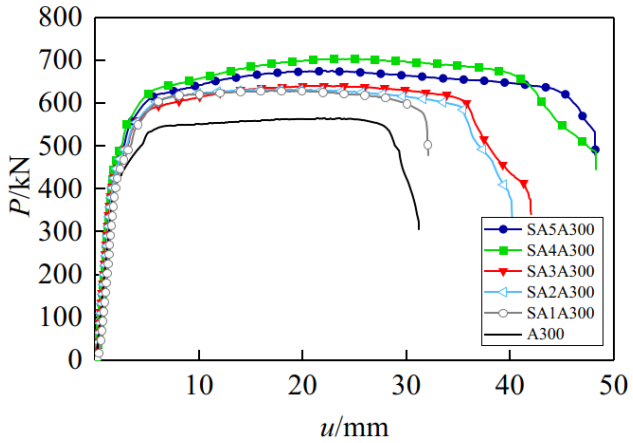


Figure 5.61. load-displacement curve (Hong et al. 2022)

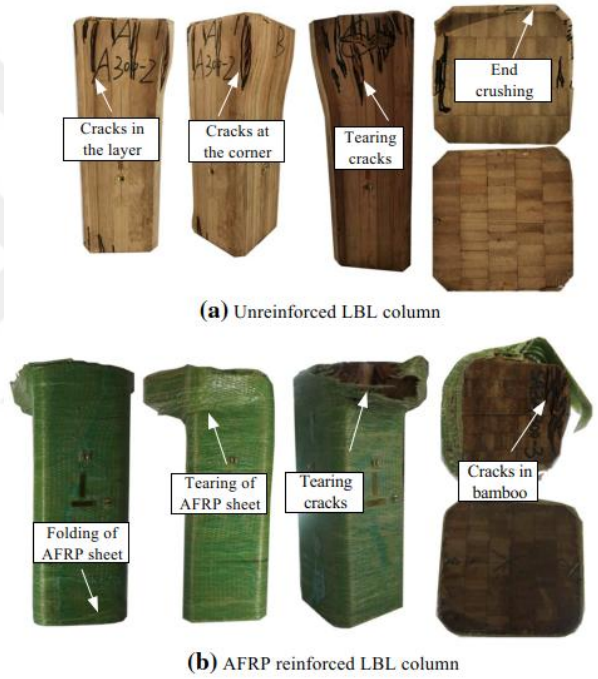


Figure 5.62. Typical failure pattern (Hong et al., 2022)

Li et al. (2022) investigates the mechanical characteristics of (AFRP) confined LBL columns subjected to cyclic loading. The study involved testing six series of short LBL columns, varying in the number of AFRP reinforcement layers from 0 to 5, to assess their failure modes, load-bearing capacity, stiffness, and ductility. The findings indicate that AFRP confinement considerably enhanced the ultimate strength by as much as 11.2% and improved the ductility coefficient by 22.2% compared to unconfined columns see Table 5.13. Figures 5.63 and 5.64 illustrate the failure modes observed during the experimental tests. Where unconfined specimens typically failed due to adhesive failure and end

crushing. Initially, the columns remained elastic, with no visible cracks or bending. As loading increased, transverse deformation and vertical cracks appeared, bamboo fibers broke, and bulging occurred, especially at the mid-length of plane-A and at junctions with other planes, accompanied by loud cracking noises. These adhesive failures were attributed to material and construction defects but did not significantly affect the ultimate bearing capacity. In contrast, AFRP-confined LBL columns failed primarily through end crushing or excessive out-of-plane bending. For end crushing, the AFRP sheet detached at the ends, followed by top surface cracking and eventual failure. For out-of-plane bending, deformation initiated on plane-A, with audible cracking, mid-height AFRP layer cracking on plane-B, and tearing of bamboo fibers, leading to significant bending and ultimate failure. Unlike unconfined specimens, AFRP confinement prevented adhesive failure and enhanced resistance to cyclic loading, shifting the failure mechanism to the bamboo lumber itself. These outcomes underscore the potential of AFRP in enhancing the seismic and mechanical performance of LBL columns under cyclic loading conditions. (Li et al., 2022)

Table 5.12. Result of specimens (Li et al., 2022)

Group		CA300	CA1A	CA2A	CA3A	CA4A	CA5A
Compressive strength /MPa	Mean	54.28	52.71	56.33	55.66	56.24	60.38
	COV	0.014	0.034	0.047	0.031	0.065	0.063
Ductility coefficient ($\mu = \Delta_u/\Delta_y$)	Mean	5.3	5.9	6.4	7.1	6.6	6.4
	COV	0.046	0.062	0	0.035	0.062	0.082



Figure 5.63:failure mode for unconfined specimen (Li et al., 2022)



(a)



(b)

Figure 5.64. AFRP confined specimen's failure mode (a) End crushing; (b) Bending (Li et al., 2022)

Wen et al. (2024) examine the buckling behavior of hybrid fiber-reinforced polymer (HFT)-timber thin-walled C-section columns see Figure 5.65 under axial compression, focusing on the local and global buckling failure modes. Their investigation involved ten HFT C-section columns with lengths of 700 mm and 2000 mm. The experimental results for hybrid fiber-reinforced polymer-timber (HFT) C-section columns showed notable differences in performance between shorter (700 mm) and longer (2000 mm) specimens under axial compression. The 700 mm specimens predominantly failed through local buckling, characterized by multiple half-sine waves and flange fracture, with a weight-specific capacity of 24.2 kN/(kg/m), higher than previous studies. The 2000 mm specimens exhibited global buckling, with failure modes depending on the buckling direction—flange crushing for web-directed buckling and flange rupture for outward buckling as illustrate in Figure 5.66. Load-displacement behavior indicated a sudden load drop after peak for 700 mm specimens, while 2000 mm specimens showed more uniform initial stiffness and gradual load reduction for some specimens. AFRP confinement enhanced axial load capacity and reduced premature adhesive failures, shifting failure to

the bamboo or composite material itself. The study demonstrated that bi-axial glass fiber reinforcement improves both stiffness and load capacity, with enhancements in weight-specific load capacity compared to thin-walled steel counterparts. (Wen et al., 2024)

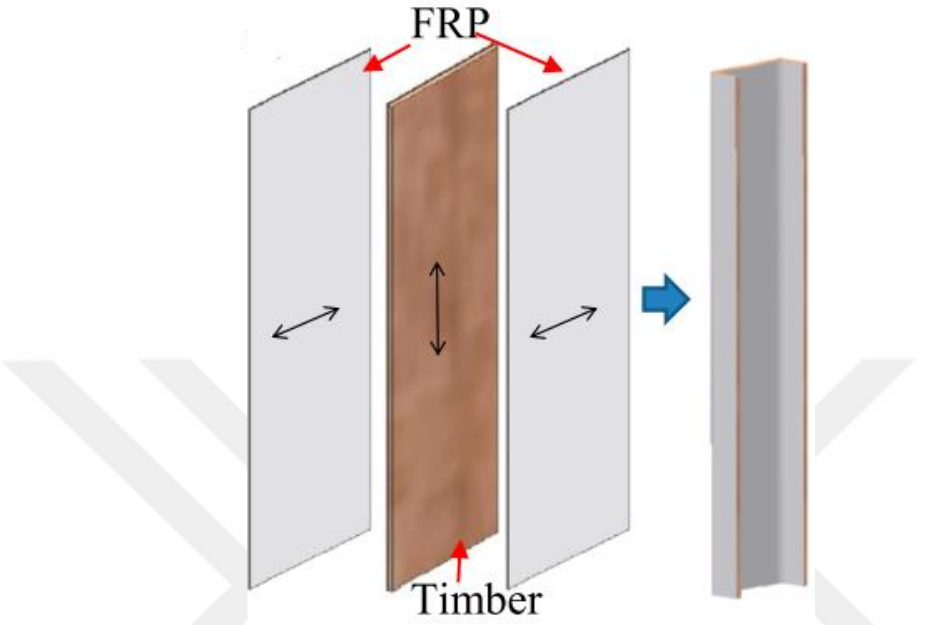


Figure 5.65. C-section of the HFT (arrow heads indicate the FRP fiber and the timber grain directions)

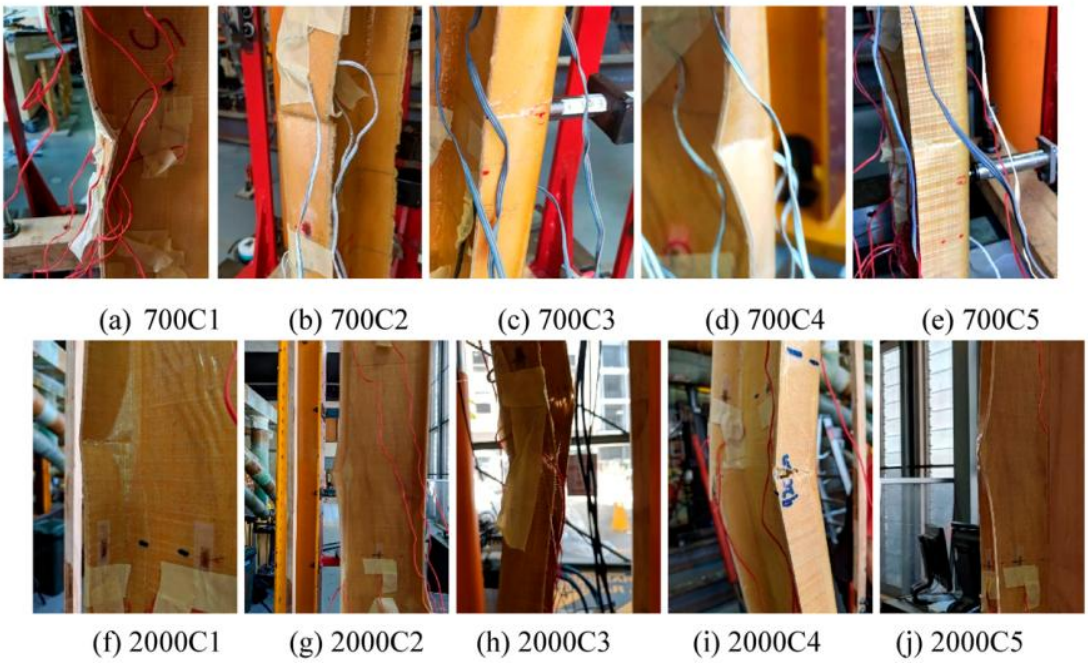


Figure 5.66. Local failure modes (Wen et al. 2024)

Table 5.13. Summary of Experimental Studies on Full-Reinforcement

Loading Method	Full-Reinforcement														
	Compression Capacity								FRP Dim,		Column Dim, (mm)			Wood Type	
	AFRP		BFRP		GFRP		CFRP		Layer						
	ST%	BC %	ST%	BC%	ST%	BC%	ST%	BC%	Type	Number	Length	Width	Height		
Axial Compression								70,0	Unidirectional	1	114	114	360	Spruce	
								83,0	Unidirectional	3	114	114	360		
Axial Compression					15.7	15.6			Unidirectional -90	1	140	140	685	Spruce-Pine-Fir	
					22.3	14.6			Unidirectional -90	3	140	140	685		
					21,6	38.7			Bidirectional perpendicular -0/90	1	140	140	685		
					26.0	24.5			Bidirectional perpendicular -0/90	3	140	140	685		
					14.3	1.3			Bidirectional 45°	1	140	140	685		
					16.5	20.2			Bidirectional 45°	3	140	140	685		

Table 5.13. (continuous) Summary of Experimental Studies on Full-Reinforcement

Loading Method	Full-Reinforcement														
	Compression Capacity								FRP Dim,		Column Dim, (mm)			Wood Type	Reference
	AFRP		BFRP		GFRP		CFRP		Layer		Length	Width	Height		
	ST%	BC%	ST%	BC%	ST%	BC%	ST%	BC%	Type	Number					
Cyclic Compression Loading Test					26.0	6.4			Unidirectional	1	105	105	200	GLT	Siha A., Changdong Zhou (2022)
					28.7	15.4			Unidirectional	2	105	105	200		
							35.9	15.8	Unidirectional	1	105	105	200		
							35.3	20.8	Unidirectional	2	105	105	200		
			12.8	8.2					Unidirectional	1	105	105	400		
			14.9	12.6					Unidirectional	2	105	105	400		
							10.6	13.5	Unidirectional	1	105	105	400		
							27.5	18.4	Unidirectional	2	105	105	400		
			36.1	18.2					Unidirectional	1	105	105	200	CLT	
			35.0	28.1					Unidirectional	2	105	105	200		
							31.0	16,2	Unidirectional	1	105	105	200		
							26.9	28.9	Unidirectional	2	105	105	200		
			19.8	22.3					Unidirectional	1	105	105	400		
			17.3	36.2					Unidirectional	2	105	105	400		
							32.2	28.8	Unidirectional	1	105	105	400		
							30.3	33.4	Unidirectional	2	105	105	400		

Table 5.13. (continuous) Summary of Experimental Studies on Full--Reinforcement

Loading Method	Full-Reinforcement														
	Compression Capacity								FRP Dim, Layer		Column Dim, (Mm)			Wood Type	Reference
	AFRP		BFRP		GFRP		CFRP				Length	Width	Height		
	ST%	BC%	ST%	BC%	ST%	BC%	ST%	BC%	Type	Number					
Axial Compression (Monotonic Loading)								16.0	Unidirectional	1	105	105	200	CLT	**Libin Wang et al., 2024**
								29.0	Unidirectional	2	105	105	200		
				20.1					Unidirectional	1	105	105	200		
				28.1					Unidirectional	2	105	105	200		
								27.4	Unidirectional	1	105	105	400		
								33.4	Unidirectional	2	105	105	400		
				22.0					Unidirectional	1	105	105	400		
				36.2					Unidirectional	2	105	105	400		
Axial Compression		10.7							Unidirectional	1	100	100	300	Laminated Bamboo Lumber (LBL)	**(Hong et al. 2022)**
		12.1							Unidirectional	2	100	100	300		
		12.8							Unidirectional	3	100	100	300		
		24.0							Unidirectional	4	100	100	300		
		21.0							Unidirectional	5	100	100	300		
Cyclic loading		-2.9							Unidirectional	1	100	100	300	Laminated Bamboo Lumber (LBL)	**Haitao Li, et al. (2022)**
		3.8							Unidirectional	2	100	100	300		
		2.5							Unidirectional	3	100	100	300		
		3.6							Unidirectional	4	100	100	300		
		11.2							Unidirectional	5	100	100	300		

Table 5.13. (continuous) Summary of Experimental Studies on Full--Reinforcement

Loading Method	Full-Reinforcement														
	Compression Capacity								FRP Dim,		Column Dim, (Mm)			Wood Type	Reference
	AFRP		BFRP		GFRP		CFRP		Layer		Length	Width	Height		
	ST%	BC%	ST%	BC%	ST%	BC%	ST%	BC%	Type	Number					
Axial Compression pinned pinned						61.2			Unidirectional	0.9mm	57.2	110	950	Glue-laminated timber (Glulam)	F. Taheri, et al. (2009)
								65.33	Unidirectional	0.55mm	57.2	110	1400		
								70.5	Unidirectional	0.55mm	57.2	110	1850		
						56			Unidirectional	0.9mm	57.2	110	1850		
Axial Compression fixed-fixed						65.7			Unidirectional	0.9mm	50.8	110	1450		
						19.3			Unidirectional	0.9mm	50.8	110	2350		
Axial compression (monotonic)		46.9							Unidirectional	1	150	150	400	Camphor pine	Dong, Yuan, et al. (2015)
		74							Unidirectional	2					
		71.9							Unidirectional	3					
				72.3					Unidirectional	2					
Lateral cyclic loading								34.9	Unidirectional	2	150D	circule	2600	(Korean Pine)	Siha A., Changdong Zhou (2022)
								39.5	Unidirectional	1					

The provided tables summarize experimental studies on the full wrapping of FRP around timber columns to evaluate improvements in bearing capacity (BC) and stiffness (ST). The studies involve different wood types, FRP materials (CFRP, BFRP, AFRP), and reinforcement configurations, including unidirectional and bidirectional layers. Results indicate that full FRP wrapping enhances both BC and ST, with variations based on FRP type, layer thickness, and wood species. CFRP generally provides the highest improvement in BC and ST, followed by BFRP and AFRP. The enhancement is more pronounced in cyclic loading conditions, emphasizing FRP's effectiveness in structural strengthening. Recommendations include optimizing FRP thickness and type based on structural requirements, conducting further studies on long-term durability, and exploring hybrid reinforcement methods to maximize performance while considering cost-effectiveness.

The bar next chart illustrates the increase in the bearing capacity of timber columns with full FRP reinforcement, categorized by different studies, wood types, reinforcement methods, and loading conditions. The y-axis represents the increase in the bearing capacity ratio, while the x-axis lists various experimental studies number of layers of FRPs sheets. Different colors indicate the type of FRP used: CFRP (blue), BFRP (gray), GFRP (orang), and AFRP (yellow). CFRP demonstrates the highest improvement, especially in spruce-pine-fir columns, reaching up to 70%, while BFRP and AFRP show moderate enhancements. CLT columns under cyclic and monotonic loading conditions also exhibit significant increases, particularly with CFRP and BFRP, reaching around 36%. AFRP provides the lowest enhancements in most cases, with some values below 10%. Among the studies, columns reinforced with CFRP under axial compression performed the best, whereas AFRP under cyclic loading showed lower gains. The comparison suggests that CFRP is the most effective reinforcement for bearing capacity improvement, followed by BFRP and GFRP, while AFRP is less effective in most configurations.

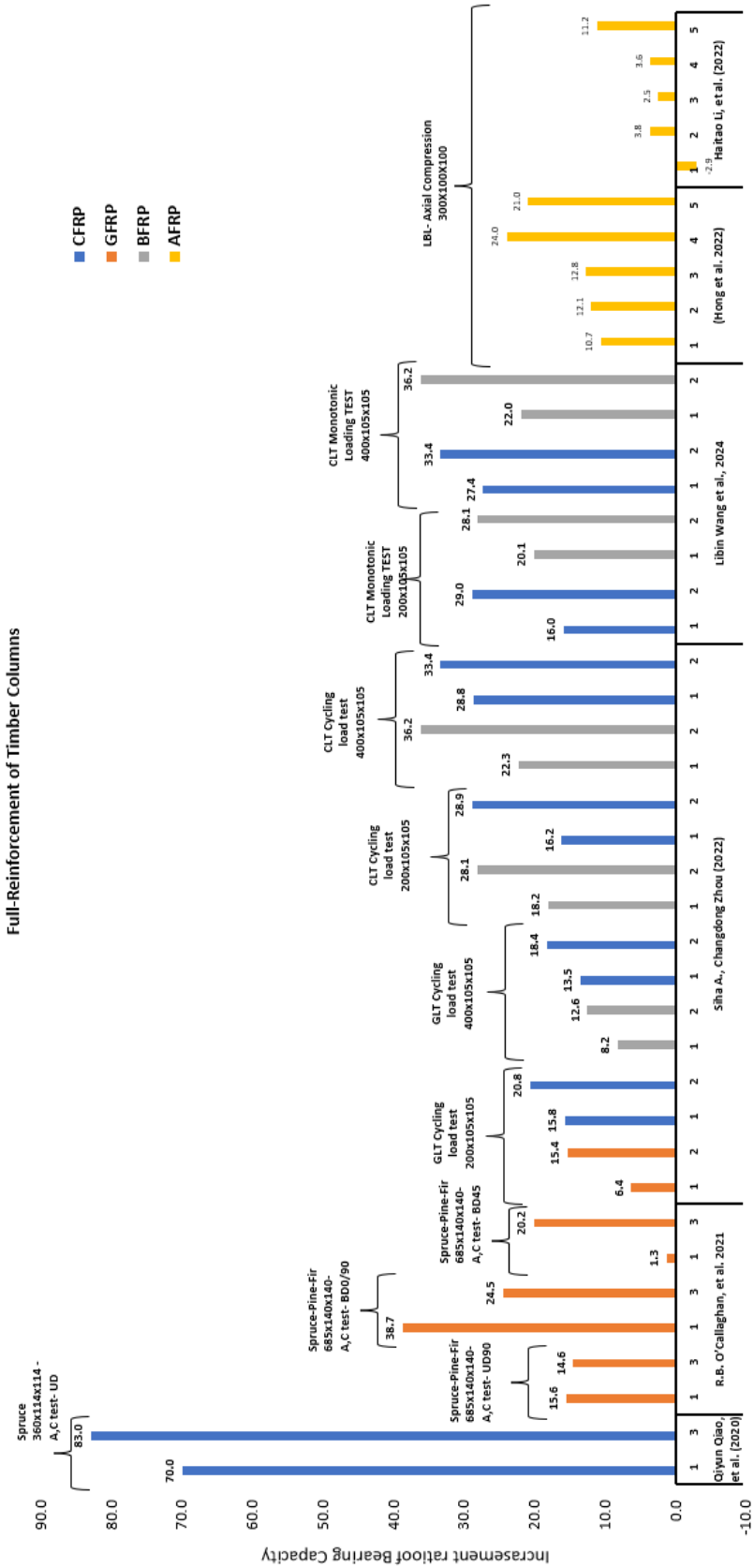


Figure 5.67. Comparative Column Capacity Results for Fully Reinforced Timber Members with Various FRP Materials

5.2.2. Studies Conduct Partial Wrapping Method

FRP is used in strips or segments, covering just a part of the surface of the column.

Zhang et al. (2012) conducted a study on the compressive behavior of timber columns with longitudinal cracks that were retrofitted using FRP sheets. The research aimed to evaluate the effectiveness of FRP wrapping in restoring the load-carrying capacity of these damaged columns and examined how factors like crack size, types of FRP sheets, and their spacing impacted performance. The timber utilized was Douglas fir, and the study involved testing 17 column specimens categorized to 5 groups shown in Table 5.16. The retrofitting process included wrapping the columns with carbon, basalt, or glass FRP sheets, with some specimens also undergoing crack-filling treatments see Figure 5.68 (a). Axial compression tests were performed using a hydraulic testing machine Figure 5.68 (b). Results indicated that FRP wrapping enhanced the load-carrying capacity of the cracked columns by up to 20%, with carbon FRP yielding the most significant recovery, followed by basalt and glass fibers. Furthermore, columns with narrower spacing of FRP sheets showed improved performance regarding stiffness and load recovery. The failure modes observed in the specimens varied among different groups as showing in Figure 5.69 Group 1 (controlled specimens) showed typical crushing failure due to wood fiber buckling (Type 1) and significant lateral deflection (Type 2) near the mid-height cross section. Group 2 specimens, which were cracked and not retrofitted, demonstrated two failure modes: one involved opposite deflection of cracked branches leading to mid-height failure (Type 3), and the other mimicked the failure of Group 1 Specimen 2 (Type 2). Group 3 specimens, cracked and retrofitted but with unfilled cracks, also displayed two failure modes; if the branches touched, the failure initiated from wood fracture with minimal FRP strain (Type 4), while if they did not touch, the tension failure of the FRP sheets led to wood fracture after significant lateral deflection (Type 5). Groups 4 and 5 had similar behaviors where FRP sheets were pulled apart (Type 5), although Group 5 sometimes experienced failure between FRP wrappings (Type 6), indicating that local wood defects could significantly impact load capacity. (Zhang et al., 2012)

Table 5.14. Details of the Specimens (Zhang et al., 2012)

Number	Dimension	Crack dimension	Crack filled	FRP property[a]	FRP spacing
Group 1: controlled specimens[b]					
1	200 × 200 × 1,800	0 × 0	—	—	—
2	100 × 100 × 900	0 × 0	—	—	—
Group 2: specimens with cracks (not retrofitted)					
3	200 × 200 × 1,800	10 × 1,500	No	—	—
4	100 × 100 × 900	10 × 710	No	—	—
5	100 × 100 × 900	10 × 710	Yes	—	—
Group 3: specimens with cracks and FRP wrapping but cracks not filled					
6	200 × 200 × 1,800	10 × 1,500	No	GF&100	250
7	200 × 200 × 1,800	10 × 1,500	No	CF&100	100
8	200 × 200 × 1,800	10 × 1,500	No	CF&100	250
Group 4: specimens with cracks and FRP wrapping and cracks filled					
9	100 × 100 × 900	10 × 710	Yes	CF&50	60
10	100 × 100 × 900	10 × 710	Yes	CF&50	115
11	100 × 100 × 900	10 × 710	Yes	CF&50	280
12	100 × 100 × 900	10 × 710	Yes	CF&50	32.5
13	100 × 100 × 900	10 × 710	Yes	BF&50	115
14	100 × 100 × 900	10 × 710	Yes	BF&50	60
Group 5: specimens with one end pinned and the other end resting on metal support					
15	100 × 100 × 900	10 × 710	Yes	CF&50	60
16	100 × 100 × 900	10 × 710	Yes	CF&50	115
17	100 × 100 × 900	10 × 710	Yes	CF&50	280

[a]CF, GF, and BF stand for carbon, glass, and basalt fiber sheets of the same thickness as that used in material property tests, respectively; and 100 is the width of the fiber sheets.
[b]All specimens were simply supported unless otherwisely specified.

Note: All units in mm.

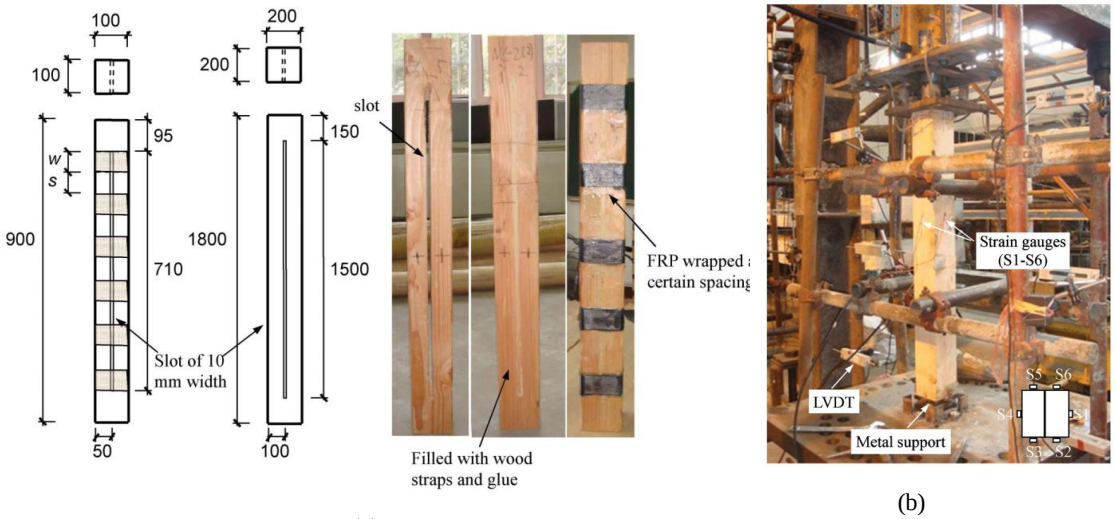


Figure 5.68. (a) Tested specimens (unit mm), (b) Test setup (Zhang et al., 2012)

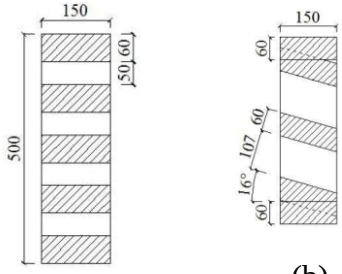


Figure 5.69. Failure Modes (Zhang et al., 2012)

Liang et al. (2013) conducted an investigation evaluating the mechanical performance of short timber columns reinforced with CFRP and AFRP, utilizing two distinct wrapping techniques: hooped and spiral configurations shown in Figure 5.70. A total of five timber columns, including one unreinforced control specimen shown in Table 5-17, underwent testing under axial compression. The findings demonstrate that the incorporation of FRP reinforcement markedly enhances compressive strength and mitigates lateral deformation. Notably, the spiral-wrapped specimen exhibited the most substantial increase in ultimate compressive strength at 57.5%, while the hooped-wrapped specimens provided more effective lateral strain restraint see Figure 5.71. Nonetheless, the presence of knags, or wood defects, influenced the performance of certain reinforced specimens, thereby limiting their effectiveness. Specimen T0 experienced failure shortly after reaching an ultimate load of 559.5 kN, with the end of the column exhibiting an extruded knag and visibly distorted wood fibers surrounding it. Initial cracking originated at the knag, followed by the development of additional cracks in nearby areas. Both HC1 and SC1A1 failed due to knags extruding from the ends of the columns, leading to the snapping of the FRP sheets. In contrast, HC1A1 and SC1 failed in the middle sections of the specimens. The FRP sheets effectively restrained crack development across all specimens, with their failure models illustrated in Figure 5.72. In summary, the adoption of FRP reinforcement significantly bolsters both strength and stiffness, with hooped wrapping outperforming spiral wrapping in terms of overall effectiveness. (Liang et al., 2013)

Table 5.15. Number of specimens and key parameters (Liang et al., 2013)

Code	Strengthening Type	Number of Plies		Twining Angle
		CFRP	AFRP	
T0	None	—	—	—
HC1	Hooped	1	—	180°
HC1A1	Hooped	1	1	180°
SC1	Spiral	1	—	16°
SC1A1	Spiral	1	1	16°



(a) (b)

Figure 5.70. (a) Hooped type, (b) Spiral type (Liang et al., 2013)

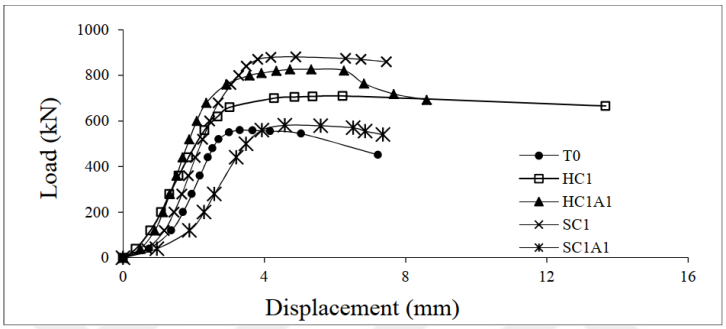


Figure 5.71. Load-displacement curve (Liang, et al. 2013)

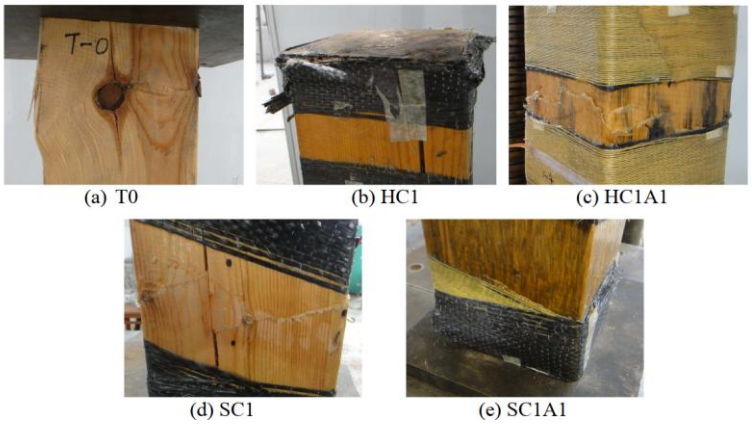


Figure 5.72. The failure modes (Liang et al., 2013)

Dong et al. 2015 carried out an experimental study involving six square timber columns (500 mm height, 150 mm width) that were reinforced with one to three layers of various FRP sheets made from aramid (AFRP), carbon (CFRP), and basalt (BFRP) fibers. The research aimed to assess the effectiveness of these reinforcements, which were applied using epoxy resin and a partial wrapping method. The columns were subjected to axial compression tests to analyze failure modes, load capacity, strain behavior, and stiffness. The results indicated that CFRP reinforcement led to a load capacity increase of 74.1% to 100.2% and a stiffness enhancement of 67.7% to 109.7%. In comparison, AFRP

improved load capacity by 70.4% to 84.6% and stiffness by 64.8% to 84.2%, while BFRP resulted in load capacity gains of 68.9% to 86.2% and stiffness increases of 63.2% to 77.9%. However, all materials exhibited a decrease in ultimate displacement, with CFRP resulting in a reduction of 46.1% to 56.9%, AFRP by 48.3% to 53.2%, and BFRP showing the least reduction. These results underscore the enhanced compressive performance and buckling resistance achieved through FRP reinforcement, with CFRP providing the most substantial improvements. (Dong et al., 2015)

Bhat (2021) examines the buckling behavior of cross-laminated poplar timber columns reinforced through various techniques: bolting, cold steel wrapping, single helix CFRP wrapping, and double helix CFRP wrapping. A total of 24 specimens Figure 5.73 underwent axial compression tests to evaluate enhancements in load-carrying capacity and stiffness. The findings revealed that double helix CFRP wrapping led to the most significant improvement, increasing the ultimate load-carrying capacity by 50.6%. In comparison, single helix CFRP wrapping produced a 35.4% increase, while cold steel wrapping improved capacity by 26.6%, and columns reinforced with bolting exhibited a modest gain of 10.1%. Figure 5.74 demonstrate the Failure patterns of columns identified during the experimental tests. In the LCLT-0 group, failures predominantly occurred due to buckling followed by cracking on the tension side, whereas LCLT-B columns exhibited combined buckling and crushing of timber fibers after initial buckling under axial loads. In the LCLT-S category, failure began with buckling, followed by debonding of the steel casing from the timber, leading to significant improvements in axial load capacity and ductile behavior. LCLT-SH columns showed elastic buckling followed by the crushing of fibers in regions not wrapped by FRP, with the FRP adding tensile strength that delayed overall buckling and enhanced ductility. Similarly, the LCLT-DH group experienced elastic buckling and fiber crushing as well, but benefited from double FRP wrapping, which provided superior confinement and further increased both load capacity and ductility compared to the LCLT-SH columns. Throughout the testing process, loads and corresponding displacements, both vertical and lateral, were meticulously recorded until failure occurred. Additionally, double helix CFRP wrapping not only enhanced stiffness but also provided better confinement, effectively delaying buckling failure and increasing ductility. (Bhat, 2021)

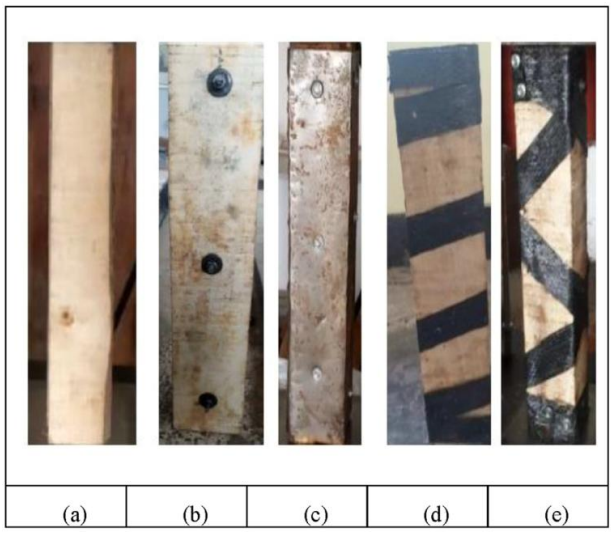


Figure 5.73. Column Samples: (a) LCLT-0, (b) LCLT-B, (c) LCLT-S, (d) LCLT-SH and (e) (Bhat 2021)

No laminates in the control column LCLT-0

Bolt-strengthened cross-laminated wood column LCLT-B

Cold steel is used to reinforce a cross-laminated timber column. LCLT-S

A single helix of FRP band LCLT-SH strengthens a cross-laminated wood column.

A cross-laminated timber column reinforced with a FRP band LCLT-DH double cross helix.

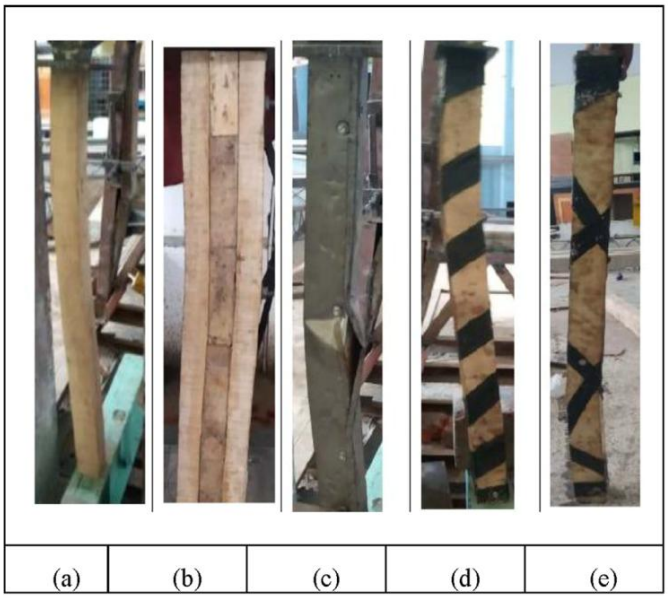


Figure 5.74. Failure patterns of columns (a) LCLT-0, (b) LCLT-B, (c) LCLT-S, (d) LCLT-SH (Bhat, 2021)

Table 5.16. Summary of Experimental Studies on Partial-Reinforcement of Timber

Loading Method	Partial-Reinforcement																
	Compression Capacity									FRP Dim,			Column Dim, (Mm)			Wood Type	Reference
	Hybrid	AFRP		BFRP		GFRP		CFRP				Layer	Length	Width	Height		
	BC	ST	BC	ST	BC	ST	BC	ST	BC	Spacing	Angle	Number					
Axial Compression									26.9	50	180	1	150	150	500	Camphor Pine	**Wei Liang, et al. 2013**
	48	1						1		50	180	2					
									57.5	107	16	1					
	3.8	1						1		107	16	2					
Axial Compression									35.4		20	1	75	75	1000	CLT	**Bhat (2021)**
									50.6		20	2					
Axial Compression pinned-pinned,							26			center	617mm	0,9mm	57,2	110	950	Glue-laminated timber (Glulam)	**F. Taheri, et al. (2009)**
							19.2			center	617mm	0,9mm	57,2	110	1850		
									32.3	center	617mm	0,55mm	57,2	110	1850		
							20			center	617mm	0,9mm	50,8	110	1450		
Axial Compression fixed-fixed							19.3			center	617mm	0,9mm	50,8	110	2350		

Table 5.16. (continuous) Summary of Experimental Studies

Loading Method	Partial-Reinforcement																
	Compression Capacity									FRP Dim,			Column Dim, (Mm)			Wood Type	Reference
	Hybrid	AFRP		BFRP		GFRP		CFRP				Layer	Length	Width	Height		
	BC	ST	BC	ST	BC	ST	BC	ST	BC	Spacing	Angle	Number					
Axial compression (monotonic)			81.4							50 spacing/ 100 Width of the FRP		1	150	150	500	Camphor pine	**J. F. Dong, et al. (2015)**
			100									2					
			95.2									3					
					103							2					
									68.9			2					
Axial compression									7.4	100S/ 100W		1	100D	circle	2000	Chinese Fir Timber	**H Wang, et al. (2023)**
									8.55	100S/100W		2	100D	circle	2000		

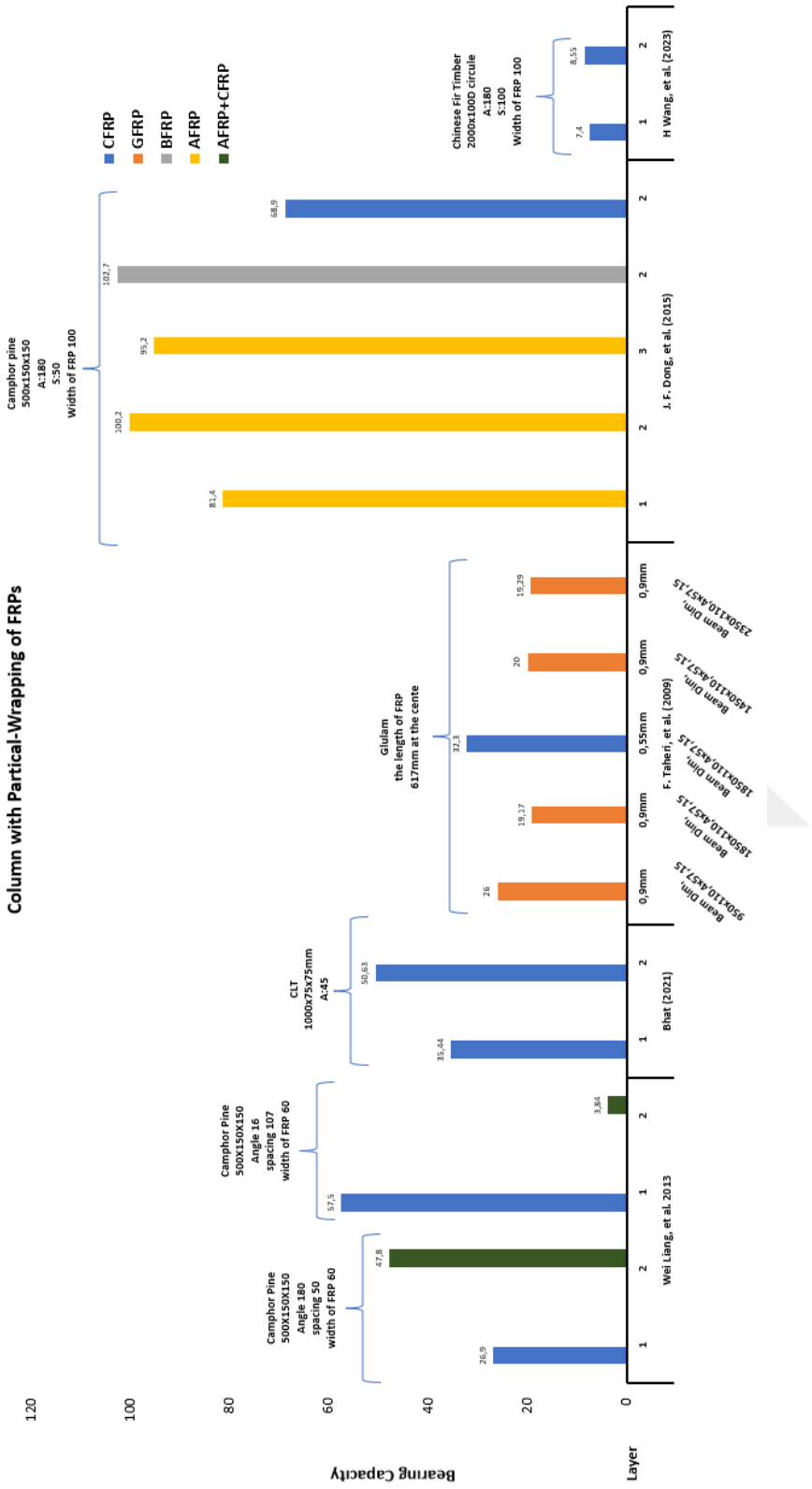


Figure 5.75: Comparative Column Capacity Results for Partially Reinforced Timber Members with Various FRP Materials

The bar chart presents the bearing capacity of timber columns with partial FRP wrapping, categorized by different wood types, number of FRP layers, and research studies. The y-axis represents the bearing capacity, while the x-axis lists various experimental setups, including number of FRP layers, research studies and different FRP types (CFRP in blue, GFRP in orange, BFRP in grey, AFRP in yellow, and hybrid AFRP+CFRP in green).

In Dong et al.'s study, using 2 layers of BFRP resulted in the highest increase in bearing capacity at 132.7%, while AFRP and CFRP provided 100.2% and 68.9%, respectively. Interestingly, CFRP, which is typically more effective, showed the lowest improvement in this case. On the other hand, when one, two, and three layers of AFRP were tested, the two-layer configuration provided the highest increase at 100.2%, whereas one and three layers achieved **81.6% and 95.2%, respectively. This trend contradicts the expectation that adding more layers would continuously improve bearing capacity.

In Bahat's study, a similar pattern was observed, where using 2 layers of CFRP resulted in a higher increase in bearing capacity (50.8%) compared to one layer (35.4%), confirming that, in some cases, increasing the number of FRP layers does not always lead to proportional strength enhancement. The study suggests that beyond an optimal point, additional layers might not be as effective due to factors such as bonding limitations and stress distribution.

5.2.3. Studies Conduct both Methods (Full + Partial)

Graybeal and Tanesi (2008) explored the performance of circular poplar timber columns under axial compression when reinforced with carbon fibers set in an inorganic matrix, specifically geopolymer. They conducted tests on forty specimens using different configurations of carbon fibers, including spirals, cross spirals, and full wraps, utilizing yarns with either 3,000 or 48,000 filaments Figure 5.76. The results indicated that carbon fiber confinement notably improved the mechanical attributes of the columns, enhancing their strength, stiffness, and reliability. The columns reinforced with 48k-tow spirals at varying spacings showed progressive gains in maximum load capacity and elastic modulus. For example, specimens with 48k-tow spirals spaced at 75 mm recorded a 9% increase in maximum load (121.8 kN) and a 17% rise in modulus (9.1 GPa), while those with spirals at 25 mm spacing achieved a 16% increase in load (129.4 kN) and a 37%

increase in modulus (10.6 GPa). Cross spirals spaced at 25 mm led to even more significant improvements, yielding a 24% increase in maximum load (138.8 kN) and a 61% increase in modulus (12.5 GPa). Full wrapping with carbon fibers resulted in the most substantial enhancements. Specimens fully wrapped with 48k-tow displayed a 32% boost in maximum load (147.9 kN) and an 80% increase in modulus (14.2 GPa). Similarly, those wrapped with 3k fabric realized a 35% increase in maximum load (150.8 kN) and a remarkable 130% increase in modulus (18.2 GPa). The 3k-fabric full wrap demonstrated the highest stiffness, while the 48k-tow wrap exhibited better toughness and resistance to loads beyond peak performance, signifying improved ductility. Additionally, the use of carbon fiber confinement led to less variability in performance among specimens, as shown by lower standard deviations for maximum load and modulus in fully wrapped configurations. These findings reinforce that carbon fiber confinement, particularly through full wrapping, effectively boosts the strength, stiffness, and reliability of timber columns subjected to axial compression, offering significant advantages for structural reinforcement. The primary failure mode observed in the tested specimens was shear failure. Another failure mode identified was localized compression failure occurring near the top and bottom of certain specimens. However, wrapped specimens demonstrated improved ductility despite experiencing shear failure. Figure 5.77 illustrates fully wrapped and spiral specimens that failed in shear. (Graybeal and Tanesi, 2008)

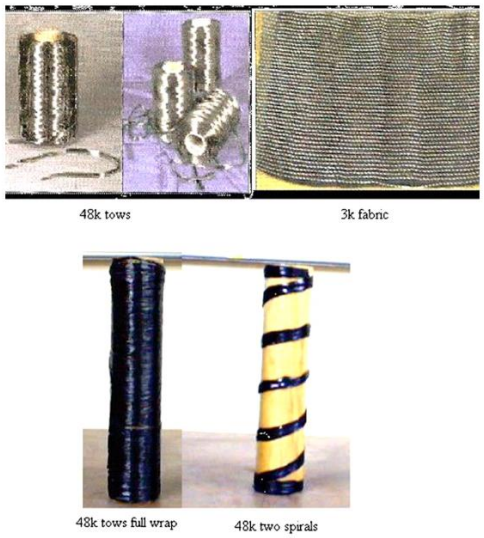
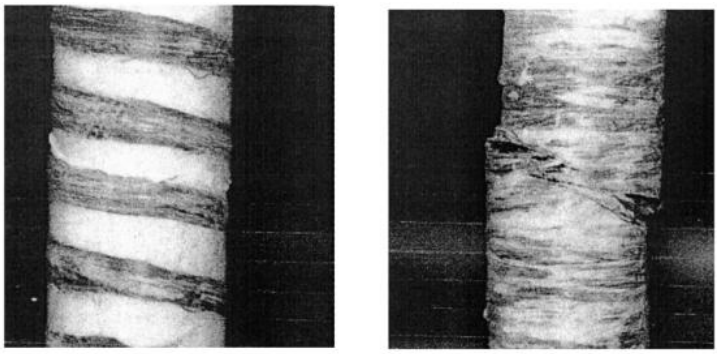


Figure 5.76. Typical carbon reinforcement and column specimens (Graybeal and Tanesi, 2008)



(a) 48k tows spirals at 25mm (a) 48k tows full wrapping

Figure 5.77. Shear failure a specimen with spirals; b specimens with full wrapping (Graybeal and Tanesi, 2008)

Taheri et al. (2009) investigated the buckling behavior of glued-laminated (glulam) timber columns reinforced with FRP sheets, emphasizing structural effectiveness and economic viability. The study involved 54 test specimens made of low-grade spruce pine fir (SPF) timber, reinforced with CFRP and GFRP in both full-length and partial-length configurations, under varying lengths and support conditions Figure 5.78. Results showed that full-length CFRP reinforcements significantly increased buckling loads by up to 52%, while partial-length reinforcements offered a cost-effective solution with a 26% strength improvement. Despite notable stiffness enhancements, particularly with CFRP, these were less pronounced than strength gains. Correlation between analytical models and experimental findings supported the effectiveness of FRP reinforcement, leading to the recommendation of partial-length CFRP reinforcement as an economical retrofitting strategy for timber structures Summary of the result that showing in Figures 5.79 and 5.80 indicate that the load-deflection analysis demonstrated a significant reduction in deflections in glulam columns when reinforced with FRP, with CFRP showing the best performance due to its superior stiffness properties. Fully reinforced columns had the lowest deflections, particularly under pinned-pinned boundary conditions. In contrast, implementing partial-length reinforcement at the mid-span proved to be a cost-effective alternative, effectively cutting deflections to approximately half of the improvements seen with full reinforcement. Columns with fixed-fixed boundary conditions displayed overall lower deflections owing to the presence of end restraints, emphasizing the critical role of boundary conditions on column performance. The findings highlighted CFRP's efficacy in enhancing both stiffness and stability, positioning it as an ideal option for both full and partial reinforcement strategies. (Taheri et al., 2009)

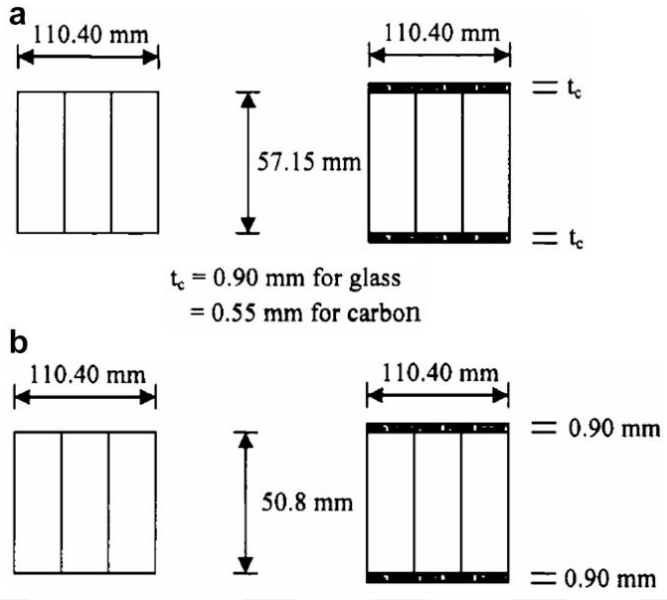
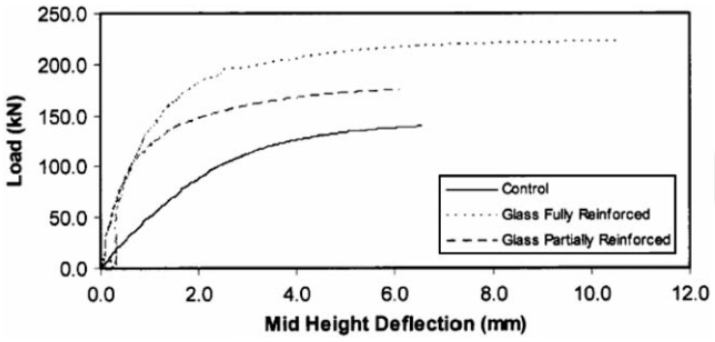
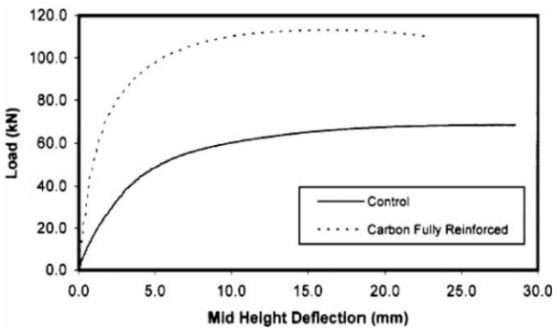


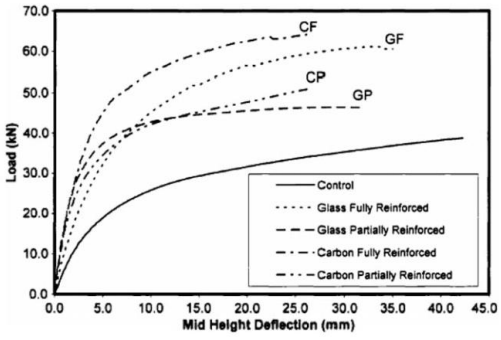
Figure 5.78. The columns' cross sections are (a) pinned and (b) fixed (Taheri et al., 2009)



(a)



(b)



(c)

Figure 5.79. Response averages for pinned–pinned GFRP columns: (a) 950 mm, (b) 1400 mm, (c) 1850 mm (Taheri et al., 2009)

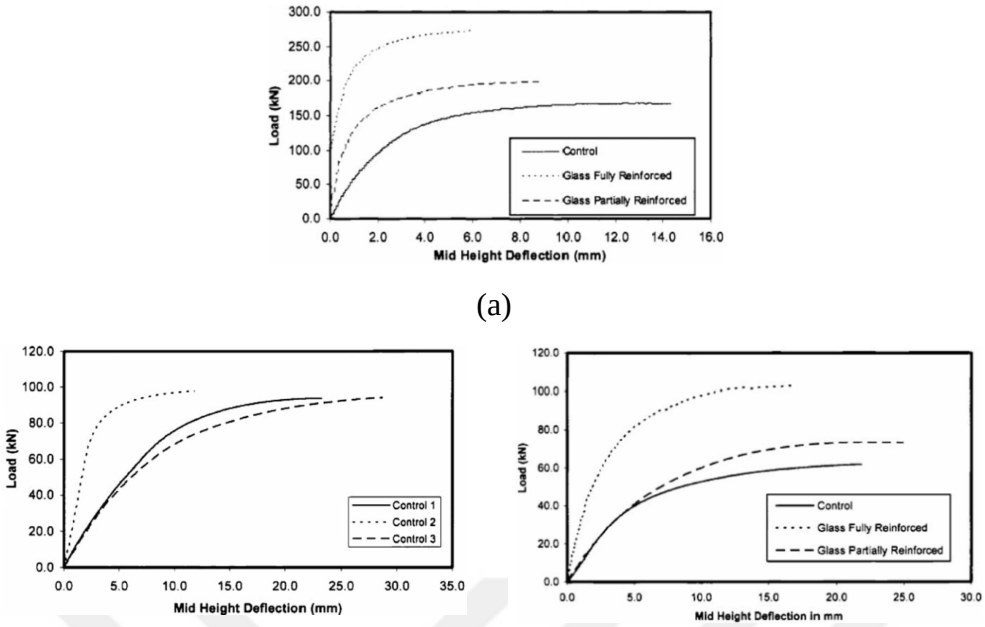


Figure 5.80. Response averages for fixed–fixed GFRP columns: (a) 1450 mm, (b) 1900 mm, (c) 2350 mm (Taheri et al., 2009)

Dong et al. (2015) conducted research examining the structural performance of timber columns reinforced with externally bonded FRP sheets, with a particular focus on the effects of fractured wood texture. The study involved fourteen timber columns featuring both circular and square cross-sections, which were subjected to axial compression tests Figure 5.81 (b) using various types of FRP—namely AFRP, BFRP, and CFRP—utilizing both full and intermittent wrapping configurations Figure 5.81 (a). The findings revealed that FRP reinforcement significantly enhanced both the load-carrying capacity and ductility of the columns. Specifically, the square columns exhibited strength increases ranging from 69% to 103%, while the circular columns showed enhancements between 35% and 83%. Notably, BFRP with intermittent wrapping led to the most substantial strength improvements, whereas AFRP was found to deliver superior ductility. Figure 5.82 demonstrates the failure modes identified during the experimental tests, which has revealed significant differences between reference columns and those that have been strengthened. The reference columns experienced sudden failure without prior signs of cracking. However, when specimens were reinforced, the manner of failure changed notably; fractures in the wood texture became apparent. Specifically, the columns that strengthen with AFRP in 1 and 3 layers transitioned from a brittle diagonal fracture to a more ductile failure due to the addition of FRP reinforcement. Conversely, the failure of

column (AFRP with 2 layers) was a result of buckling in the wood structures at knots where AFRP sheets were not used. Ultimately, the research concluded that FRP sheets effectively strengthen timber columns, mitigate crack propagation, and enhance load-bearing capacity; however, the advantages may diminish with the application of excessive layers of reinforcement. (Dong et al., 2015)



(a) (b)

Figure 5.81. (a) Illustration of wrapping of FRP methods, (b) Test setup (Dong et al., 2015)

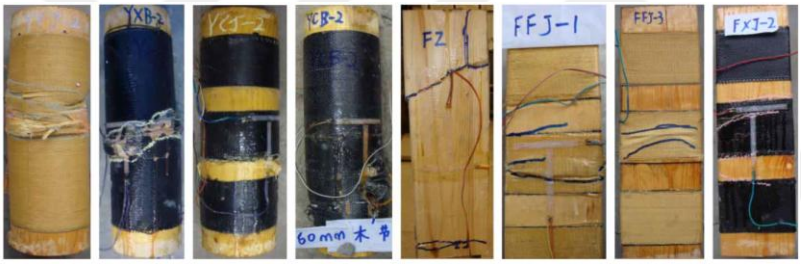


Figure 5.82. Failure modes of specimens tested (Dong et al., 2015)

Zhou (2022) conducted an experimental investigation to improve the seismic performance of Korean pine timber columns using a composite reinforcement technique that combines near surface mounted (NSM) steel bars with CFRP strips. In their study, eight specimens underwent lateral cyclic loading shown in Figure 5.84, with variations in the number of steel bars (0, 2, or 4) and different CFRP wrapping configurations (none, partial wrapping, or full wrapping) shown in Figure 5.83. The results indicated that the specimens with mounted steel bars and interval-wrapped CFRP strips exhibited a significant increase in peak load (32.3% to 35.1%) and deformation (67.9% to 74.4%). In contrast, specimens with mounted steel bars and fully jacketed CFRP strips achieved an even greater increase in peak load, ranging from 59.5% to 60.1%, while ultimate displacement improved between 70.3% and 89.4%. The findings suggest that the composite reinforcement method effectively enhances the performance of timber columns. However, when the number of mounted steel bars is constant, interval-wrapped

CFRP strips do not contribute to the improvement of bearing capacity, whereas fully jacketed CFRP strips do enhance peak load. Even without mounted steel bars, the fully jacketed CFRP strips positively impacted the lateral bearing capacity of the timber columns. The failure of specimens primarily occurred near the base of the columns, where the interval-wrapped CFRP strips failed to adequately restrain the vertical deformation of the timber grain, leading to rapid development of tensile strain and eventual brittle rupture parallel to the grain. For specimen TC-0-F, the ultimate displacement increased by about 30.6% compared to the reference specimen, while specimens TC-4-S and TC-4-F showed increases of 67.9% and 70.3%, respectively. This indicates that the wrapped CFRP strips significantly enhance the deformation capacity of strengthened timber columns. The experimental results highlight that mounted steel bars improve the bearing capacity of timber columns, with the arrangement of these bars being a crucial factor. In specimens TC-4-N, TC-4-S, and TC-4-F, two steel bars positioned near the neutral axis of the timber column cross-section did not significantly contribute to the enhancement of bearing capacity. The failure modes observed during the tests, illustrated in Figure 5.85, revealed that full CFRP wrapping was more effective than interval wrapping, and the addition of NSM steel bars provided further improvements, particularly under high deformation conditions.(Zhou and shi, 2022)

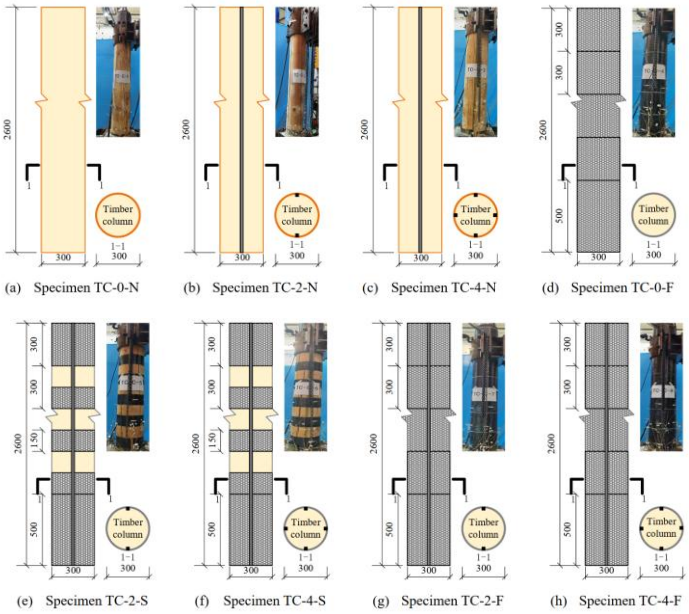
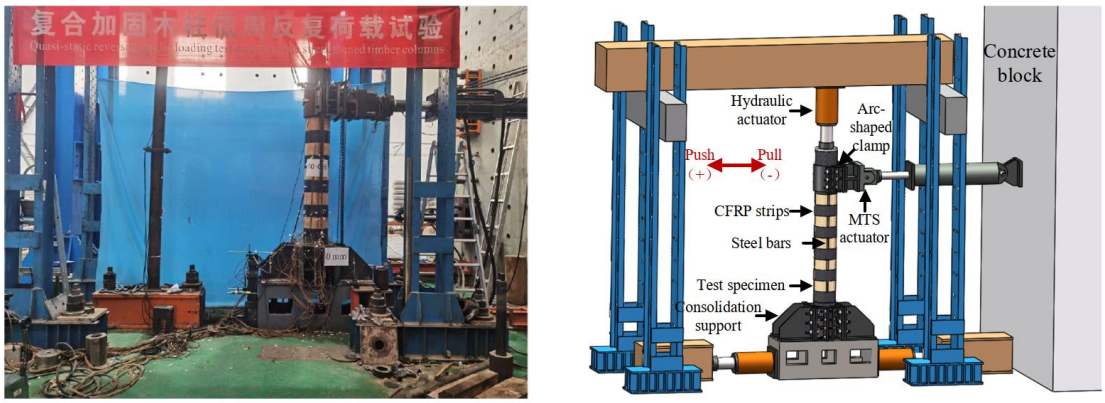
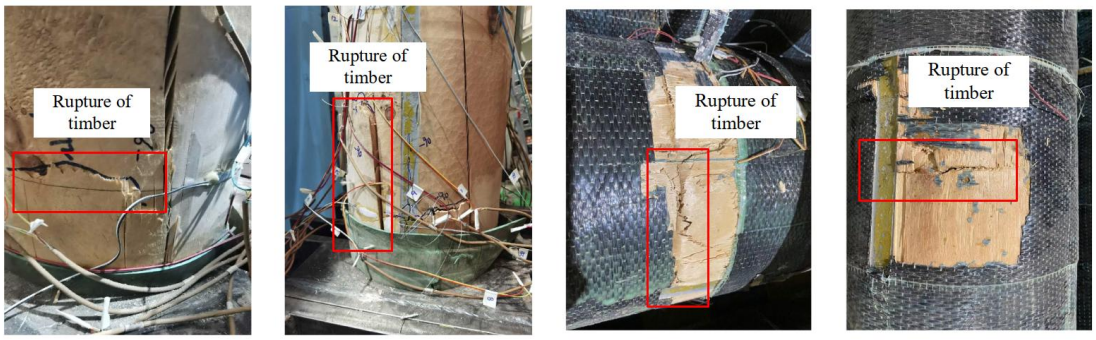


Figure 5.83. Strengthening scheme of timber columns (mm))TC-number: number of bars, N: None, S: Confined with partial strips, F: Fully confined. (Zhou and shi, 2022)



(a) Photo of test setup (b) Diagram of test setup

Figure 5.84. Test setup (Zhou and shi, 2022)



(a) Specimen TC-0-N (b) Specimen TC-2-N (c) Specimen TC-2-S (d) Specimen TC-2-F

Figure 5.85. Modes of specimen failure (Zhou and shi, 2022)

Wang et al. (2023) carried out an experimental investigation involving 36 long timber columns to evaluate the compressive behavior of six different types of Hybrid Fiber Reinforced Polymer (HFRP) sheets Figure 5.86. The study utilized three reinforcement methods: 100 mm weft wrapping, full wrapping, and warp-weft partial wrapping see Figure 5.87, with two unreinforced columns serving as a control group. In the first group, which used weft wrapping, significant improvements in bearing capacity were observed, with CFRP1 showing a 7.40% increase and C2A1G1 achieving the highest enhancement among unidirectional sheets at 10.12%. Bidirectional sheets outperformed the unidirectional variants with CoGa reaching a 22.42% increase. The ductility improvements were also notable, especially with C2A1G1 demonstrating a substantial 374.89% increase in ultimate displacement, while CoAa achieved the maximum ductility enhancement at 502.20% see Table 5.19. (Wang et al., 2023)

In the second group employing full wrapping, CFRP2 exhibited an 8.55% increase in bearing capacity, with C2G1 and C1A2G1 showing similar improvements of 7.02% and

8.35%, respectively Figure 5.90. C2A1G1 achieved an 11.07% increase, but it was CoGa and CoAa that excelled further, with capacity improvements of 23.18% and 18.71%. Full wrapping proved to maximize strength across all specimens, largely benefiting from its bidirectional fiber configuration, although warp-weft interval wrapping emerged as an efficient alternative, yielding up to 20.15% improvement while using less material. Overall, the study underscored the effectiveness of HFRP reinforcement for enhancing the compressive strength, ductility, and stability of long timber columns, particularly highlighting the advantages of bidirectional sheets and well-optimized reinforcement strategies. (Wang et al., 2023)

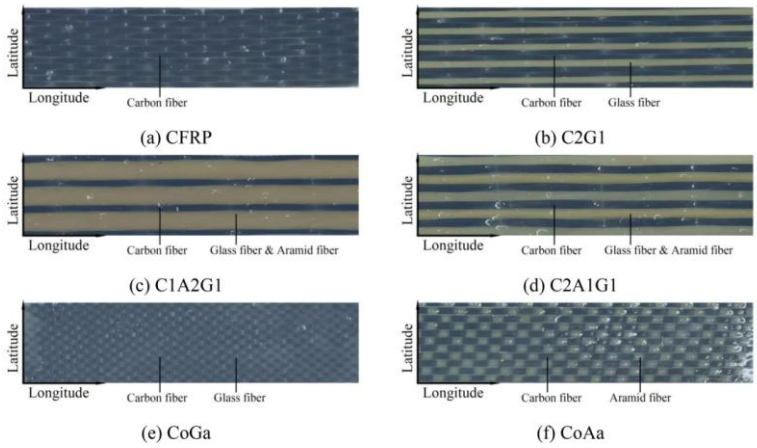


Figure 5.86. FRP types (Wang et al., 2023)

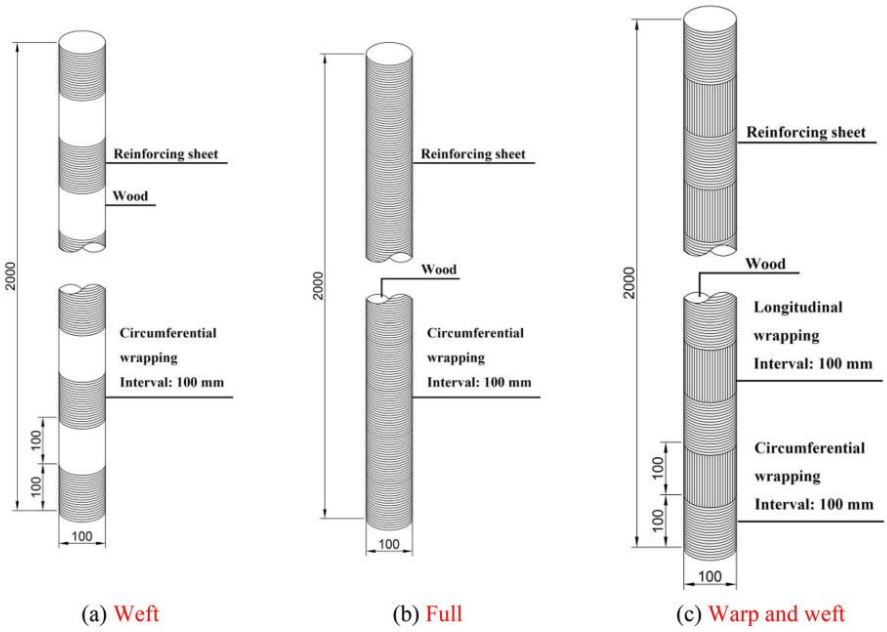
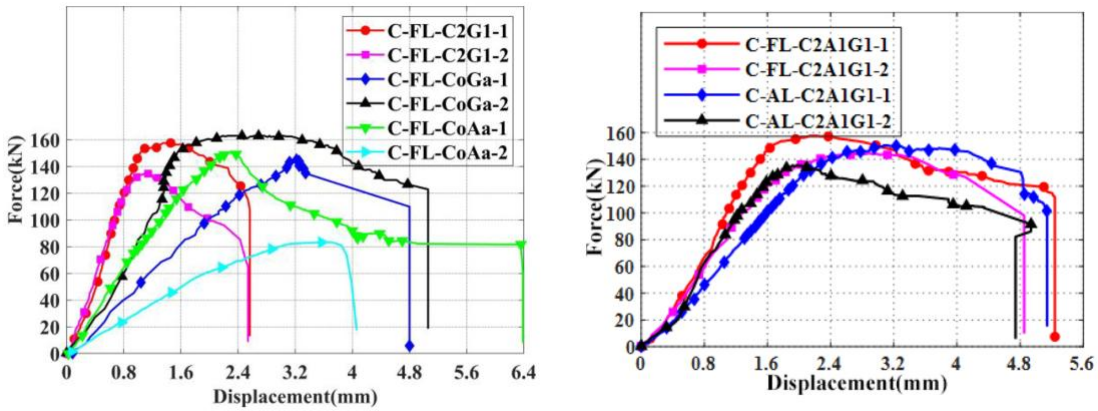


Figure 5.87. Test specimens (Wang et al., 2023)

Table 5.17. Results of group one (Wang et al., 2023)

Material parameter	Control group	(CFRP)1	(C2G1)1	(C1A2G1)1	(C2A1G1)1	(CoGa)1	(CoAa)1
The ultimate bearing capacity	119.06 (kN)	127.88 kN	124.37 kN	127.62 kN	131.11 kN	145.76 kN	139.38 kN
The increasing rate	\	7.40%	4.46%	7.18%	10.12%	22.42%	17.06%
The ultimate displacement	0.550 (mm)	1.108 mm	1.060 mm	1.973 mm	2.610 mm	1.700 mm	3.309 mm
The increasing rate	\	101.53%	92.89%	259.06%	374.89%	209.42%	502.20%
The softening displacement	0.755 (mm)	1.965 mm	2.008 mm	4.041 mm	4.026 mm	3.900 mm	6.066 mm
The increasing rate	\	160.44%	166.07%	435.59%	433.60%	416.90%	703.91%
Material parameter	**Control group**	**(CFRP)2**	**(C2G1)2**	**(C1A2G1)2**	**(C2A1G1)2**	**(CoGa)2**	**(CoAa)2**
The ultimate bearing capacity	119.06 (kN)	129.25 kN	127.43 kN	129.01 kN	132.24 kN	146.66 kN	141.34 kN
The increasing rate	\	8.55%	7.02%	8.35%	11.07%	23.18%	18.71%
The ultimate displacement	0.559 (mm)	0.683 mm	1.063 mm	1.308 mm	3.042 mm	2.488 mm	2.944 mm
The increasing rate	\	22.18%	90.21%	134.14%	444.49%	345.31%	426.99%
The softening displacement	0.767 (mm)	1.913 mm	1.822 mm	4.044 mm	4.711 mm	4.909 mm	5.366 mm
The increasing rate	\	205.16%	188.78%	586.65%	706.05%	741.50%	823.31%



(a) Full wrapping (b) Interval wrapping

Figure 5.88. Ultimate load–displacement curve of group two (Wang et al., 2023)

5.2.4. Studies Conduct Longitudinal FRP Reinforcement

FRP bars or strips are installed longitudinally on the column to enhance both axial and flexural strength.

Lee et al. (2021) conducted a study to evaluate the compressive strength performance of (FRP) and steel-reinforced laminated timber constructed from small-diameter Larix timbers. The primary objective was to improve seismic resistant performance while retaining aesthetic qualities. The research involved testing six different specimen types, which included unreinforced controls and those reinforced with CFRP plates, CFRP bars, GFRP plates, GFRP bars, and steel bars see Figure 5.89. These reinforcements were bonded with adhesives and incorporated into a multi-layered laminated timber column structure with dimensions of 120 × 120 × 450 mm. The compression strength tests were

performed at a loading rate of 1.35 mm/min. Results indicated that columns reinforced with GFRP bars and steel bars achieved the most significant strength enhancements, with increases of 38% and 37%, respectively, compared to the control specimens. In contrast, CFRP bars and plates yielded modest gains in strength of 7% and 6%, respectively, while GFRP plates exhibited a strength reduction of 5% due to cohesive failure. Notably, the modulus of elasticity saw increases of up to 21% for specimens reinforced with steel bars. The study revealed that the reinforced specimens demonstrated reduced diagonal fractures compared to the unreinforced controls, which typically failed due to issues related to fiber slope angles. The findings underscored the effectiveness of GFRP and steel bars in improving strength, along with revealing the variability in strength outcomes depending on the type of reinforcement used and the bonding methods applied. All specimens, apart from those with GFRP plates, exhibited low strength variation, ranging from 2% to 10.4%, and effectively dampened fractures associated with fiber slope angles, thereby enhancing their seismic design performance. Figure 5.90 demonstrate the compression failure modes identified during the experimental tests, which varied depending on reinforcement type and wood characteristics. Control specimens exhibited diagonal failure due to the fiber slope angle, with strength influenced by defects such as grain splitting, knots, or bonded part splitting. Control-3 showed high strength due to minimal defects, while Control-2 and Control-5 exhibited lower strength due to significant knot failures. Reinforced specimens with CFRP plates showed diverse failure modes, including splitting at the plate-wood bond, diagonal fractures, plate collapse, and cohesive failure of the CFRP plates, with variations based on knot presence and plate bonding integrity. GFRP plate-reinforced specimens primarily failed at knots through splitting along the grain, cohesive failure of the GFRP plate, or splitting of bonded parts. The GFRP plates were less effective due to weak phenolic adhesive strength. CFRP bar-reinforced specimens generally failed at the top under compressive load, except CFRP bar-3, which fractured near a large knot. GFRP bar-reinforced specimens failed through splitting initiated at knots or brittle timber fracture at the bar insertion point, with GFRP bars themselves compressively damaged. Steel bar-reinforced specimens displayed consistent strength, with wood failure occurring even at large knots. (Lee et al., 2021)

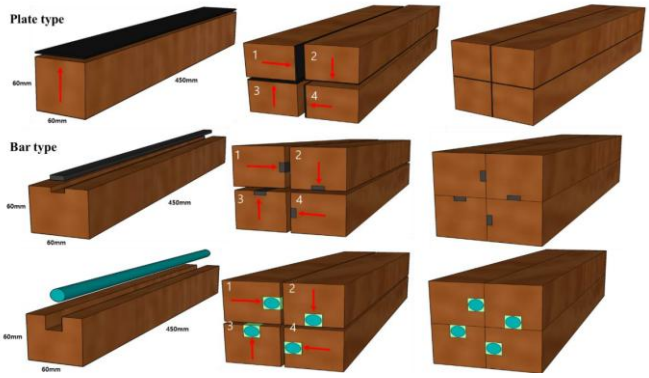


Figure 5.89. Shape of the compression strength specimen (Lee, et al. 2021)



Figure 5.90 .The reinforced-specimen failure modes (Lee, et al. 2021)

5.2.5. Studies Conduct Hybrid Reinforcement Techniques

Integrates FRP with additional reinforcement methods, like steel coverings or grout-filled sleeves.

Qiao, Yang, and Mou (2020) examine the axial compressive behavior of Square timber-filled Steel Tube (TFST) stub columns that are confined with (CFRP) see Figure 5.93. In this study, a total of twelve specimens were tested under axial compression showing in Figure 5.94, including bare timber, hollow steel tubes, and TFST columns, with variations in timber conditions, specifically the presence or absence of knots, as well as different configurations of CFRP confinement layers. The findings indicate that TFST columns exhibit significantly enhanced axial compressive strength and ductility when compared to bare timber and hollow steel tube columns. Specifically, the ultimate strength of TFST columns was found to be twice that of timber and 1.7 times that of hollow steel tubes. The application of CFRP confinement further improved the performance, resulting in an 11% increase in ultimate strength when three layers of CFRP were used. However, the

presence of knots in the timber reduced strength by approximately 10–11%. The combined strength of the timber and steel components was observed to be slightly less than the theoretical predictions, likely due to interaction effects. Additionally, TFST columns demonstrated exceptional strength-to-weight ratios, being 6.5 to 7 times greater than those of traditional concrete-filled steel tube (CFST) columns, indicating their potential for use in seismic-resistant structures. The The failure modes observed across the three specimen groups highlight distinct behaviors influenced by material and structural interactions see Figure 5.95. Bare timber columns (Group 1) failed through brittle fracture, with cracks forming parallel to the grain and more rapid failure occurring in specimens with knots. Hollow steel tube specimens (Group 2) experienced outward and inward buckling, with CFRP tearing due to outward local buckling. Timber-filled steel tubes (TFST, Group 3) displayed a combination of steel tube buckling and timber shear or extrusion failures. The timber failures transitioned from grain splitting in bare specimens to shear and local extrusion under steel tube confinement, fully utilizing the timber's axial capacity. The CFRP and infilled timber significantly mitigated both outward and inward buckling of steel tubes, enhancing their deformation resistance compared to hollow tubes. (Qiao et al., 2020)

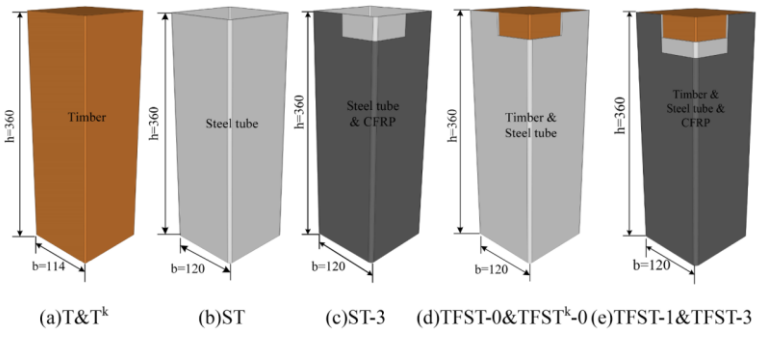


Figure 5.91. Specimen types.(Qiao et al., 2020)

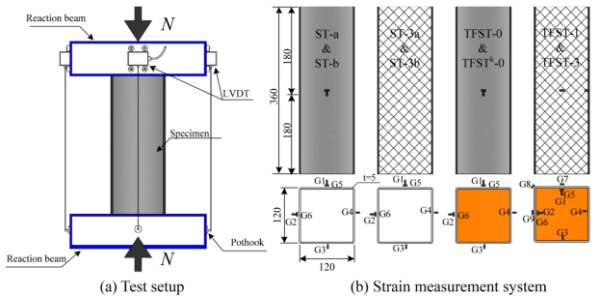
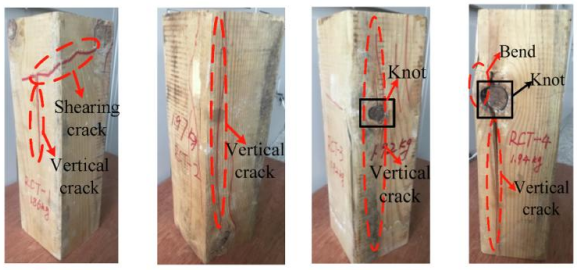
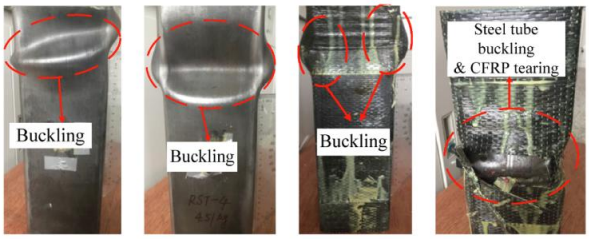


Figure 5.92. Illustration of the loading mechanism and measurement apparatus (Qiao et al., 2020)



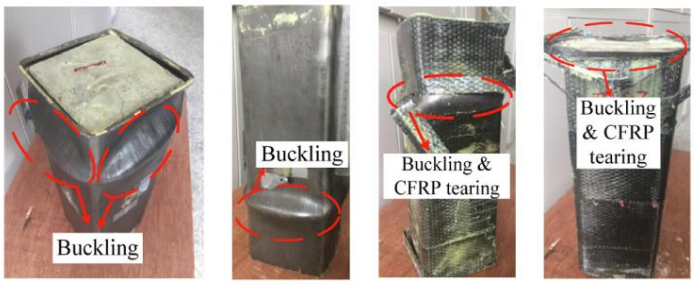
(a) T-a (b) T-b (c) T^k-a (d) T^k-b

Group 1



(a)ST-a (b)ST-b (c)ST-3a (d)ST-3b

Group 2



(a)TFST-0 (b) $TFST^k$-0 (c)TFST-1 (d)TFST-3

Group 3

Figure 5.93. (a) Group 1, (b) Group 2, (c) Group 3 (Qiao et al., 2020)

Otoom et al. 2022 investigate the flexural performance of circular timber columns that have been enhanced with GFRP wrapping systems subjected to three-point bending tests Figure 5.97. Eight specimens included both unwrapped columns and those wrapped with GFRP, either combined with epoxy or cementitious grout infills shown in Figure 5.94 and Table 5.20. Additionally, some samples were reinforced with CFRP straps. The findings indicated substantial increases in both flexural capacity and energy absorption, with columns wrapped in GFRP and epoxy demonstrating the highest flexural strength—up to 95% greater than that of the unwrapped columns see the summary result in Table 5.21. Furthermore, the incorporation of CFRP straps significantly improved energy absorption,

resulting in a 207% increase. The failure modes of the columns were influenced by the type of infill used, with epoxy showing superior performance in stress transfer and a reduction in premature failures compared to grout. Both numerical simulations and theoretical models corroborated the experimental findings, highlighting the effectiveness of GFRP and CFRP in enhancing the performance of timber columns. (Otoom et al., 2022)

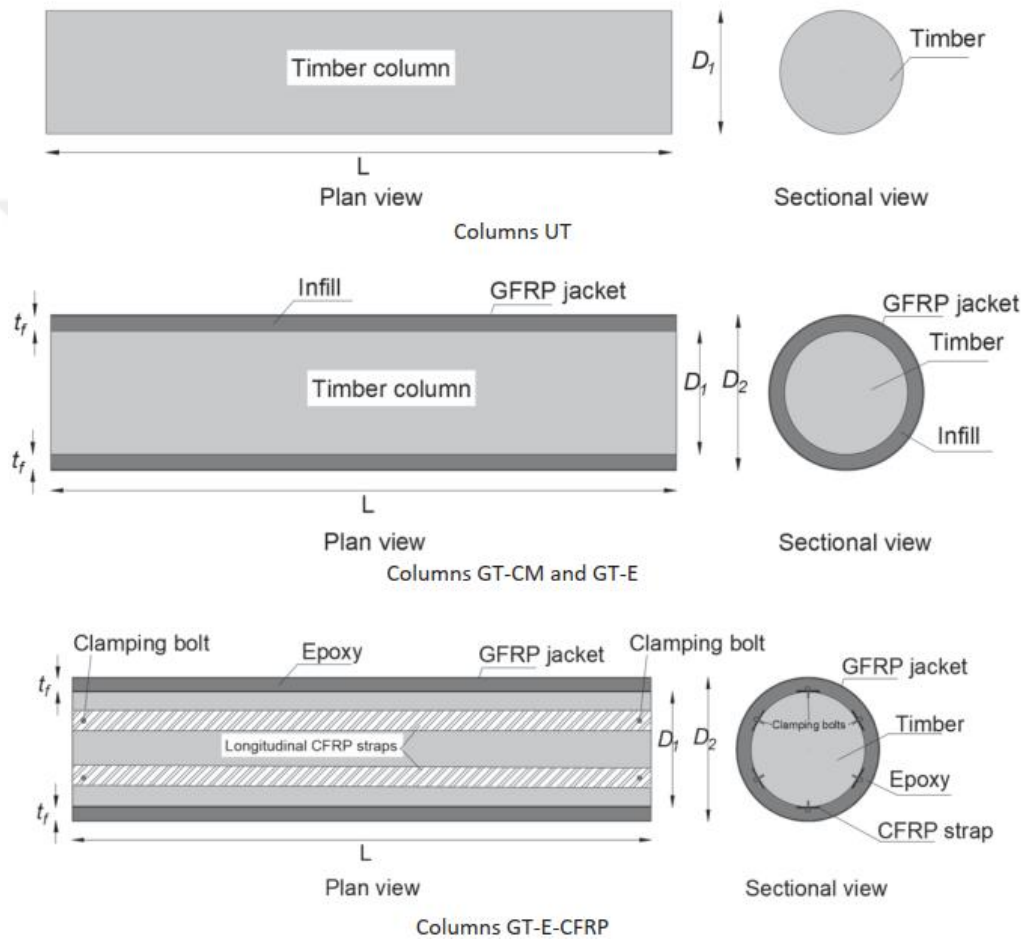


Figure 5.94. Plan and sectional views of full-scale (Otoom et al., 2022)

Table 5.18. Details of tested specimens (Otoom et al., 2022)

Column	Average diameter (mm)		Infill	Strengthening with CFRP straps
	Unwrapped (D_1)	Wrapped (D_2)		
UT1	239 ± 10.0	–	–	–
UT2	251 ± 18.9	–		
GT-CM1	232 ± 7.5	295	Grout	–
GT-CM2	227 ± 13.5	287		
GT-E1	213 ± 11.3	273	Epoxy	–
GT-E2	225 ± 5.7	285		
GT-E-CFRP1	248 ± 17.5	302	Epoxy	Six CFRP straps
GT-E-CFRP2	242 ± 31.0	308		

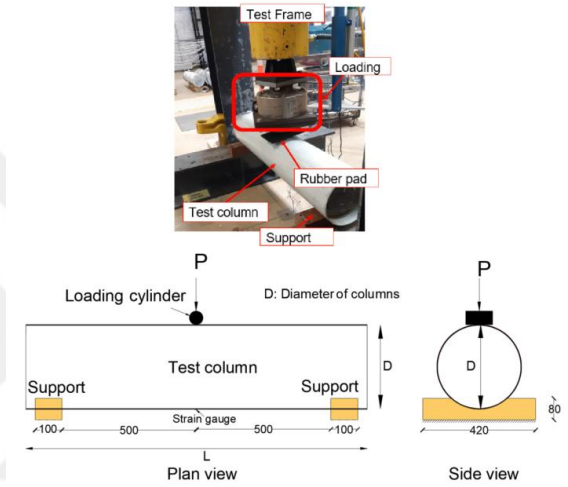


Figure 5.95. Full-scale column test arrangement and schematic design (mm) (Otoom et al., 2022)

Table 5.19. Summary of results (Otoom et al., 2022)

Column	Experimental	
	Peak load (kN)	Deflection at peak (mm)
UT1	474	50.6
UT2	555	53.2
GT-CM1	523	52.3
GT-CM2	572	49.5
GT-E1	592	58.8
GT-E2	644	56.9
GT-E-CFRP1	867	73.4
GT-E-CFRP2	1001	72.0

Zhang et al. (2023) conducted an investigation into the mechanical performance of GFRP-timber-steel tube-concrete composite columns (GTSCs) see Figure 5.96 subjected to axial compression. The research included tests on eight specimens, which varied based on timber core diameters, the number of GFRP laminates, and laminate orientations shown in Figure 5.97. Their findings indicated that increasing the timber core diameter led to a significant decrease in both the ultimate bearing capacity and stiffness of the columns,

primarily due to diminished confinement effects from the timber core. Specifically, the specimens G2-90-T30, G2-90-T40, and G2-90-T50 exhibited reductions in ultimate bearing capacity of 10.5%, 27.5%, and 50.7%, respectively, when compared to the reference specimen G2-90-T0. Despite these reductions in axial load capacity, the weight reductions achieved corresponded to only minor decreases in load-to-weight ratios (P/W), specifically 2.7%, 15.9%, and 35.8%. The optimal lay-up angle for GFRP laminates to achieve maximum ultimate bearing capacity was identified as 90°. In contrast, using angles of 45° and 60° resulted in reductions of 14.7% and 18.1%, respectively. Furthermore, specimens with increased layers of GFRP, such as G1-90-T50, G2-90-T50, and G3-90-T50, showed enhancements in ultimate bearing capacity, with improvements of 11.2% and 18.7% observed for specimens with two and three layers, respectively, although the rate of improvement became less pronounced with additional laminates. Energy dissipation characteristics were also affected by the diameter of the timber core. Generally, larger timber diameters resulted in higher energy dissipation (TA) and improved TA-to-weight (TA/W) ratios. The study demonstrated that GFRP laminates with 90° lay-up angles maximized energy dissipation, with significant increases in TA observed when the number of laminates was increased to two. Regarding stiffness, an increase in timber core diameter resulted in a reduction of up to 22.4%, as exemplified by the comparative analysis of G2-90-T40 and G2-90-T0. Nevertheless, the stiffness-to-weight ratio (K/W) remained relatively constant. The introduction of GFRP laminates helped to compensate for the loss in stiffness, with the specimen G3-90-T50 achieving comparable stiffness to G2-90-T30 despite having a larger timber core. The 60° GFRP lay-up angle was found to provide the best balance of stiffness and overall performance metrics. The analysis of failure modes in Figure 5.98 demonstrated the intricate relationships between the timber core, GFRP laminates, and other materials present in the composite. Although the timber core contributed to a reduction in ultimate capacity, it also enhanced ductility and energy dissipation. The researchers suggested that reinforcing the FRP constraints could mitigate the capacity losses attributed to the timber core. A theoretical model developed during the study was shown to closely correlate with the experimental results, highlighting the potential of GTSCs to achieve an optimal balance between weight reduction, energy dissipation, and structural performance. (Zheng and Zhou, 2024)

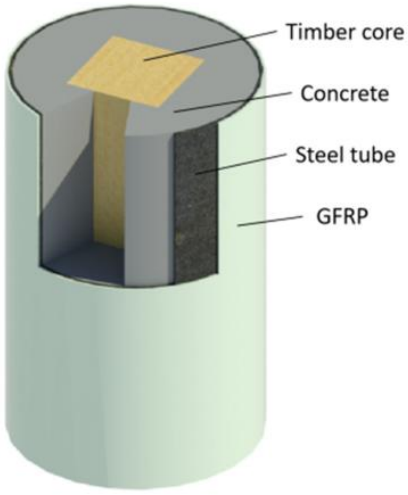


Figure 5.96. A typical composite column made of concrete, steel tubes, timber, and GFRP (Zheng and Zhou, 2024)

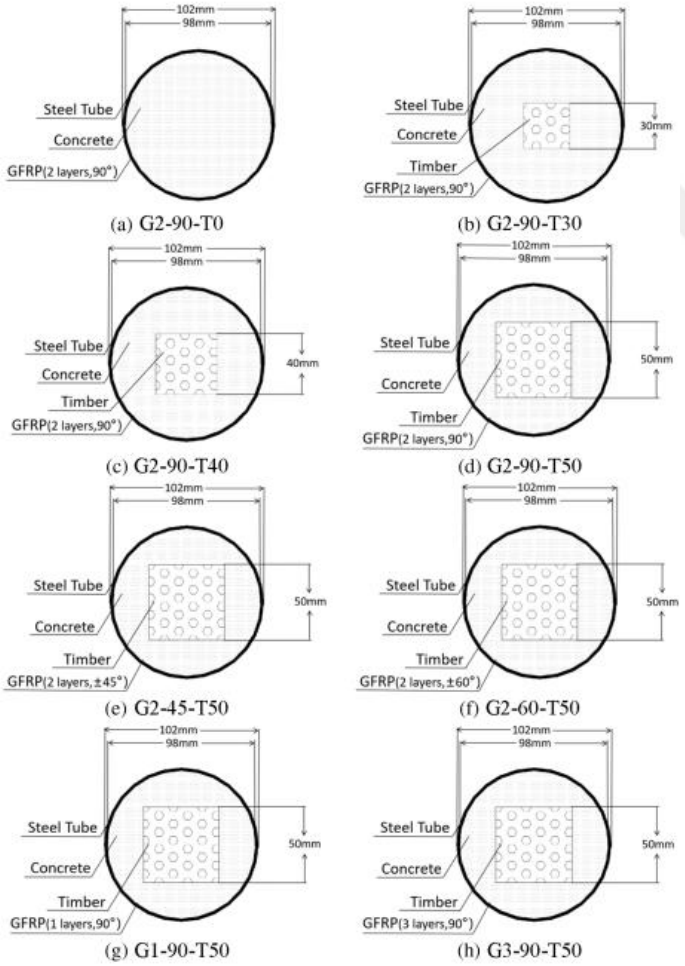


Figure 5.97. Cross-sections of all specimens (Zheng and Zhou, 2024)



(e) G2-45-T50 (f) G2-60-T50 (a) G2-90-T0 (b) G2-90-T30

(g) G1-90-T50 (i) G3-90-T50 (c) G2-90-T40 (d) G2-90-T50

Figure 5.98. Modes of failure of GTSCs (Zheng & Zhou, 2024)

6. CONCLUSION AND RECOMMENDATIONS

Optimization of FRP Reinforcement Strategies: The effectiveness of FRP reinforcement in both beams and columns is significantly influenced by the number of layers, bond length, and width. Studies indicate that while increasing FRP layers enhances strength and ductility, excessive layering may lead to bonding inefficiencies and premature failure (Vahedian et al., 2019; Dong et al., 2015). Future research should focus on identifying the optimal number of FRP layers tailored to different timber species and structural configurations to achieve a balance between performance and cost-effectiveness.

Selection of FRP Type and Hybrid Configurations: CFRP has consistently demonstrated superior improvements in both flexural and compressive strength, making it the preferred reinforcement choice. However, BFRP and GFRP provide cost-effective alternatives with notable performance gains, particularly in hybrid configurations (Shi et al., 2022; Corradi et al., 2017). Further studies should explore the potential of hybrid reinforcements, such as CFRP combined with AFRP or BFRP, to optimize both structural performance and economic feasibility (Zhang et al., 2022; Li et al., 2022).

Enhancing Bonding and Confinement Efficiency: The efficacy of FRP reinforcement is largely dependent on bonding techniques, with Near-Surface Mounted (NSM) reinforcement demonstrating superior adhesion and reduced delamination risks (Yeboah and Gkantou, 2021). Additionally, hybrid reinforcement methods, such as integrating FRP with steel or grout-filled sleeves, provide better stress distribution and structural confinement (Zhou et al., 2022; Qiao et al., 2020). Future investigations should focus on advanced bonding adhesives and reinforcement layouts to mitigate debonding failures and maximize load transfer efficiency.

Strengthening Strategies for Specific Structural Needs:

Flexural Strength: Bottom-face reinforcement is highly effective in beams, but the fiber orientation and reinforcement coverage should be optimized to prevent localized stress concentrations (Triantafillou, 1997).

Shear Resistance: Side-face reinforcement significantly enhances shear strength, particularly when CFRP sheets are applied to critical shear zones. Future studies should

explore alternative fiber orientations and hybrid materials to improve shear behavior further.

Compression Performance: Full wrapping provides the most significant enhancement in timber columns, but spiral and hooped wrapping techniques also offer effective lateral strain resistance for retrofitting applications (Liang et al., 2013; Zhang et al., 2012).

Sustainability and Long-Term Performance Considerations: The long-term durability of FRP-reinforced timber structures remains an area requiring further exploration. Future studies should investigate the impact of environmental conditions such as moisture exposure, temperature variations, and cyclic loading to ensure sustained mechanical performance (Wang et al., 2023). Additionally, research should focus on developing eco-friendly FRP alternatives, such as natural fiber-reinforced composites, to enhance sustainability without compromising structural efficiency. (Otoom et al., 2022)

REFERENCES

Abrahamsen, R. B., Malo, K. A. (2014). Structural design and assembly of "treet" - A 14-storey timber residential building in Norway. *WCTE 2014 - World Conference on Timber Engineering, Proceedings*, *April 2014*, 3–10.

Aghayere, A., Vigil, J. (2007). Structural Wood Design: A Practice-Oriented Approach Using the ASD Method. Hoboken, New Jersey: John Wiley & Sons.

Al-Hayek, H., Svecova, D. (2014). Flexural Strength of Posttensioned Timber Beams. *Journal of Composites for Construction*, *18*(2), 1–7. DOI: 10.1061/(asce)cc.1943-5614.0000431

Al-Katib, A., Alkhudery, H., Al-Tameemi, A. (2022). Structural behavior of standard timber beams strengthened using CFRP sheet. *Asian Journal of Civil Engineering*, *23*(5), 727–739. DOI: 10.1007/s42107-022-00452-w

Alam, P., Ansell, M. P., Smedley, D. (2009). Mechanical repair of timber beams fractured in flexure using bonded-in reinforcements. *Composites Part B: Engineering*, *40*(2), 95–106. DOI: 10.1016/j.compositesb.2008.11.010

Alfieri, P. V., García, R., Rosato, V., Correa, M. V. (2016). Biodegradation and biodeterioration of wooden heritage: Role of fungal succession. *International Journal of Conservation Science*, *7*(3), 607–614.

Alfred, J. (2002). Density of wood substance, adsorption by wood, and permeability of Wood. *The Journal of Physical Chemistry*, *112*, 399–414.

Alhayek, H., Svecova, D. (2012). Flexural Stiffness and Strength of GFRP-Reinforced Timber Beams. *Journal of Composites for Construction*, *16*(3), 245–252. DOI: 10.1061/(asce)cc.1943-5614.0000261

Ali, A. C. (2011). Physical-Mechanical Properties and Natural Durability of Lesser Used Wood Species from Mozambique. *Doctoral Thesis, Swedish University of Agricultural Sciences, Faculty of Forest Sciences, Department of Forest Products, Uppsala*.

Andor, K., Lengyel, A., Polgár, R., Fodor, T., Karácsonyi, Z. (2015). Experimental and statistical analysis of spruce timber beams reinforced with CFRP fabric. *Construction and Building Materials*, *99*, 200–207. DOI: 10.1016/j.conbuildmat.2015.09.026

Arriaga, F., Wang, X., Íñiguez-González, G., Llana, D. F., Esteban, M., Niemz, P. (2023). Mechanical Properties of Wood: A Review. *Forests*, *14*(6). DOI: 10.3390/f14061202

Bączek, P., Borysiuk, P. (2024). Parallel strand lumber made from pine veneer. *Annals of WULS, Forestry and Wood Technology*, *125*, 23–37. DOI: 10.5604/01.3001.0054.6641

Bedon, C., and Louter, C. (2017). Numerical analysis of glass-FRP post-tensioned beams – Review and assessment. *Composite Structures*, *177*, 129–140. https://doi.org/10.1016/j.compstruct.2017.06.060

Bhat, J. A. (2021). Buckling behavior of cross laminated poplar timber columns using various performance improvement techniques. *Materials Today: Proceedings*, *44*, 2792–2796. DOI: 10.1016/j.matpr.2020.12.785

Blaß, H.J., Sandhaas, C. (2017). Timber Engineering: Principles for Design. Karlsruhe: KIT Scientific Publishing. DOI: 10.5445/KSP/1000069616

Chang, W. S. (2015). Repair and reinforcement of timber columns and shear walls - A review. *Construction and Building Materials*, *97*, 14–24. DOI: 10.1016/j.conbuildmat.2015.07.002

Chai, H., So, C., & Yuan, P. F. (2021). Manufacturing double-curved glulam with robotic band saw cutting technique. *Automation in Construction, 124*, 103571.

Chrisp, T. M., Cairns, J., & Gulland, C. (2003). The development of roundwood timber pole structures for use on rural community technology projects. *Construction and Building Materials*, *17*(4), 269–279. DOI: 10.1016/S0950-0618(02)00114-9

Corradi, M., Borri, A., Righetti, L., Speranzini, E. (2017). Uncertainty analysis of FRP reinforced timber beams. *Composites Part B: Engineering*, *113*, 174–184. DOI: 10.1016/j.compositesb.2017.01.030

Corradi, M., Mouli, C., Edmondson, V., Pologanathan, K. (2021). Local FRP reinforcement of existing timber beams. *Composite Structures*, *258*(August 2020), 113–363. DOI: 10.1016/j.compstruct.2020.113363

De La Rosa García, P., Escamilla, A. C., Nieves González García, M. (2013). Bending reinforcement of timber beams with composite carbon fiber and basalt fiber materials. *Composites Part B: Engineering*, *55*, 528–536. DOI: 10.1016/j.compositesb.2013.07.016

Dong, J. F., Jia, P., Yuan, S. C., Wang, Q. Y. (2015). Compressive behaviours of square timber columns reinforced by partial wrapping of FRP sheets. *Materials Research Innovations*, *19*, 1465–1468. DOI: 10.1179/1432891715Z.0000000001593

Dong, J. F., Yuan, S. C., Wang, Q. Y., Liang, W. (2015). Influence of fractured wood texture on structural behaviour of timber columns with fibre reinforced polymer reinforcement. *Materials Research Innovations*, *19*, 5546–5550. DOI: 10.1179/1432891714Z.0000000001149

Fédération Internationale du Béton (FIB). (2001). *Externally Bonded FRP Reinforcement for RC Structures* (Bulletin No. 14). Lausanne: International Federation for Structural Concrete.

Fossetti, M., Minafò, G., Papia, M. (2015). Flexural behaviour of glulam timber beams reinforced with FRP cords. *Construction and Building Materials*, *95*, 54–64. DOI:

10.1016/j.conbuildmat.2015.07.116

Franke, S., Franke, B., Harte, A. M. (2015). Failure modes and reinforcement techniques for timber beams-State of the art. *Construction and Building Materials*, *97*, 2–13. DOI: 10.1016/j.conbuildmat.2015.06.021

Gilfillan, J. R., Gilbert, S. G., Patrick, G. R. H. (2003). The use of FRP composites in enhancing the structural behavior of timber beams. *Journal of Reinforced Plastics and Composites*, *22*(15), 1373–1388. DOI:10.1177/073168403035583

Globa, A., Subhani, M., Moloney, J., Al-Ameri, R. (2018). Carbon Fiber and Structural Timber Composites for Engineering and Construction. *Journal of Architectural Engineering*, *24*(3), 1–14. DOI:10.1061/(asce)ae.1943-5568.0000318

Grabner, M., Wolf, A., Schwabl, E., Schickhofer, G. (2016). Methods of forming veneer structures. *WCTE 2016 - World Conference on Timber Engineering*. 849–85. https://www.researchgate.net/publication/316286076

Graybeal, B., Tanesi, J. (2008). Compression Tests of Circular Timber Column Confined with Carbon Fibers Using Inorganic Matrix. *Transport Research Arena Europe 2008*, *1561*(February), 454–461. DOI:10.1061/(ASCE)0899-1561(2007)19

Günaslan, S. E., Karaşin, A., Öncü, M. E. (2014). *Properties of FRP Materials for Strengthening*. *1*(9), 656–660.

Halicka, A., Ślósarz, S. (2021). Strengthening of timber beams with pretensioned CFRP strips. *Structures*, *34*(May), 2912–2921. DOI: 10.1016/j.istruc.2021.09.055

Hong, C., Li, H., Yang, D., Li, H., Zhang, H., Lorenzo, R. (2022). Compressive performance of AFRP reinforced laminated bamboo stub columns. *Archives of Civil and Mechanical Engineering*, *22*(1), 1–12. DOI: 10.1007/s43452-021-00354-9

Iskander, M. G., Hassan, M. (1998). State of the Practice Review in FRP Composite Piling. *Journal of Composites for Construction*, *2*(3), 116–120. DOI: 10.1061/(asce)1090-0268(1998)2:3(116)

İşleyen, Ü. K., Ghoroubi, R., Mercimek, Ö., Anil, Ö., Erdem, R. T. (2021). Behavior of glulam timber beam strengthened with carbon fiber reinforced polymer strip for flexural loading. *Journal of Reinforced Plastics and Composites*, *40*(17–18), 665–685. DOI: 10.1177/0731684421997924

Joist, F. T. *Timber Strand, Microllam, and Parallam Beams, Headers, and Columns Specifier's Guide*. 1–44.

Kilinçarslan, Ş., Türker, Y. Ş., Avcar, M. (2023). Numerical and Experimental Evaluation of the Mechanical Behavior of FRP-Strengthened Solid and Glulam Timber Beams. *Journal of Engineering Management and Systems Engineering*, *2*(3), 158–169. DOI: 10.56578/jemse020303

Kliger, R., Al-Emrani, M., Johansson, M., Crocetti, R. (2008). Strengthening timber with

CFRP or steel plates - Short and long-term performance. *10th World Conference on Timber Engineering 2008*, 414–421.

Lam, F. (2001). Modern structural wood products. *Progress in Structural Engineering and Materials*, *3*(3), 238–245. DOI: 10.1002/pse.79

Leblon, B., Adedipe, O., Hans, G., Haddadi, A., Tsuchikawa, S., Burger, J., Stirling, R., Pirouz, Z., Groves, K., Nader, J., LaRocque, A. (2013). A review of near-infrared spectroscopy for monitoring moisture content and density of solid wood. *Forestry Chronicle*, *89*(5), 595–606. DOI: 10.5558/tfc2013-111

Lee, I. H., Song, Y. J., Hong, S. (2021). Evaluation of the Compression Strength Performance of Fiber-reinforced Polymer (FRP) and Steel-reinforced Laminated Timber Composed of Small-diameter Timber. *BioResources*, *16*(1), 633–642. DOI: 10.15376/biores.16.1.633-642

Li, H., Chen, B., Fei, B., Li, H., Xiong, Z., Lorenzo, R., Fang, C., Ashraf, M. (2022). Mechanical properties of aramid fiber reinforced polymer confined laminated bamboo lumber column under cyclic loading. *European Journal of Wood and Wood Products*, *80*(5), 1057–1070. DOI: 10.1007/s00107-022-01816-4

Li, H., Wang, L., Wei, Y., Semple, K. E., and Dai, C. (2023). Out-of-plane bending behavior of cross-laminated timber members enhanced with fiber-reinforced polymers. *Journal of Building Engineering*, *66*(January), 105–862. DOI: 10.1016/j.jobe.2023.105862

Liang, W., Dong, J. F., Wang, Q. Y. (2013). Mechanical study on short timber columns reinforced by different methods of FRP under axial compression. *Applied Mechanics and Materials*, *405–408*, 968–971. DOI: 10.4028/www.scientific.net/AMM.405-408.968

Ling, Z., Liu, W., Shao, J. (2020). Experimental and theoretical investigation on shear behaviour of small-scale timber beams strengthened with Fiber-Reinforced Polymer composites. *Composite Structures*, *240*(September 2019), 111–989. DOI: 10.1016/j.compstruct.2020.111989

Manninen, H. (2014). *Long-term outlook for engineered wood products in Europe.* European Forest Institute, Technical Report 91.

McKay, A. R. J. (2021). Exploring physical and mechanical properties of OSB and underutilized species to be used in the Glulam industry. *Pharmacognosy Magazine*, *75*(17), 399–405.

Mohammad, M., Gagnon, S., Douglas, B. K., Podesto, L. P. E. (2012). Introduction to Cross Laminated Timber. *Wood Design Focus 22,* 3–12.

Nogueira, E. M., Nelson, B. W., Fearnside, P. M. (2005). Wood density in dense forest in central Amazonia, Brazil. *Forest Ecology and Management*, *208*(1–3), 261–286. DOI: 10.1016/j.foreco.2004.12.007

Nowak, T. P., Jasieńko, J., Czepizak, D. (2013). Experimental tests and numerical analysis of historic bent timber elements reinforced with CFRP strips. *Construction and Building Materials*, *40*, 197–206. DOI: 10.1016/j.conbuildmat.2012.09.106

O'Callaghan, R. B. (2021). *Effects of GFRP reinforcement on the compressive behaviour of square SPF timber columns*. http://hdl.handle.net/10012/17479

O'Ceallaigh, C., Sikora, K., McPolin, D., Harte, A. M. (2020). Modelling the hygro-mechanical creep behaviour of FRP reinforced timber elements. *Construction and Building Materials*, *259*, 119–899. DOI: 10.1016/j.conbuildmat.2020.119899

Ong, C.B. (2015). *Glue-laminated timber (Glulam)*. In Wood Composites (pp. 124-140). Elsevier. DOI: org/10.1016/B978-1-78242-454-3.00007-X

Otoom, O. F., Lokuge, W., Karunasena, W., Manalo, A. C., Ozbakkaloglu, T., Ehsani, M. R. (2022). Flexural behaviour of circular timber columns strengthened by glass fibre reinforced polymer wrapping system. *Structures*, *38*, 1349–1367. DOI: 10.1016/j.istruc.2022.02.070

Porteous, J., Kermani, A. (2007). Structural Timber Design to Eurocode 5. Oxford: Blackwell Publishing.

Qi, Y., Xiong, W., Liu, W., Fang, H., Lu, W. (2015). Experimental study of the flexural and compression performance of an innovative pultruded glass-fiber-reinforced polymer-wood composite profile. *PLOS ONE*, *10*(10). DOI: 10.1371/journal.pone.0140893

Qiao, Q., Yang, Z., Mou, B. (2020). Experimental study on axial compressive behavior of CFRP confined square timber filled steel tube stub columns. *Structures*, *24* , 823–834. DOI: 10.1016/j.istruc.2020.02.007

Raftery, G. M., Rodd, P. D. (2015). FRP reinforcement of low-grade glulam timber bonded with wood adhesive. *Construction and Building Materials*, *91*, 116–125. DOI: 10.1016/j.conbuildmat.2015.05.026

Raquel, R. A. (2019). Global Overview of the Cross-Laminated Timber Industry. *Young*, 1–128.

Sahoo, K., Bergman, R., Puettmann, M. (2021). *Cradle-to-Grave Life-Cycle Assessment of North American Laminated Strand Lumber Production*. *November*. https://www.fs.usda.gov/research/treesearch/63643

Schmid, J., Konig, J., & Köhler, J. (2010). Fire-exposed cross-laminated timber - Modelling and tests. *11th World Conference on Timber Engineering 2010, WCTE 2010*, *4*, 3268–3276.

Schober, K. U., Harte, A. M., Kliger, R., Jockwer, R., Xu, Q., Chen, J. F. (2015). FRP reinforcement of timber structures. *Construction and Building Materials*, *97*, 106–118. DOI: 10.1016/j.conbuildmat.2015.06.020

Shekarchi, M., Vatani Oskouei, A., Raftery, G. M. (2020). Flexural behavior of timber beams strengthened with pultruded glass fiber reinforced polymer profiles. *Composite Structures*, *241*, 112062. DOI: 10.1016/j.compstruct.2020.112062

Siha, A., Zhou, C. (2022). Experimental study on hysteretic behavior of circular timber columns strengthened with wrapped CFRP strips and near surface mounted steel bars. *Engineering Structures*, *263*(January), 114416. https://doi.org/10.1016/j.engstruct.2022.114416

Shi, F., Wang, L., Du, H., Zhao, M., Li, H., Wang, F., Wang, S. (2022). Axial Compression Behavior of FRP Confined Laminated Timber Columns under Cyclic Loadings. *Buildings*, *12*(11), 1–16. DOI: 10.3390/buildings12111841

Śliwa-Wieczorek, K., Ostrowski, K. A., Jaskowska-Lemańska, J., Karolak, A. (2021). The influence of cfrp sheets on the load-bearing capacity of the glued laminated timber beams under bending test. *Materials*, *14*(14). DOI: 10.3390/ma14144019

Song, H., Chun, Q., Han, Y., Gao, X., Cui, Z. (2024). Research on flexural behavior of square and circular cross-section timber beams strengthened with externally bonded and near-surface-mounted hybrid FRP plates. *Construction and Building Materials*, *451*(June), 138–742. DOI: 10.1016/j.conbuildmat.2024.138742

Svecova, D., Eden, R. J. (2004). Flexural and shear strengthening of timber beams using glass fibre reinforced polymer bars - an experimental investigation. *Canadian Journal of Civil Engineering*, *31*(1), 45–55. DOI: 10.1139/l03-069

Swedish Wood. (2015). Design of timber structures, Volume 1: Structural aspects of timber construction. *Swedish Wood*, *3*, 1–64. https://www.swedishwood.com/siteassets/5-publikationer/pdfer/sw-design-of-timber-structures-vol1-2022.pdf

Taheri, F., Nagaraj, M., Khosravi, P. (2009). Buckling response of glue-laminated columns reinforced with fiber-reinforced plastic sheets. *Composite Structures*, *88*(3), 481–490. DOI: 10.1016/j.compstruct.2008.05.013

Triantafillou, T. C. (1997). Shear Reinforcement of Wood Using FRP Materials. *Journal of Materials in Civil Engineering*, *9*(2), 65–69. DOI: 10.1061/(asce)0899-1561(1997)9:2(65)

URL-1: https://whc.unesco.org/en/list/58 (Access date: 10th January, 2024).

URL-2: https://chiloepatrimoniomundial.gob.cl/en/iglesias/iglesia-de-achao/ (Access date:10th January, 2024).

URL-3: http://www.greenstedchurch.org.uk/index.html (Access date: 12th January, 2024).

URL-4: https://www.designboom.com/architecture/white-arkitekter-tallest-timber-building-completed-skelleftea-sweden-09-08-2021/ (Access date: 12th January, 2024).

URL-5: https://cutthewood.com/guides/wood-types/oriented-strand-board/ (Access date: 8thJune, 2024).

Vahedian, A., Shrestha, R., Crews, K. (2019). Experimental and analytical investigation on CFRP strengthened glulam laminated timber beams: Full-scale experiments. *Composites Part B: Engineering*, *164*, 377–389. DOI: 0.1016/j.compositesb.2018.12.007

Wang, H., Chun, Q., Zhang, C., Ma, S., Cao, G., Dong, Q. (2023). Experimental study on the compression behavior of long timber column strengthened with the novel hybrid fiber sheets. *Journal of Wood Science*, *69*(1). DOI: 10.1186/s10086-023-02077-2

Wang, L., Shi, F., Zhao, M., Wang, B. J., Li, H., Zou, X., Du, H. (2024). Axial compressive behavior of FRP-confined laminated timber columns. *Archives of Civil and Mechanical Engineering*, *24*(1), 1–16. DOI: 10.1007/s43452-023-00827-z

Wei, P., Wang, B. J., Li, H., Wang, L., Peng, S., Zhang, L. (2019). A comparative study of compression behaviors of cross-laminated timber and glued-laminated timber columns. *Construction and Building Materials*, *222*, 86–95. DOI: 10.1016/j.conbuildmat.2019.06.139

Wen, Y., Fernando, D., Gilbert, B. P., Bailleres, H., Hu, R., Bisby, L., Roy, D. (2024). An investigation into the buckling behaviour of hybrid fibre reinforced polymer-timber thin-walled C-section columns. *Advances in Structural Engineering*, *27*(14), 2409–2428. DOI: 10.1177/13694332241269249

Weyerhaeuser. (2024). *Trus Joist® Beam, Header, and Column Specifier's Guide TJ-9000*.https://www.weyerhaeuser.com/woodproducts/document-library/document_library_detail/tj-7001/

Wilson, J. B., Dancer, E. R. (2005). Gate-to-gate life-cycle inventory of laminated veneer lumber production. *Wood and Fiber Science*, *37*, 114–127.

Woodall, C. W., Ince, P. J., Skog, K. E., Aguilar, F. X., Keegan, C. E., Sorenson, C. B., Hodges, D. G., Smith, W.B. (2024). an overview of the Forest Products Sector Downturn in the United States. 61(8), 595–603. https://www.researchgate.net/publication/275560939

Xu, M., Zhou, L., Gao, S., Xie, Q., Guo, N. (2024). Experimental study and theoretical analysis on mechanical properties of prestressed bolted glulam connections under cyclic loading. *Construction and Building Materials*, *457*(2024), 139352. DOI: org/10.1016/j.conbuildmat.2024.139352

Yang, H., Liu, W., Lu, W., Zhu, S., Geng, Q. (2016). Flexural behavior of FRP and steel reinforced glulam beams: Experimental and theoretical evaluation. *Construction and Building Materials*, *106*(March 2018), 550–563. DOI: 10.1016/j.conbuildmat.2015.12.135

Yang, J., Haghani, R., Al-Emrani, M. (2019). Innovative prestressing method for externally bonded CFRP laminates without mechanical anchorage. *Engineering*

Structures, *197*, 109416. DOI: 10.1016/j.engstruct.2019.109416

Yeboah, D., Gkantou, M. (2021). Investigation of flexural behaviour of structural timber beams strengthened with NSM basalt and glass FRP bars. *Structures*, *33*(April), 390–405. DOI: 10.1016/j.istruc.2021.04.044

Zahn, J. J., Rammer, D. R. (1995). Design of Glued Laminated Timber Columns. *Journal of Structural Engineering*, *121*(12), 1789–1794. DOI: 10.1061/(asce)0733-9445(1995)121:12(1789)

Zhang, C., Chun, Q., Wang, H., Lin, Y., Shi, J. (2022). Experimental study on the flexural behaviour of timber beams strengthened with high ductility and low cost hybrid fibre sheets. *Construction and Building Materials*, *322*(January), 126514. DOI: 10.1016/j.conbuildmat.2022.126514

Zhang, W., Song, X., Gu, X., Tang, H. (2012). Compressive Behavior of Longitudinally Cracked Timber Columns Retrofitted Using FRP Sheets. *Journal of Structural Engineering*, *138*(1), 90–98. DOI: 10.1061/(asce)st.1943-541x.0000423

Zheng, Y., Zhou, C. (2024). Mechanical behavior of timber columns reinforced with high-performance bamboo-based composites and self-tapping screws under axial compression. *Structures*, *70*(July), 107836. DOI: 10.1016/j.istruc.2024.107836

PUBLICATIONS AND WORKS

Suliman, S. S. A. (2023). State-of-the-Art of Fiber Reinforced Polymer (FRP) in Timber Structures*, 5th International ACHARAKA Congress on Life, Engineering*, *and Applied Sciences*, İzmir, Turkey, November 11–13, 2023.

BIOGRAPHY

Suhaib Suliman and completed his foundational education in Sudan, where he attended primary, secondary, and high school. He then pursued a bachelor’s degree in civil engineering at Karary University, graduating in 2017 with the highest GPA in his department, thus earning First Class with Honors. Suhaib further advanced his academic career by obtaining a master's degree in Structural Engineering from Khartoum University in 2022, achieving an excellent academic standing. During his master's program, he authored a research article focused on improving the strength and durability of concrete using waste glass powder. In 2021, he received the Turkish Government Scholarship (Turkiye Burslari) and began his higher education journey at Kocaeli University in Türkiye. There, he dedicated a year to learning the Turkish language before embarking on a second master's degree in the Civil Engineering department.